Compressor Stability Management

A Thesis
Presented to
The Academic Faculty

by

Manuj Dhingra

In Partial Fulfillment
of the Requirements for the Degree
Doctor of Philosophy

School of Aerospace Engineering
Georgia Institute of Technology
May 2006

Compressor Stability Management

Approved by:

Dr. J. V. R. Prasad, Advisor
School of Aerospace Engineering
Georgia Institute of Technology

Dr. Jerry Sietzman
School of Aerospace Engineering
Georgia Institute of Technology

Dr. Lakshmi Sankar
School of Aerospace Engineering
Georgia Institute of Technology

Dr. Aspi Wadia
GE Aircraft Engines

Dr. Yedidia Neumeier
School of Aerospace Engineering
Georgia Institute of Technology

Date Approved: January 9, 2006

To my Family

ACKNOWLEDGEMENTS

I would like to thank several people who have helped me during my years at Georgia Tech, and have made this dissertation possible. I would like to thank Dr. J.V.R. Prasad for the advice and support during the various stages of my doctoral program. I deeply value the opportunities that Dr. Prasad has made available and the freedom I have enjoyed while working under his guidance. Dr. Yedidia Neumeier has managed to fill a surprising number of roles: a mentor, a champion, and a friend. I have gained immensely from his insight and intuitive grasp of physical systems, as well as a unique approach to problem solving. I would like to thank Dr. Lakshmi Sankar, Dr. Jerry Seitzman and Dr. Aspi Wadia for serving on my committee. The thoughtful and pertinent feedback I have received from my committee has added to the quality of this dissertation.

I have had the fortune to interact with some exceptional people at GE Aircraft Engines. Andy Breeze-Stringfellow, Hyoun-Woo Shin and Peter Szucs have repeatedly helped me in any way they could. I can safely say that without them, I would not be where I am today. The design perspective provided by Andy and Peter has been invaluable. Dr. Shin has provided high quality compressor data, simply upon asking, which has been extremely useful for my research.

My work at Georgia Tech has been funded in part by the GEAE University Strategic Alliance, a project led by Dr. Dave Wisler at GEAE. Funding has also been generously made available by NASA under the URETI on Aeropropulsion and Power Technology. I am grateful for these sources of funding and would like to thank people involved.

I would like to thank several people at the School of Aerospace Engineering for their help. In particular, Carole Gains, Howard Simpson, Loretta Carroll, and Vivian Robinson have helped with various administrative matters. I have enjoyed my interactions with fellow students at AE, especially Assaad Krichene, Adam Sampley, Jim Armor, Suraj Unnikrishnan, Rama Sattigeri, Suresh Kannan, Geoffrey Jeram and Chang Chen.

On a personal note, I would like to thank my family for always being there for me. I would also like to thank Sameer for his unwavering friendship through the years. Last, but definitely not least, I would like to thank my wife, Poulomi, for her friendship, love and support. She has been my motivation and comfort during the downs, and has celebrated the ups with me. Her help with technical as well as linguistic aspects of this dissertation has been invaluable.

I would like to acknowledge the contributions of open-source software. I have benefited from several excellent tools and utilities, and I am grateful to people behind open-source software.

TABLE OF CONTENTS

LIST OF TABLES

LIST OF FIGURES

LIST OF SYMBOLS AND ABBREVIATIONS

$\mathbf{W_{f_{mod}}}$	Fuel modulation utlized by limit avoidance control.
μ	Average Number of Events
τ	Time between consecutive events, seconds
$C(t)$	Correlation Measure
C_{th}	Theshold value of correlation measure. An event is generated when correlation measure falls below this threshold.
D^+	Right hand derivative
$F(.)$	Distribution Function, also known as Cumulative Distribution Function
i	Index
N_g	Gas Generator Speed
N_p	Power Turbine Speed
P	Pressure signal
$P(x)$	Probability that x is true
P_2	Compressor Inlet Pressure
P_3	Compressor Outlet Pressure
P_{41}	Gas Turbine Inlet Temperature
P_{45}	Power Turbine Inlet Pressure
$shaft$	Number of samples in one shaft revolution
SM_{trig}	Stall margin below which limit detection alarm is triggered

t	Time, Current sample time
T_2	Compressor Inlet Temperature
T_{41}	Gas Turbine Inlet Temperature
$u_0(t)$	Probability that zero events will occur in time interval $(0, t)$
W_f	Fuel Flow Rate
Wa_2	Compressor Inlet Mass Flow Rate (Air)
wnd	Correlation window size in number of samples
ECDF	Empirical Cumulative Distribution Function
ECU	Electrical Control Mechanical Unit
EPDF	Empirical Probability Density Function
HMU	Hydro-Mechanical Unit
LDS	Load Demand Spindle
NG	Gas Generator Speed
TBE	Time Between successive Events

SUMMARY

Dynamic compressors are susceptible to aerodynamic instabilities while operating at low mass flow rates. These instabilities, rotating stall and surge, are detrimental to engine life and operational safety, and are thus undesirable. In order to prevent stability problems, a passive technique, involving fuel flow scheduling, is currently employed on gas turbines. The passive nature of this technique necessitates conservative stability margins, compromising performance and/or efficiency. In the past, model based active control has been proposed to enable reduction of margin requirements. However, available compressor stability models do not predict the different stall inception patterns, making model based control techniques practically infeasible. This research presents a viable alternative in the form of active stability management. In particular, a limit detection and avoidance approach has been used to maintain the system free of instabilities. Simulations show significant improvements in the dynamic response of a gas turbine engine by using this approach.

A novel technique has been developed to enable real-time detection of stability limits in axial compressors. It employs a correlation measure to quantify the chaos in the rotor tip region. Analysis of data from four axial compressors shows that the value of the correlation measure decreases as compressor loading is increased. Moreover, sharp drops in this measure have been found to be relevant for stability limit detection. The significance of these drops can be captured by tracking events generated by the downward crossing of a selected threshold level. It has been observed that the average number of events increases as the stability limit is approached in all the compressors studied. These events appear to be randomly distributed in time. A stochastic model for the time between consecutive events has been developed and incorporated in an engine simulation. The simulation has been used to highlight the importance of the threshold level to successful stability management. The compressor stability management concepts have also been experimentally demonstrated on a laboratory axial compressor rig.

The fundamental nature of correlation measure has opened avenues for its application besides limit detection. The applications presented include stage load matching in a multi-stage compressor and monitoring the aerodynamic health of rotor blades.

CHAPTER I

INTRODUCTION

1.1 Overview

Compressors are an integral part of gas turbine engines. While turbo-fan and turbo-jet engines used in fixed wing aircrafts predominantly incorporate axial compressors, turbo-shaft engines used in helicopters also utilize centrifugal or axial-centrifugal hybrid varieties. Both the basic types of compressors, along with the hybrid are susceptible to aerodynamic instabilities. The instabilities, rotating stall and surge, impose limits on the safe operation of a gas turbine engine. The onset of instabilities is represented by the surge line on a compressor map (Figure 1). The surge line demarcates the stable and unstable operating regimes of the compressor. The distance between a given operating point and the surge line is designated as stall margin. To date, numerous efforts have been undertaken to analyze, understand, control and/or mitigate the impact of these phenomena. However, the solution adopted for production engines continues to be an open-loop avoidance of the limit in question. This is accomplished by establishing an operating line sufficiently below the surge limit. The open-loop nature of this avoidance coupled with the detrimental effects of these instabilities on the engine, necessitate conservative margins. Contributing factors also include effects such as aging, speed as well as thermal transients, and engine control tolerances. Inlet distortions, e.g. during an aggressive maneuver, can significantly reduce the transient stall margin, adding to the margin requirement.

The need to reduce the stall margin is two-fold. A certain part of efficiency is usually sacrificed in order to meet design stall margin requirements. It follows that an excessive stall margin requirement acts as an efficiency penalty. Thus from the perspective of continuous steady operation, it would be beneficial to trim any extra stall margin requirement built into a compressor design. Secondly, the conservative stall margin negatively impacts the emergency response of the engine. For example, aborted carrier landings of fixed-wing

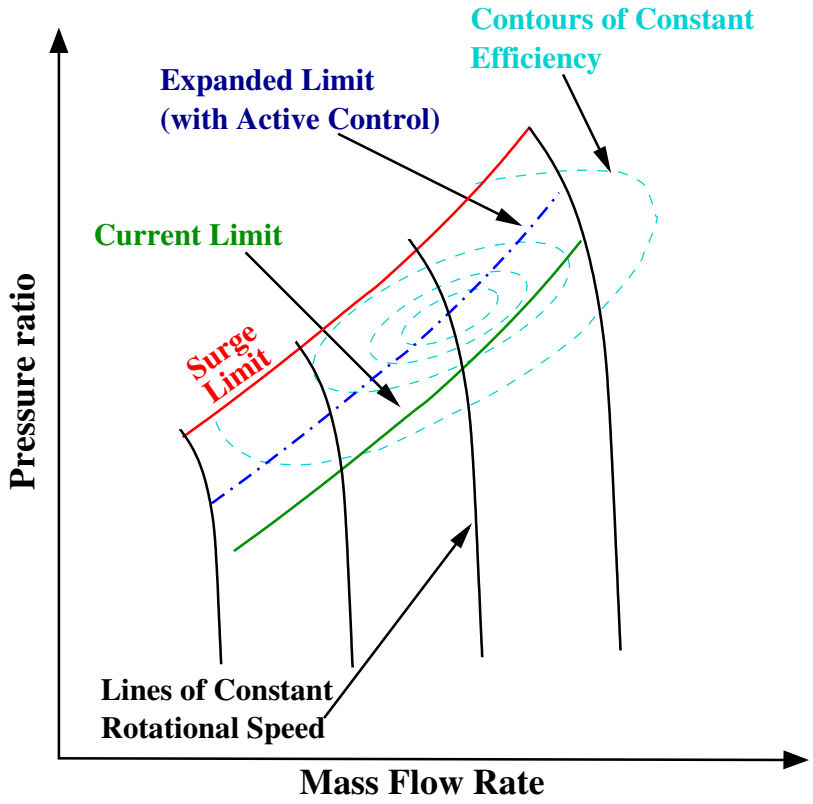

Figure 1: Expected performance enhancement with active control.

aircraft, or auto-rotation recovery for helicopters both demand a sharp increase in thrust or power from the gas turbine. The open-loop scheduling, while keeping the engine safe even in the worst case scenario, significantly increases the engine response time.

In most cases, a reactive control action, executed after the stall line has been crossed, is unacceptable. Any occurrence of such an event raises safety concerns and adds to the maintenance costs. The guidelines usually require dismantling of the engine and at least a visual inspection after any reported event.

The current chapter surveys the previous work in this area. This survey is divided into distinct parts. It starts with a discussion of different efforts that contributed to the model development. The review of model development stops at the Moore-Greitzer model, not because this model is the final word on compressor modeling, but because the later models inherit key problems associated with it. Next, some representative efforts on model based rotating stall control are outlined. A separate section is accorded to operability enhancement. Although the operability enhancement is also model based, its goals are sufficiently

different to warrant this. This is followed by a slightly detailed discussion of research on stall inception. A key outcome of this research is the existence of non-modal routes to stall, i.e. a route which is not captured by current compressor modeling approaches. Finally, the survey highlights four different efforts that aim to capture precursors to stall. Although some of these efforts are motivated by modal growth of rotating stall, they also seem to capture some aspects of non-modal inception.

1.2 Literature Review

1.2.1 Model Development

Emmons, Pearson and Grant (1955)

Emmons et al. [18] were probably the first to differentiate between rotating stall and surge. They described surge as a Helmholtz "organ-pipe" resonance in larger chambers of the machine. On the other hand, rotating stall was defined as a blade row instability characterized by the propagation of stall from blade to blade. They studied both a centrifugal as well as a single stage axial compressor and claimed that both systems were susceptible to the two phenomena. Emmons et al. correctly inferred that these two phenomena frequently interact to produce complex performance characteristics. It may be noted that the term "stall propagation" was used for what is currently called rotating stall. During the evaluation of experimental data obtained with the centrifugal compressor, Emmons et al. observed the existence of rotating stall in the low mass flow part of the surge cycle. On the nature of rotating stall, they discovered that it may involve multiple cells, with each cell spanning multiple blades. They further found that the shape, size and number of cells can vary with the operating condition, even for a given compressor. Emmons et al. provided a qualitative explanation for rotating stall. Moreover, they derived linear models for both rotating stall and surge.

Although the efforts of Emmons et al. did not eventually yield useful models, they successfully identified the main aspects of the problem. The discussion generated by their work indicates that similar experimental results were obtained at Cambridge University, England. Further, flow visualization studies carried out at Caltech around the same time

confirmed the method of propagating stall cells.

E. M. Greitzer (1976)

Continuing the analogy proposed by Emmons et al., Greitzer [22, 21] based his compressor surge model on the lines of a Helmholtz oscillator. He assumed that all the kinetic energy (KE) was limited to the compressor, inlet and throttle ducts, whereas all the potential energy (PE)was contained in the plenum. The compressor itself was modeled as an actuator disk. In contrast to Emmons et al. however, Greitzer's model captured some non-linear aspects of the compression system. At the time, it had already been observed that a compression system can surge under certain circumstances, while exhibit rotating stall under others. Greitzer's main concern then was the following: For a particular system at a given operating point, would it be possible to predict the final state of the system when subjected to a small throttle perturbation? Would the system return to steady operation, enter rotating stall, or undergo surge oscillations? Greitzer formulated a parameter, called Greitzer's parameter or sometimes simply the B-parameter, defined as,

$$B = \frac{U}{2a}\sqrt{\frac{V_p}{A_c L_c}}$$

where,

$$\begin{aligned} U &= \text{Rotor tip speed.} \\ a &= \text{Speed of sound.} \\ V_p &= \text{Plenum Volume.} \\ A_c &= \text{Characteristic compressor area.} \\ \text{and } L_c &= \text{Effective length of equivalent duct.} \end{aligned}$$

Greitzer's model assumed that the performance characteristic of the compressor, including the in-stall performance, was known. The numerical simulations of his model showed that the compression system exhibits rotating stall for low values of B-parameter. On the other hand, for larger values of B, surge was shown to be the dominant mode of aerodynamic instability. Greitzer conducted experiments using a low-speed three stage axial compressor. The results obtained were qualitatively consistent with the numerical simulations. Consequently, Greitzer proposed that there exists a critical value of the B-parameter for a given

compression system, which delineates preference for the two aerodynamic instabilities.

I. J. Day, E . M. Greitzer and N. A. Cumpsty (1978)

The effort by Day et al. [14] was focused on the understanding of the in-stall characteristics of the compressor. Specifically, they wanted to elucidate the impact of different design variables, such as design mass-flow rate, hub to tip ratio, number of stages etc., on the in-stall performance. The approach followed was heuristic, the idea being to correlate experimental data to the relevant design variables. Day et al. built on a hypothesis by Mckenzie *, which stated that stalled compressors produce approximately constant total-to-static pressure rise per stage, irrespective of the details of a compressor. Day et al. proposed the "blockage" concept. As per this concept, they assumed that the stalled part of the annulus operates with zero axial velocity, and that the unstalled part could be regarded as operating on the unstalled steady state characteristic. The blockage factor λ, defined as the fraction of annulus that has no net flow though it, played an important part in their model. They postulated that there were critical values of λ, λ_{ps} and λ_{fs}. The factor λ_{ps} was the maximum blockage with part-span stall, whereas λ_{fs} was the minimum blockage with full-span stall. Upon analyzing the experimental data, Day et al. concluded that

$$\lambda_{ps} = \lambda_{fs} = 30\%$$

and thus,

- There is a critical value of cell blockage, equal to 30 %, above which part-span stall breaks down into full-span stall, and below which full-span stall either ceases, or changes into part-span stall.
- The nature of stall onset may be determined by the blockage at a non-dimensional pressure rise of 0.17 per stage.
- The flow rate at which stall cedes is the rate when the blockage corresponding to non-dimensional pressure rise of 0.11 per stage drops below the critical value.

*No reference is available

Based on these guidelines, Day et al. predicted the influence of certain design parameters on rotating stall behavior, simply by estimating their respective influence on the unstalled compressor characteristic. Specifically they deduced that,

- The slope of throttle characteristic plays an important role on the in-stall performance.
- The higher the design value of flow coefficient, larger the hysteresis loop and the compressor is more likely to exhibit full-span stall at stall onset.
- The higher the number of stages, the larger the hysteresis loop and the compressor is more likely to suffer full span stall at stall onset.

Stetson (1982)

Stetson illustrated the importance of compressor stability from a design perspective [40]. He did not provide any new models of compressor instabilities, rather highlighted the different factors which interact with the compressor and impact its stability. Upon evaluation of aircraft engine usage he found that with the increase in engine thrust to weight, the engine spent less time at the maximum turbine temperature. On the other hand, the number of major throttle transients per sortie increased. Moreover, the increased thrust to weight of the engines increased the maneuverability of the aircraft, leading to increased distortion of the inlet flow. Stetson divided the flight envelopes into regions based on afterburner transient stability, arguing that as opposed to turbojets, the turbofans were not isolated from the after-burner by a choked turbine. Stetson dwelt on the importance of non-recoverable stall. Sometimes also called the "hung" stall, this term denotes the inability of the control system to clear rotating stall, and is the result of rotating stall hysteresis coupled with limits on effective throttle opening. Stetson's work was mainly concerned with the avoidance of "hung" stall. He proposed a stall recovery factor, based on the application of the B-parameter to Pratt and Whitney engines. He did not, unfortunately, provide an expression for the same.

F. K. Moore (1984)

In his work, presented as a three part paper [34], Moore attempted to develop a theory of rotating stall. He initially started with a small disturbance analysis and later extended it to finite amplitude disturbances. Moore restricted his formulation to completely developed rotating stall, i.e. he did not address the stall inception problem. Further, he assumed a system which exhibited rotating stall alone, and not surge. Two fundamental assumptions made by Moore are discussed below.

The unsteady response of each blade row was modeled as a first order lag. Specifically,

$$\frac{\Delta p}{\frac{1}{2}\rho U^2} = F(\phi) - \tau\dot{\phi}$$

where

$$\begin{aligned} \Delta p &= \text{Pressure rise across the blade row,} \\ U &= \text{Rotor tip speed,} \\ \phi &= \text{Non dimensional axial velocity,} \\ F(\phi) &= \text{Steady state blade row performance,} \\ \text{and } \tau &= \text{Time lag parameter.} \end{aligned}$$

The second key assumption involved the stall pattern of the compressor. Moore assumed that any disturbance in axial velocity is purely a function of circumferential location and that the stall pattern must proceed straight through the machine. He further assumed that the disturbance was steady in some rotating frame of reference. Moore's idea was to find the necessary conditions for such a set of disturbances to exist, while pressure far upstream and downstream remained constant.

Using a small disturbance analysis, Moore obtained an estimate of stall propagation speed. Comparison of calculated stall propagation speeds to experimental data showed that the estimate was qualitatively correct. Moore was able to achieve quantitative agreement by tweaking the lag parameters.

Moore postulated the existence of compressor characteristic function. This was defined as the pressure rise versus mass flow performance curve with steady, axisymmetric flow. He found that a necessary condition for weak stall pattern to exist was that this curve should

be locally flat. He argued that this was also true for finite amplitude disturbances, if the compressor characteristic was purely parabolic.

Moore tried to calculate the effect of rotating stall on the average compressor performance. A comparison with experimental data showed that his estimate was significantly off in certain cases.

Moore and Greitzer (1986)

This collaborative effort by the two successfully combined their respective earlier work, to yield an integrated theory of post stall transients [35, 36]. While Greitzer had assumed that the compressor performance curve under rotating stall, including the hysteresis region, as known, Moore had considered a compressor under isolation and hence subjected to rotating stall in the absence of surge. The combined theoretical model was represented by a set of three coupled, non-linear partial differential equations, one each for pressure rise, average axial flow coefficient, and the perturbation axial flow coefficient. Significantly, the combined theory retained Moore's original assumption that any axial disturbance is a function of circumferential location alone. In other words, any disturbance that enters the compressor passes straight through it. Moore and Greitzer demonstrated that pure rotating stall (as modeled by Moore) and pure surge were special cases of the combined model. To illustrate the model and to investigate transient behavior, they assumed a cubic compressor characteristic. Moreover, they used a single term Galerkin procedure to reduce the 3 PDEs into a system of 3 non-linear ODEs. The analysis of this reduced model led the authors to conclude that a fully developed rotating stall is stable in the presence of small axisymmetric disturbances. On the other hand, they found that a fully developed surge may be susceptible to circumferential disturbances, depending on the phase of the surge cycle at which the disturbance is introduced. Moore and Greitzer used a numerical simulation of their model to confirm Greitzer's previous conclusion regarding the importance of the B-parameter. In particular, they found that for low values of the B-parameter, initial small disturbances will grow into a steady rotating stall, whereas larger values favor the limit cycle behavior. Moore and Greitzer found that the compressor behavior was

not sensitive to reasonable variations of the initial disturbance amplitude. Finally, they calculated the instantaneous compressor pumping characteristics to show that the transient performance could be significantly different from both the axisymmetric and the steady state performance.

1.2.2 Model Based Active Control

Epstein, Ffowcs Williams and Greitzer (1986)

Epstein et al. evaluated the theoretical benefits of active control when applied to the compressor aerodynamic instabilities [19]. They claimed that active control would allow for operation in previously unstable high performance region. Moreover, as the proposed scheme operated on small disturbances, they argued that it would require relatively low control authority. Although the validity of the latter may be argued, the first claim is not quite correct. The high-performance region is usually not unstable. It is simply close to the stability boundary, and thus susceptible during transient operation, or when large disturbances are encountered. The researchers used the Moore-Greitzer model to study three example scenarios: Active suppression of small disturbances that develop into rotating stall, destabilization of steady rotating stall leading to stall recovery, and stabilization of surge. Epstein et al. assumed that the control input is a vortical perturbation which could be generated in any of the following ways:

- far upstream, using unsteady jets or wiggling stators,
- wiggling inlet guide vanes, or,
- a downstream perturbation via pulsing combustor.

They concluded that a control input, proportional to the circumferential perturbation of the compressor flow coefficient, could be used to significantly affect the compressor's stable operating range. Epstein et al. further showed that the *stable* stalled state can be similarly *destabilized*. As a consequence, they hypothesized, the compressor operating point could be moved up the throttle characteristic via active control.

For the purpose of surge control, Epstein et al. considered both a moving plenum wall and throttle area variation as the control input. They suggested that a speaker could be used as a moving plenum wall. For either case, they considered a linear control law, i.e. the control input was proportional to the plenum pressure variations. As with the rotating stall scenario, they concluded that control had a significant impact on the point of surge initiation.

In general, Epstein et al. were of the view that the operating range of the compressor can be significantly extended via active control.

D. L. Gysling and E. M. Greitzer (1994)

Following the control concepts proposed by Epstein et al., Gysling and Greitzer developed and experimentally demonstrated a strategy to stabilize rotating stall [23]. They significantly deviated from the earlier approaches in the choice of the actuators. While the researchers before them had employed mechanical actuators, Gysling and Greitzer used aeromechanical feedback actuation. They argued that aeromechanical feedback was inherently superior, stressing that it did not require external inputs, and eliminated sensors and actuators. In a sense aeromechanical feedback combines sensing and actuation into a single unit, and enables a control strategy based on locally reacting feedback.

Gysling and Greitzer used simple physical arguments to claim that dynamic feedback, specifically aeromechanical feedback, worked by local modification of the effective compressor characteristic. The particular form of aeromechanical feedback employed by them was based on reed valves. They developed a simple model of the combined system, with assumption analogous to the original Moore-Greitzer model. They deduced that the reed valves introduced two additional modes for each spatial harmonic of rotating stall. Gysling along with Greitzer designed an experimental facility to evaluate their concepts. In order to account for the effects of steady injection, they compared all results obtained to *rigid* reed valves, i.e., they used steady injection, and not the nominal baseline, as the basis for range extension via aeromechanical feedback calculations. They found that aeromechanical feedback had no apparent effect on the nominally stable steady-state performance, while

it extended the stable operating regime. The maximum range extension observed in their experiments corresponded to a 10% decrease in stalling flow coefficient. Finally, Gysling and Greitzer argued that the reed valves act as high bandwidth actuators. They showed that for the optimally tuned reed valves, reed valve deflection was 180^o out of phase with the velocity perturbations, for frequencies up to two times the rotor frequency.

H.J. Weigl, J.D. Paduano, L.G. Frechette, A.H. Epstein, E.M. Greitzer, M.M. Bright, A.J. Strazisar (1998)

Weigl et al. studied the active control of rotating stall for high speed compressors using a single stage transonic compressor [48]. They reiterated that the modes introduced by compressibility effects in a high speed compressor have significant implications for its control. They further argued that the new modes could be critical both in frequency and stability. In terms of stability they pointed to the work of Tryfonidis et al. [45] which suggested the possibility of the first *compressible* mode leading to instability in a high speed compressor.

With regards to the frequency, Weigl et al. argued that the compressible modes, in contrast with their incompressible counterparts, do not scale with rotor frequency. Thus, they argued, the two types of modes could have absolute natural frequencies that are relatively close to each other, especially at high speeds. Simply, Weigl et al. were concerned about the excitation of the compressible modes by the feedback from the control system.

Weigl et al. used twelve high bandwidth injectors in their effort to control rotating stall experimentally. They employed a non zero mean steady injection to allow for symmetric, i.e. positive and negative, unsteady actuation. Consistent with the earlier results on low speed compressor, they found that steady blowing significantly impacted the compressor performance curve. Weigl et al. obtained the transfer function of their system by forcing it with rotating sinusoidal waves. They designed the control laws based on this experimentally identified transfer function.

Weigl and co-workers found that while a simple constant gain control law could stabilize the rotating stall when the compressor was operated at 70% of design speed, it was not effective at the design speed. To obtain benefits at the design speed, they synthesized a model based, H_∞ control law, which simultaneously controlled multiple harmonics of

rotating stall. The use of this H_∞ control law yielded 3.5% range extension over the steady injection scenario. Weigl et al. claimed that the control law was robust with respect to modeling errors. In order to show that the control law was also robust in terms of disturbance rejection, they switched off the controller at a nominally unstable operating point. The control was then switched back on after a time lapse. Weigl et al. argued that when the controller is re-activated in this fashion, it has to stabilize the system, starting with a large initial condition which approximates the effect of a finite amplitude disturbance.

Finally, Weigl et al. stressed that forced response testing was a useful tool for investigating compressor dynamics, regardless of implications for rotating stall control.

J.V.R Prasad, Y. Neumeier, M. Lal, S. H. Bae and A. Meehan

Prasad et al. investigated a combination of passive and active control methods for stall suppression [38]. They used a laboratory axial compressor facility to evaluate passive flow separators, bleed, as well as recirculation control. The flow separators in the compressor inlet were motivated by the Moore-Greitzer model, which assumed that the stall pattern flows unmodified through the compressor. Prasad et al. argued that in the presence of separators in the inlet, traveling waves could not develop in the entire machine. They found that the same idea was reached independently by Moore, who recommended a single separator and, in fact, had patented the idea. Prasad and co-workers found that a single separator had a minimal impact on the flow pattern in the compressor. They increased the number of separators and concluded that any number of separators were unable to eliminate rotating stall. However, the increased number of separators delayed the onset of rotating stall and moderated its amplitude.

Prasad et al. used different steady bleed rates to show that steady bleed did not alter the flow through the compressor. Specifically, they showed that pressure versus inlet mass flow characteristic was not affected by steady bleed. Further, they showed that active recirculation can be used to extend the unstalled operating range of the compressor, and that recirculation did not degrade the performance of the compressor. They combined fuzzy logic based active control with passive flow separators and showed that the benefits

of active control can be augmented by passive control. Finally, Prasad et al. showed that heat addition acts analogous to a downstream throttle and postulated its use for compressor control.

A.J. Strazisar, M. M. Bright, Thorp, D. Cully and Suder (2004)

Motivated by the open-loop injection results of Weigl et al., Strazisar and co-workers evaluated the effectiveness of end-wall recirculation for stall control [43]. Their work encompassed injector development, testing on a single stage transonic compressor, and assessment of recirculation on a multistage high speed compressor. Strazisar et al. found the previously used injectors unsuitable for multistage compressors as they protruded into the flow. Consequently they concentrated on compact injectors, flush with the compressor casing. After evaluating the results obtained through CFD calculations, they concluded that angled slot injectors were not suitable for injecting air into the the tip region. They used *coanda*-type injectors instead. As per the coanda effect, the static pressure gradient across the curved streamlines within the injector keeps the flow attached to the end-wall. With the aim of minimizing the amount of circulation, Strazisar et al. conducted an experimental survey of injector throat height. They found that for a fixed ratio of circumferential coverage, results were similar for two injector designs, one half as high as the other. They obtained a 6% reduction in stalling mass flow of the single stage transonic compressor using the half height injectors.

Following the tests on the single stage machine, Strazisar et al. conducted recirculation experiments on a high speed, technology development, multistage compressor. They claimed that the high speed valves for the injection system were not rated for high temperature air bled from the compressor. Hence they simulated recirculation by injecting ambient temperature air from an external source, while bleeding an equivalent, temperature corrected mass flow from the rear of the compressor. Strazisar et al. tested both steady injection and actively pulsed injection with this setup. They found that both active and steady injection had some stabilizing effect on the compressor. Further they inferred that the main advantage of active control, as compared to steady injection, was that it reduced the amount

of injection for the same improvement in stability. Finally, Strazisar et al. claimed that the main benefit of recirculation in a high speed multistage compressor is towards stage matching, i.e. an ability to throttle individual stages with respect to others.

1.2.3 Operability Enhancement

An alternative look at stall control has been provided by the proponents of operability enhancement. In relation to compressor control, operability enhancement could be defined as the elimination of the hysteresis associated with the rotating stall. The hysteresis in not a characteristic of the compressor in isolation, but arises due to interaction between the throttle characteristics and the bifurcation of the compressor performance curve. However, it is a major concern for the safe operation of the gas-turbine engine. Due to its impact, the initial work on compressor stability was essentially concerned with determining which instability was favored by a given compressor.

D. Liaw and E. H. Abed (1993)

Liaw and Abed performed bifurcation analysis of the three state Moore-Greitzer model [30]. In general, bifurcation analysis deals with the emergence of new equilibria in a non-linear system, when a given parameter crosses some critical value. Liaw and Abed emphasized the importance of local bifurcations on the nature of post-stall flow in an axial compressor. They considered the throttle parameter as the bifurcation parameter, and showed that the system undergoes a pitch-fork bifurcation at a critical value which corresponds to the stall inception point. Further, they showed that this bifurcation was sub-critical, i.e., the resulting bifurcated equilibria were unstable. Liaw and Abed contended that this instability of bifurcated equilibria was responsible for the hysteresis associated with the rotating stall. Using throttle as the control input, they proceeded to show that the axisymmetric branch of the equilibria could not be stabilized by linear feedback control. They used a purely quadratic control law, in which control throttle input was proportional to the square of the amplitude of the first rotating stall harmonic. Such a law, Liaw and Abed calculated, could render the bifurcation at the stall inception point super-critical, i.e. the bifurcated equilibria can be locally stabilized.

Liaw and Abed's work essentially suggested that a 1-D actuation of throttle parameter could suitably modify the 2-D behavior of the system, eliminating the hysteresis associated with rotating stall.

Badmus, Chowdhury, Eveker, Nett and Riviera (1993)

Badmus et al. [1, 2] advocated a simplified approach to rotating stall control. They outlined the likely scenario of its application to gas turbine engines. According to Badmus et al., the benefits of active stall control would not be available to most existing designs. As the efficiency of the compressor is optimized at the design point, moving the operation away from it would in fact be detrimental. However, they said, a reduced stall margin requirement can be the part of new design process, where the new design point would carry lower than previous levels of stall margin.

Badmus et al. contrasted their approach to that followed previously, highlighting that they did not aim to extend the theoretical stability limit of the axisymmetric flow. Instead, the stated goal was to eliminate the abrupt jump into rotating stall while eliminating the hysteresis with respect to the onset and cessation of rotating stall. This approach was fundamentally similar to that proposed by Liaw and Abed [30]. Badmus et al. extended the analysis by introducing domains of attraction, a concept from non-linear systems theory. They mentioned that if the domain of attraction of an axisymmetric equilibrium point in the hysteresis region is small, internal system noise can perturb the system sufficiently to push it to the stalled branch. The goal thus, according to Badmus et al., was to enlarge the domain of attraction of the inherently stable axisymmetric branch of the compression system.

The control law considered by Badmus et al. was the constant gain quadratic feedback, proposed by Liaw and Abed. Although not explicitly discussed, they apparently encountered the critical gain associated with such a law, as discovered by Markopoulos et al. [32] later.

Badmus et al. used a compressor rig to experimentally demonstrate their approach. They performed open loop tests which illustrated the bifurcation at the stall inception.

To compute rotating stall amplitude required for the closed loop control, they used six circumferentially distributed pressure sensors at the compressor inlet. They were able to eliminate the hysteresis in the closed loop system. Further, they showed that closed loop control was effective in the presence of a small persistent disturbance. However, when they used a larger persistent disturbance, the system entered a limit cycle. They hypothesized that this behavior was caused by the non-linearities introduced by the actuator limits. They also suggested that due to the experimental tuning of their control law in the absence of a model of their system, its parameters were not optimal.

The work of Badmus et al. provided partial experimental demonstration of rotating stall control via 1-D actuation.

R. D'Andrea, R. L. Behnken and R. M. Murray (1997).

D'Andrea and co-workers utilized pulsed air injection for rotating stall control [11]. Essentially, their idea was to modify the compressor characteristic, which in turn would change the bifurcation behavior of the Moore-Greitzer model. In their experimental work, they used three circumferentially distributed air injectors and six wall mounted static pressure transducers. The setup employed permitted them to vary the orientation of the injected air, relative to the rotor face. The experimental results led them to conclude that the air-injection can be modeled as a local shift of the compressor characteristic. D'Andrea et al. used the 3-state Moore-Greitzer model to show that the bifurcation behavior of the non-linear ODEs can be changed by a linear shift of the compressor characteristic. Specifically, they showed that the slope of the locus of the stalled equilibria at the stall inception point can be changed from its nominal positive value to a negative value. They argued that the negative slope of the bifurcation diagram would eliminate the hysteresis associated with rotating stall.

D'Andrea et al. successfully demonstrated the elimination of hysteresis on their experimental rig. The experimental results were augmented with a simulation study, performed with a mid-fidelity model. D'Andrea et al. concluded that the modeling of air injection as a local shift in compressor characteristic was a valid approach.

This work also demonstrated the coupling between rotating stall and surge. They conducted a set of experiments with a large value of the B-parameter, to allow surge cycles to occur. They induced surge by a controlled perturbation of the throttle. They found that the uncontrolled system entered a stable limit cycle. On the other hand, in the controlled system, surge was eliminated within three cycles after air-injection was turned on.

Markopoulos, Neumeier, Prasad and Zinn (1998)

Markopoulos et al. [32] considerably generalized the results obtained by Liaw and Abed. They considered the throttle area as the control variable, along with a relatively large class of control laws of the form,

$$u = kA^p$$

where A is the amplitude of the first mode, gain $k \geq 0$ and $p > 0$. Thus the control laws were proportional to the amplitude of the first rotating stall harmonic, raised to a strictly positive exponent. Markopoulos et al. discovered a critical value for the gain, k_{crit}, defined in terms of compressor parameters. Incidentally, k_{crit} which is nominally a positive number, was determined to be significant for the closed-loop as well as open-loop stability. Markopoulos et al. found that the stability of the axisymmetric branch was invariant under throttle feedback control, irrespective of the form of control law used. Besides evaluating the stability of the bifurcated axisymmetric and non-axisymmetric branches, they looked at the local stability of the stall inception point (SIP). They found that the sign of k_{crit} determined the stability of SIP, both for the open-loop case, as well as the higher than quadratic control laws. In either case, SIP was stable for $k_{crit} < 0$ and unstable if $k_{crit} > 0$. If quadratic control law was used, SIP was stable for all gains larger than k_{crit}, whereas it was stable for all positive gains with a sub-quadratic control law. The stability of non-axisymmetric equilibria was found to be similar to that of SIP. The sign of k_{crit} determined the stability of the non-axisymmetric branch for open-loop and higher than quadratic feedback control laws, with $k_{crit} < 0$ implying stability and $k_{crit} > 0$ implying instability. Markopoulos et al. found that quadratic control laws ensured stability, provided the gain was greater than k_{crit}. Finally, they found that the closed-loop system was stable for all positive gains,

when a sub-quadratic control law was assumed. Markopoulos et al. observed that the non-axisymmetric branch was tangential to the axisymmetric branch at the stall inception point, when the control law was sub-linear. Consequently they claimed that a sub-linear control law was a superior choice for throttle based rotating stall control. This conclusion was a sharp contrast from previous work which, in general, did not consider linear or sub-linear control laws.

Y. Wang, S. Yeung and R. M. Murray (2002)

Wang et al. studied the effects of magnitude and rate limits in a bleed actuator on the operability enhancement achievable via active control in an axial compressor[46, 47]. Their analysis was restricted to low B-parameter values, i.e. surge free operation of the compressor. They performed a model order reduction based on the stability of the invariant manifold connecting the axisymmetric and stalled equilibria. Using this reduced model, they concluded that the presence of noise in a compression system causes stall inception to occur at the right of the peak performance. Wang et al. defined operability enhancement as the extension of operating range through active control, for which fully developed rotating stall can be avoided. They applied bifurcation analysis tool to the reduced order model and concluded that a rate saturated control law yields optimal operability enhancement. In other words, when bleed actuation is used for rotating stall stabilization, and the actuator is subjected to rate and magnitude limits, the optimal control law is the one which opens the bleed valve to its maximum value, as fast as possible.

Continuing their analysis of operability enhancement, Wang et al. showed that it is affected by the shape of compressor characteristic, magnitude and rate limits of the actuator, and time delay of the control system. In particular, they showed that the achievable enhancement is inversely impacted by the curvature of the characteristic, and when the unstable part is steeper than the stable part. Wang et al. validated these results through experiments in which a family of compressor characteristics was obtained with the use of continuous air injection. For a fixed operability enhancement, the experimental results were

qualitatively similar to those predicted by theory. However, the theory consistently under-predicted the required actuator rates. Further the actuator used by them was capable of bleeding 12% of flow at stall inception, thus may not have been magnitude limited. Finally, Wang et al. only considered quadratic feedback control law of the type proposed by Liaw and Abed [30]. The sub-linear control laws proposed by Markopoulos et al.[32], which theoretically do not have a minimum gain requirement, may yield different results.

1.2.4 Non-modal Stall Inception

I. J. Day (1991)

Day [12] studied the problem of stall inception in axial flow compressors. His investigation was experimental in nature, for which he utilized two low speed compressors. The first compressor was a single stage machine and lacked inlet guide vanes. The second compressor, on the other hand, had four identical stages. He utilized hot wire anemometers to measure the velocities in front of the first rotor in both cases. It may be recalled that prior to Day's work, the accepted theory of stall was the growth of a modal disturbance, which smoothly transitioned into stall cells, close to the compressor performance peak. The data reduction methods thus included the spatial Fourier transform, to check for any modal waves. Day was able to observe modal growth in some of the data from his experiments. Further, using an array of circumferentially distributed air injectors, he studied the forced response of the system. He found that the response of the compressor peaked at a frequency equal to that of naturally occurring modal perturbations prior to stall. He also found that the amplitude of excited waves increased almost linearly, as the flow rate was reduced. This ability to excite modal waves, Day noted, was limited to a small range of the compressor flow coefficient.

During the experiments, Day observed a hitherto unknown phenomenon, which he termed the formation of finite stall cells. He divided these cells, based on their relative size into two classes: short length scale, also known as *spike*, and long length scale stall cell. The distinction was somewhat arbitrary, according to him, and that the real difference lied in the speed at which the cells traveled. Day observed that the short length scale stall was localized to two or three blade passages and had relatively high speed of rotation. The

coupling between the short length scale stall and modal waves, if present, was minimal. The modal wave, Day found, affected the formation of a *spike* cell in that the spike initiated at the trough of the modal wave. The large length scale cell had a larger amount of coupling with the modal wave. Day concluded that the large length scale cell inception was consistent with the Moore-Greitzer model. He also found that in some cases both short and long length scale cells appeared prior to stall. Exploring the properties of short length scale cells, Day found that multiple cells could form in the compressor, and that these could be non-uniformly distributed. He further found that the spike had the tendency to occur at the same circumferential location. Moreover, for the single stage compressor, he found that the spike occurred at the same location even in the relative frame. In other words, the short scale cells originated when a particular part of the rotor was under a particular part of the casing, at least in the single stage compressor. Day concluded that geometric non-uniformities were important for this type of stall inception.

Day postulated that modal oscillations and formation of finite stall cells were separate events. He found that the occurrence of the two was not necessarily consecutive, and if short length scale cells were formed first, the modal waves did not appear prior to stall. Day's work highlighted that rotating stall inception is a complex phenomenon and that the Moore-Greitzer model did not capture all the routes to stall.

Longley, Shin, Plumley, Sikowski, Day, Greitzer, Tan and Wisler (1994)

Longley et al. [31] were interested in analyzing the impact of a rotating inlet distortion on compressor stability. This scenario arises in multispool engines, where a stall in the upstream compressor imposes a rotating distortion on its downstream counterpart. The significance of their work to the problem under consideration arises due to the particular method they used to experimentally simulate this situation. They used a rotating screen upstream of four different compressors and measured the stall margin degradation as a function of its speed and direction of rotation. They divided the compressors into two groups based on the observed response. The first group showed a single peak in stall margin degradation, whereas the second had two distinct peaks. Incidentally these peaks occurred for

co-rotating inlet distortion. Longley et al. observed that the second peak was sharper than the first and occurred at higher (about 70% of rotor speed) speeds. This difference motivated them to study the natural stall inception behavior of the four compressors. They found that the compressors in the first group with a single peak exhibited a modal, long length scale type of stall inception pattern. One of the compressors in the second group favored a spike type of stall inception. The propagation speed of the small scale cell coincided with the second peak in the forced response measurements. Longley et al. stated that sufficient information on stall inception process was not available for the second compressor in this group.

It is worthwhile to note that Longley et al. used a theoretical model, based on the Moore-Greitzer type 2-D flow-field stall inception process, to predict the stall margin degradation for all four compressors. The predictions for the first group were qualitatively acceptable, whereas those for the second group were not. This highlights the fact that the available models of compressor rotating stall do not capture the 3-D, spike type of stall inception. In regards to the problem investigated by Longley et al., they concluded that counter rotation of fan and core spools would be beneficial to the compressors tested.

J. F. Escuret and V. Garnier (1996)

Following the work of Day [12], Escuret and Garnier [20] studied the stall inception process in a high speed multi-stage compressor. They used a four stage compressor which had a larger than usual axial blade spacing. This larger spacing, according to Escuret and Garnier, was mandated by inter blade-row instrumentation requirements. For the stall inception studies they employed high bandwidth wall mounted pressure transducers. They conducted experiments to determine the stalling process for the entire operating range, varied inlet guide vanes (IGV) to understand the effect of stage matching and conducted fast transients to simulate transients encountered in military engines. For the compressor used, Escuret and Garnier found that it stalled via a short length scale stall inception pattern over the entire map. Further, they found that the only effect of IGV setting angle was on the axial location of the first flow disturbance detected. They studied the effect of IGVs at

three different speeds and found that opening the IGVs moved the first detected disturbance to the first stage, whereas closing them moved it to the fourth stage. Escuret and Garnier found that fast transients did not have any effect on the stall inception behavior of their compressor. To confirm the absence of modal waves prior to stall inception, they used the traveling wave energy method, pioneered by Tryfonidis et al.[†] They did not find any peak of propagating wave energy and concluded the absence of modal waves. Finally Escuret and Garnier tried to determine the relative and absolute angular location of the spike inception. Like Day [12] before them, they found good coherence in the circumferential location of spike onset in both the frames. Consequently, they concluded that circumferential non-uniformities played an important part in the short length scale cell stall inception.

The unique, unusual feature of Escuret and Garnier's work was the complete absence of modal waves prior to stall.

T. R. Camp and I. J. Day (1997)

These two researchers [6] utilized detailed measurements to illustrate the differences between spikes and modal oscillations. Camp and Day analyzed a combination of velocity measurements, circumferential and axial, along with pressure data from sensors located at the hub and tip of the compressor. They concluded that a spike was a localized blockage in the flow-field with an accompanying upstream stagnation region. They also found that a spike type of disturbance originates near the rotor tip and initially occupies only part of the span. Modal oscillations on the other hand, according to Camp and Day, did not have a specific origin in time or space. They emphasized that modal oscillations were usually of equal intensities from inlet to exit, in a low speed compressor, and that these oscillations occur at the peak of the pressure rise coefficient.

Camp and Day proceeded to identify the operating conditions which facilitate each of the stall inception mechanisms. They conducted a series of stage matching experiments by utilizing the variable geometry of the compressor. They divided the compressor into two blocks *stage 1* and *stages 2-4*. They found that the compressor stalled via spikes

[†]This technique is discussed in following section.

whenever *stage 1* was at a higher loading than *stages 2-4*. They also found that whenever the compressor stalled via spikes, rotor 1 incidence angles at stall were nearly constant. After analyzing the total-to-static pressure rise characteristics, Camp and Day found that modal oscillations appeared in cases where the slope of the compressor characteristic was zero or slightly positive at the stall point.

Camp and Day combined these two observations and proposed a simple model. As per this model, there exists a critical value of rotor incidence angle. If the peak of overall characteristic is reached before the rotor incidence angle exceeds the critical value, modal oscillations will occur in the compressor. On the other hand, if the critical value of rotor incidence angle is exceeded while the compressor characteristic is still negatively sloped, spike will appear before modal oscillations have developed.

To study the effect of radial redistribution of flow, Camp and Day used a single stage compressor. They found that prior to stall, spikes appeared when the flow was directed towards the hub, whereas modal activity was apparent when it was directed towards the tip region. Camp and Day showed that the two types of stall inception mechanisms have different stability criteria. The occurrence of one versus the other depended on which criteria was first violated.

I. J. Day, T. Breuer, J. Escuret, M. Cherrett and A. Wilson (1999)

In a collaborative European effort, Day and his co-workers tested four different high speed compressors in order to identify the generic features of stall inception [13]. In spite of differences in design, Day et al. considered the four compressors to be typical of aero-engine practice. They pointed out that in a high speed compressor, the stage matching automatically changes with the rotation speed. The compressibility effects shift the position of highest loading from the front of the compressor to the rear, as the speed of rotation is increased. With the above in mind, Day et al. expected spike type of stall inception at low and high speeds, with modal oscillations visible at the mid-speeds. They found that in three out of the four compressors, spike type of stall was indeed observed at low speeds, whereas modal oscillations could be observed prior to stall in the mid-speed range. At high speeds

however, Day et al. discovered, the stalling process developed so quickly that it was difficult to classify the stalling pattern. Moreover, for one of the compressors [‡] modal activity was limited to a very narrow speed range, only about 2% wide. The fourth compressor, which incidentally was the one used by Escuret and Garnier [20] in their work, always stalled via spike type of inception. Day and co-workers sought to address the effect of IGV settings on stall inception. They obtained inconclusive results in this respect. Only two of the four compressors had variable geometry. In terms of stall inception, one was very sensitive to IGV setting angle while the other was not affected by it at all.

Besides analyzing the stall inception patterns, Day et al. sought to assess the range of signals that an active control system would be expected to cope with in regular operation. They found "front-end" or "start-up" stall in three of the four compressors. This kind of stall is usually benign, unless additional throttling forces the small cells present in this condition to coalesce into one large cell.

On the high speed side, Day et al. found that each of the four compressors stalled in a different way. They found that all the compressors were sensitive to circumferential non-uniformities, where flow breakdown was associated with specific locations. They also observed a new phenomenon, which they designated as non-rotating stall. In this phenomenon, they observed rising pressures in the form of a slow ramp that occurred over a large circumferential area, prior to complete flow breakdown. Another previously unknown phenomenon was reported by Day et al., which they called the high frequency stall. They encountered high frequency stall in two compressors. In one of the compressors, they were able to attribute it to multiple part-span cells rotating at high speeds. For the other one, they found that the disturbance was apparently axisymmetric and could not be similarly explained.

Moreover, Day et al. found that shaft order perturbations were present in all the compressors at high speeds, while they were exhibited by one compressor at all speeds. Finally, the researchers also looked at the impact of inlet distortion. They found that inlet distortion could introduce spikes which did not lead to flow breakdown, and in one compressor

[‡]VIPER engine

distortion amplified the modal oscillations which in turn triggered spikes.

B. Hoss, D. Leinhos and L. Fottner (2000)

Hoss et al. studied the stall inception in a two stage low pressure compressor, part of a twin spool turbofan engine [24]. They throttled the compressor by reducing the secondary nozzle area. Hoss et al. used pressure transducers, total as well as static, to investigate the flow-field in the compressor. They used a series of techniques to reduce experimental data, which were used not only to isolate the stall inception process, but also to generate a pre-stall warning alarm. The existing techniques that they used, included filtering in time domain, frequency spectra via FFT, and the traveling wave energy method. Hoss and co-workers introduced a new scheme, based on the wavelet transform.

The compressor studied, according to Hoss et al. was unusual because the first stage exhibited a positive pressure rise characteristic for all throttle settings, at all speeds. They found that the compressor stalled via spikes at low-speeds, while modal oscillations could be observed prior to stall at mid-speeds. They found that the stall inception at high speeds was dominated by the shaft frequency. Moreover at high speeds, specifically at 90% corrected rotor speed, Hoss et al. observed significant perturbations in the shaft frequency which damped out prior to stall. Based on the spike-like signature of this disturbance, they concluded that a stall cell fixed to a particular blade was responsible for the observed phenomena.

The wavelet analysis performed by Hoss and co-workers led them to suggest that it could provide significant stall warning lead times, and thus could form the basis of an active avoidance approach.

Hoss et al. observed some high frequency content located between third harmonics of the low and high pressure compressors. This was accompanied by another mode, on shaft frequency step above it. They speculated that this could be the result of the interactions between the low and high pressure compressors. Finally, Hoss et al. investigated stall inception in the presence of inlet distortion. They found that the compressor always stalled via spike-type cells, and no modal oscillations were observed prior to stall for the entire

speed range.

1.2.5 Precursor based avoidance

M. Inoue, M. Kuroumaru, T. Iwamoto and Y. Ando (1991)

In their work, Inoue et al. were concerned with the early detection of precursors to rotating stall [27]. The rapid growth of a stall cell in many cases, led them to exclude the stall inception triggered control action from the set of viable options. Continuing with the practical aspects of compressor control, they sought precursors in pressure fluctuations at the casing wall, while ruling out velocity measurements via hot-wire anemometers.

In particular, Inoue et al. conducted tests using two rotor designs. Their setup included a provision for several tip clearance settings for each design. They reported that in all the cases stall occurred at the tip in their compressor. In a detailed study, Inoue et al. evaluated the contour maps of ensemble averaged wall pressure, as well as the variation around the average. They observed that although the mean pressure maps for different operating points close to the stall inception were nearly indistinguishable, the pressure variation increased significantly as the flow rate was reduced. Inoue et al. drew on concepts from statistical analysis to illustrate and capture the nature of the increased pressure fluctuation. They concluded that the fluctuation was caused by the intermittent separation at the leading edge of the rotor blade.

Inoue et al. used, what they called, the pseudo spatial correlation contour map to study the nature of the fluctuations. They found a periodicity associated with the blade spacing under normal operating conditions. This periodicity decreased and even vanished as the flow rate was reduced. Although this loss could be due to random disturbances, the spatial correlation contour maps led Inoue et al. to suggest the existence of a coherent propagating disturbance.

To quantify the collapse of periodic nature, Inoue et al. defined a similarity parameter. They showed that the similarity parameter decreased rapidly as stalling flow rate was approached. They emphasized that the similarity parameter was computationally intensive and could not be calculated in real-time. Finally, they defined a cross-correlation coefficient,

which in essence behaved similar to the similarity coefficient.

It is worth mentioning that the method proposed by Inoue et al. only required a single pressure transducer. However, the definition of both the similarity coefficient and the cross-correlation parameter required ensemble averages. The ensemble averaging was performed over 200 revolutions, and hence the detection parameter reflected conditions over 200 revolutions. The ensemble averaging may make such a technique unsuitable for control during rapid transient scenarios.

M. Tryfonidis, O. Etchvers, J. D. Paduano, A. H. Epstein and G. J. Hendricks (1995)

Tryfonidis et al. evaluated pre-stall data from several high speed compressors for indicators to impending stall [45]. In order to do this, they developed a new data reduction technique, called the traveling wave energy (TWE). This method involves the computation of spectral Fourier coefficients, and thus needs data from circumferentially distributed sensors. Once the spectral Fourier coefficient, say for the first harmonic, is obtained, its power spectra are calculated. Tryfonidis et al. emphasized that such spectra may not be symmetric about the zero frequency (i.e. y-axis on the power spectrum plot). The integral difference between the *positive* and the *negative* spectra was defined as the quantitative measure of the traveling wave energy. Tryfonidis et al. claimed that all the compressors studied, exhibited rotating disturbances prior to *surge*. They also claimed that all the compressors showed some evidence of rotating waves prior to stall.[§] Tryfonidis et al. emphasized that in the noisy engine environment it would be difficult to identify small amplitude pre-stall waves by a linear phase or increased magnitude in the spatial Fourier coefficients. The researchers evaluated the pre-stall power spectra of the first spatial Fourier coefficient using data from the various compressors. They found that the shaft frequencies dominated at 100% speed for all the cases, though other modes were present at part speeds. Tryfonidis et al. calculated the traveling wave energy for one of the compressors, integrating from 25% to 125% of rotor speed, to obtain its value as a function of time. They found that the traveling wave energy

[§]Note: This claim is in contradiction with that of Day et al. [13] who found rotating waves existed only for a very limited range in the VIPER engine

was related to the stall margin for that compressor.

Tryfonidis et al. used a compressible version of the 2-D Moore-Greitzer model to show that compressibility introduces additional axial modes. Application of this theoretical model to a four stage compressor led Tryfonidis to conclude that the compressible modes could lose stability before the incompressible modes, especially at the design speed. They also found that the frequency of the compressible mode was close to the shaft frequency at this speed.

M. M. Bright, H. K. Qammer, H. J. Weigl and J. D. Paduano (1997)

Motivated by the focus on the spike type of stall inception, Bright and co-workers sought a new precursor detection scheme, one which could detect linear as well as non-linear flow phenomena [5]. They based the method on concepts from chaos theory. The fundamental assumption made by this group of researchers was that complex, chaotic events influence the pre-stall regime. They sought to identify the underlying structure of any such events and relate the changes in this structure to impending stall. Bright et al. used four different configurations in their experiments. Two of the configurations consisted of rotors alone, while the other two were single stage compressors. They benchmarked the new method by comparing it to the traveling wave energy (TWE) method, as applied to the data from the four configurations. They found reasonable lead times of stall warning for three of the four cases when the TWE method was used. To quantify the non-linear changes in the structure of chaotic events, Bright et al. used the correlation integral, a standard measure in chaos theory. According to them, an increase in this measure signifies an increase in the complexity of the events and vice-versa.

By applying the new method to pressure data from the same four configurations, Bright et al. showed that the correlation integral decreased as the compressors were throttled into stall. This result showed that the pressure signal became less chaotic as the stall inception point was approached. By thresholding the measure, in a manner analogous to the TWE method, they were able to obtain advanced stall warning for all the four cases. Bright et al. pointed out that longer warning times were obtained via the correlation integral approach,

relative to the TWE method.

Continuing the comparison to the TWE method, Bright et al. mentioned that the correlation integral was not implemented in a real-time friendly form. However, they said, that the need to use a single transducer, as opposed to a circumferential array required by TWE, was a considerable advantage. In general, Bright et al. considered the correlation integral method to be a complimentary approach to the traveling wave energy.

J.V.R. Prasad, A. Krichene and Y. Neumeier (2000)

Another approach to precursor based stall control was demonstrated by Prasad et al. on a centrifugal compressor [37]. They analyzed pressure measurements from a single sensor located at the compressor inlet with a real-time observer. This observer was used to identify the frequency and magnitude of the dominant wave in any given signal. Prasad et al. verified the observer's performance with off-line Fourier analysis of open-loop test data. They implemented a fuzzy logic based controller to transform the identified frequency and amplitude into a control command. Using this controller, Prasad and co-workers showed that both surge avoidance and surge recovery can be achieved in a precursor based scheme.

Prasad et al. found that the frequency of the precursor waves was a function of compressor RPM. However, they demonstrated that the controller tuned for one speed successfully stabilized the system with compressor operating at a different speed. Thus they concluded that the controller was robust to uncertainties. Significantly, Prasad et al. used two actuation schemes, a bleed valve or throttle actuation, and fuel flow modulation. They showed that either method could be used for stall control. They emphasized that fuel flow actuation was better suited for application in an engine, as the reduction in fuel flow reduced the temperature and consequently would reduce the risk of component damage.

1.3 Objectives

A review of available literature highlights numerous efforts in the active control of compressor. However, researchers have been unable to transition these past efforts to production engines. This can be attributed to limitations of the compressor instability models, dependence on high bandwidth actuators or new actuation mechanisms, and above all, a lack of

clear demonstration of system level benefits. In this light, the objectives of this work have been defined as:

- Develop a practical approach to active compressor control with an emphasis on system level benefits. In particular, the approach should not require improvements in actuator technology and, in fact, should only use existing actuation mechanisms routinely employed on production engines.
- Develop a method to detect compressor stability limits with a focus on real-time implementation.
- Demonstrate the universality of any new methods developed via application to different axial compressors.
- Develop a simulation framework to aid in the design and development of controllers for the new approach. This framework can also be used for quick evaluations of the overall methodology.

1.4 Summary

In terms of overall compressor stall research, the survey presented is by no means exhaustive. The aim has been to present a broad mix of experimental and analytical efforts representative of compressor stall control. Besides this, a plethora of work has been performed using computational methods. It spans all aspects of compressor rotating stall, e.g. Hoying et al. [25] used CFD to study the role of blade passage structures on stall inception, Stein et al. [39] studied compressor control using air injection, and Inoue et al. [28] investigated install flow field. As the computational techniques mature, they become a good complement to experimental and analytical methods, providing tools to design and develop advanced gas turbines.

CHAPTER II

COMPRESSOR CONTROL: PHILOSOPHY AND STRATEGY

A review of available literature, presented in Chapter 1, highlighted the limitations of model-based compressor stability control. The existence of alternate routes to stall, not predicted by current compressor models, nullify any potential advantage such schemes may offer. A precursor based approach, provided it captures the different stall inception mechanisms and yields sufficient warning time, is superior in this respect. There exists a fundamental question regarding the goals of compressor control. Should control strive to reconcile the design point and the peak performance point? To answer this question, it is necessary to understand the reasons behind establishing the design point at a pressure ratio lower than the peak value. It should be emphasized that aerodynamic instabilities alone are not responsible for this gap. One of the goals of compressor design is to attain high efficiency at the design point. In general, any performance gain accompanied by reduction in design point efficiency is detrimental from a systems perspective. After all the design point of a system is where it is expected to operate for the majority of its lifetime. The peak pressure point of a compressor, with high blade loading, is associated with higher losses. It follows that efficiency considerations make it undesirable to situate the design point of a compressor at its peak pressure ratio.

Another aspect is the operating line excursions that are fundamental to transient operations. The sheer act of engine acceleration requires additional pressure rise capability, over and above that delivered in steady state operation for a given compressor speed.

In order to be successful, any approach to compressor control should be cognizant of the overall system requirements. It is necessary that improvements at the compressor level are translated into engine or vehicle level benefits. A series of observations play an important role in defining the current approach. As outlined above, the compressor design point should

not be its peak pressure point. There are uncertainties associated with the point of stall onset, or equivalently surge line. A part of these uncertainties, for example introduced by phenomena like inlet distortions, cannot be eliminated *a* priori. Open-loop avoidance control currently employed, is based on worst case scenarios. This introduces conservatism in the stall margin requirements at the operating line. The idea central to the current approach can be stated as follows: Stall margin requirements can be reduced by reducing the uncertainties associated with the stall line. The open-loop controller is designed with worst case scenarios, which leaves extra stall margin, neither needed nor utilized for majority of operating lifetime. Active monitoring of available margin can either translate this back to reduced stall margin requirements, or into improved engine performance.

To ensure that potential benefits are not lost due to additional actuators and/or complexity, the current approach proposes to utilize control systems and actuators routinely utilized on engines today. In particular, actuation is limited to fuel flow rate, compressor variable geometry and mass flow bleeding.

This chapter starts with an overview of the different tools utilized as part of the current investigation on compressor stability management. These tools include experimental as well as simulation techniques. The experimental facilities have been used to develop a method for real-time detection of compressor stability limits. As a motivation, a simulation study has been used to highlight the benefits of active stability management. The results show that engine dynamic response can be improved by this approach, without the use of compressor stability extension. The chapter concludes with a discussion of the relationship between stall margin requirements and compressor efficiency.

2.1 Experimental Facilities

Different aspects of the current approach to compressor control have been developed using three compressor rigs. While two of the rigs are low speed facilities, the third is an advanced high speed facility which emulates a production engine. As there are two configurations of the high speed compressor, a total of four compressors have been analyzed. Closed loop control has been demonstrated on a low speed rig, the GTAxial facility. A brief description

of these facilities is given below.

2.1.1 GTAxial Rig

The axial compressor rig located in the School of Aerospace Engineering at Georgia Institute of Technology has been established to facilitate control-oriented studies in surge and rotating stall. It includes an inlet duct, a single-stage axial fan, a compressor discharge duct, a plenum, exhaust duct and a throttle. The low speed single-stage fan delivers a pressure ratio of about 1.035. It has fourteen blades on the rotor and eleven blades on the stator. The design speed is about 11800 RPM at which the tip Mach number is about 0.3. The plenum is a large metal chamber, capable of withstanding pressures up to 400psi. It incorporates a self-entraining burner and is thus capable of simulating a combustor. The compressor load is varied by a butterfly valve downstream of the plenum. The compressor used is known to have a very abrupt characteristic near the stall inception point. The compressor is instrumented using six high bandwidth pressure sensors. The sensors are mounted flush to the inside of the compressor casing in order to maintain a large overall bandwidth. Significantly, all the measurements obtained as part of the present work are from a single sensor. Further details regarding this facility are available in Appendix A.

2.1.2 Low Speed Research Compressor (LSRC)

The LSRC is a GE experimental facility that duplicates the relevant aerodynamic features of axial flow compressors in modern gas turbine engines in a large, low-speed machine where very detailed investigations of the flow can be made. Aerodynamic similarity for Mach number and Reynolds number is used in scaling the high speed airfoils to their low speed counterparts. This method of testing has proven reliable for over fifty years in understanding and designing HP compression systems provided the phenomena being studied are Reynolds number dependent and not compressibility dependent.

The LSRC, which has a constant casing diameter of 1.524 m (60.0 in), was set up with four identical stages in order to simulate the repeating stage environment. The data analyzed here is from the fourth stage. The configuration used is typical of modern engines and has a high hub/tip ratio of 0.85 with low aspect-ratio, high-solidity blading and shrouded

stators. The compressor is a low-speed aerodynamic model of the middle block of highly loaded, high reaction HP compressor in commercial gas turbine engines currently in service. Additional information about the LSRC testing technique and the blading is available in Storace et al.[41].

2.1.3 High Speed Compressor: Build-A and Build-B

The High Speed Compressor (HSC) is a six-stage technology development compressor with high stage loading, higher than that currently found in commercial aircraft engines. The blading designs employed the latest three-dimensional aerodynamics, including forward swept rotors and bowed and swept stators. The compressor rig employs several features designed to model engine environment. These include a settling chamber to model the goose-neck between low pressure and high pressure spools, and a volume downstream of the compressor that models a combustor and emulates the surge dynamics of a production environment. A distortion screen at the inlet generates the pressure-only equivalent of pressure and temperature distortions due to typical low-pressure compressors. Finally, appropriate amount of mass is bled to account for customer as well as turbine cooling bleeds, a part of the production environment.

Data have been acquired on two configurations of HSC. The configurations utilize different blade designs for some of the stages. Moreover they also differ in the stage loading distribution. In current context, the configurations can be considered as two different compressors, and are designated as HSC-A and HSC-B.

2.1.4 Data overview

In all four cases, data consists of pressure signals from sensors mounted on the compressor casing, located over the rotor. As much as possible, the sensors are flush to the interior of the casing wall, to minimize the cavity and maximize available pressure sensing bandwidth. Moreover, the pressure sensors are high bandwidth, fast response sensors manufactured by Kulite Inc.

Between the four compressors, the available data encompass a range of parameters. Unless otherwise specified, each set consists of pressure data acquired under steady operating

Table 1: A summary of available data and associated parameters.

	GTAxial Rig	LSRC Rig	HSC-A	HSC-B
Compressor RPM (%)	90, 95, 100	88, 94, 100	92, 97, 100	92, 97, 100
Sensor Location	Mid-Chord	Multiple	Multiple	Mid-Chord
Stages	Single	4^{rth} only	1,2,3	2^{nd} only
Repeat runs	Yes	No	No	No

conditions, with each run characterized by its stall margin. The different parameters are summarized in Table 1. Data corresponding to three compressor speeds is available on each rig. For GTAxial Rig as well as HSC-B, pressure signals from a single sensor over the rotor are available. In both cases, this sensor is located near the rotor mid-chord. On the other hand, data from multiple sensor locations on LSRC and HSC-A are available. Each sensor location is identified by its axial distance from the rotor tip leading edge. This distance is normalized with respect to the axial projection of the rotor tip chord. In particular 0% chord signifies a location over the rotor tip leading edge, 100% chord the corresponding trailing edge, and negative values signify locations in front of the leading edge. This nomenclature is used without qualification hereafter. Data for multiple stages are available for HSC-A tests. Finally, experiments on the GTAxial Rig have been conducted multiple times on different days.

2.2 Engine Simulation

A digital simulation has been used to complement the experimental facilities. The simulation incorporates various aspects of a gas turbine engine, including engine dynamics, sensor dynamics, and the engine control system. Consequently, it can provide a realistic test bed to evaluate ideas and demonstrate the advantages of active stability management. It simulates a turbo-shaft engine and has been developed on the basis of a component-type model of the T700-GE-700 engine. A variant of this engine has been deployed on the Sikorsky Black-Hawk utility helicopter. The component model is described in detail by Ballin [3]. Ballin has used it for real-time simulation studies conducted in the cited work. The model has been slightly extended, and some of the simplifications originally made have been dropped.

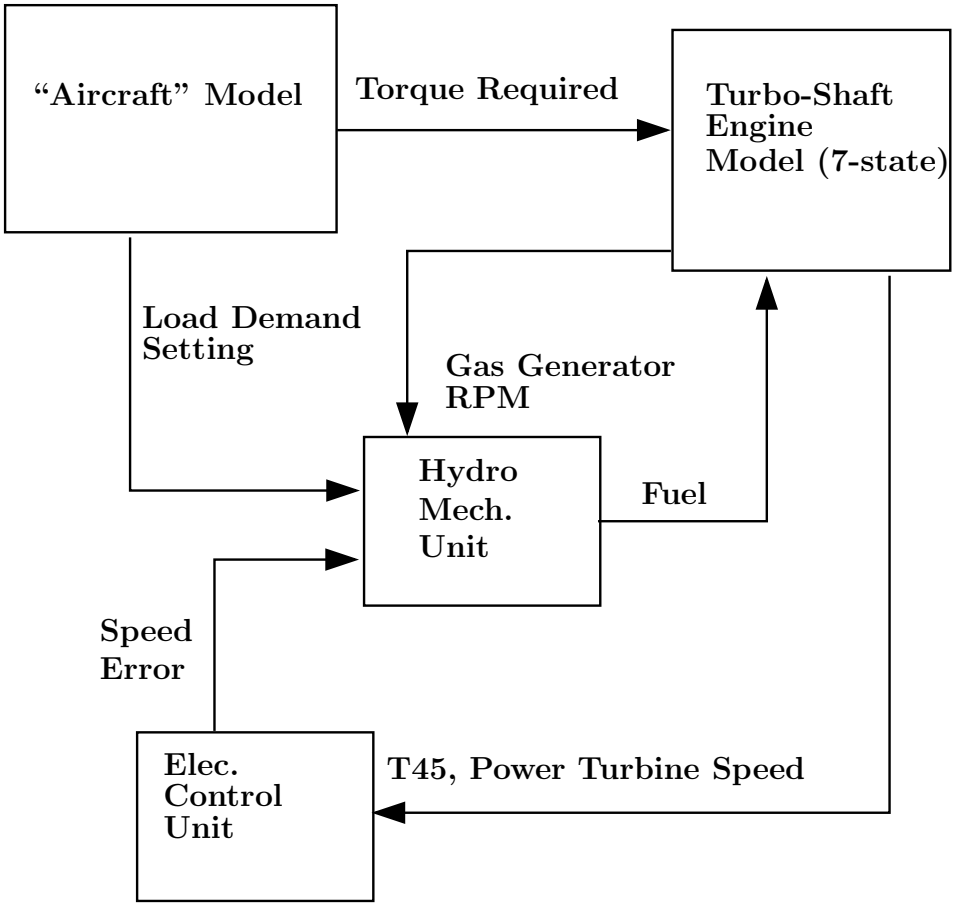

Figure 2: A block diagram representation of turbo-shaft engine simulation.

Following a brief overview, only the pertinent differences between the original model, hereafter referred to as the Ballin model, and the current implementation are described here. The complete details of the engine model are available in Ref.[3].

The simulation essentially consists of a seven state engine model and the fuel control system.

The engine consists of a five stage axial and a single stage centrifugal flow compressor, a flow-through annular combustion chamber, a two stage axial flow gas turbine, and a two stage independent power turbine. The mathematical model is a component-type, with four major components separated by fluid mixing volumes, each of which is associated with flow passages within the engine where thermodynamic states are quantifiable. States of gas in each control volume are expressed in terms of pressure, temperature, and mass flow, which are determined as functions of energy transfer across each component. Dynamics of rotating

components are modeled by relating changes of angular rotation of a given component to applied torque on the component. Inputs consist of ambient temperature and pressure at the inlet, pressure at the exhaust, fuel flow, and load torque. The seven-degree-of-freedom model, which is used here, is of the following form:

$$\dot{N_p} = f_1(N_p, N_g, T_{41}, P_3, P_{41}, P_{45}, P_{amb}, T_2, Q_{dmd}) \tag{1}$$

$$\dot{N_g} = f_2(N_g, T_{41}, P_3, P_{41}, P_{45}, P_2, T_2) \tag{2}$$

$$\dot{T_{41}} = f_3(N_g, T_{41}, P_3, P_{41}, P_2, T_2, W_f) \tag{3}$$

$$\dot{Wa_2} = f_4(N_g, P_3, P_2, T_2) \tag{4}$$

$$\dot{P_3} = f_5(N_g, Wa_2, P_3, P_{41}, P_2, T_2) \tag{5}$$

$$\dot{P_{41}} = f_6(T_41, P_3, P_{41}, P_2, T_2, W_f) \tag{6}$$

$$\dot{P_{45}} = f_7(N_g, T_{41}, P_3, P_{41}, P_{45}, P_{amb}, P_2, T_2) \tag{7}$$

where T_2, P_2 are determined using ambient conditions. The control input is fuel flow W_f and the output is power turbine speed N_p.

As depicted in Figure 2, the fuel control system further consists of a hydro-mechanical unit (HMU) and an electrical control unit (ECU). The "aircraft" model is simply a prescribed torque demand profile along with an appropriate load demand spindle setting. The load demand spindle (LDS) input is a function of pilot collective setting and provides a feed-forward collective compensation to improve transient response. The HMU is responsible for acceleration limiting, stall and flameout protection, gas generator speed (NG) control, and rapid response to power demand. The ECU trims the rotor speed within acceptable limits, while also providing over-temperature protection. The controller parameters are multivariate functions of the engine operating conditions and they are fine-tuned based on a trade-off between controller complexity and performance.

In order to enable closed-loop compressor stability management simulations, the fuel control system has been slightly modified. The ability to modulate the fuel flow rate has been incorporated as a multiplicative factor, and significantly, is applied at the input of the fuel metering valve. The model for the fuel metering valve contains a pure time delay, which accounts for the fuel transport phenomena. Thus, the additional control actuation

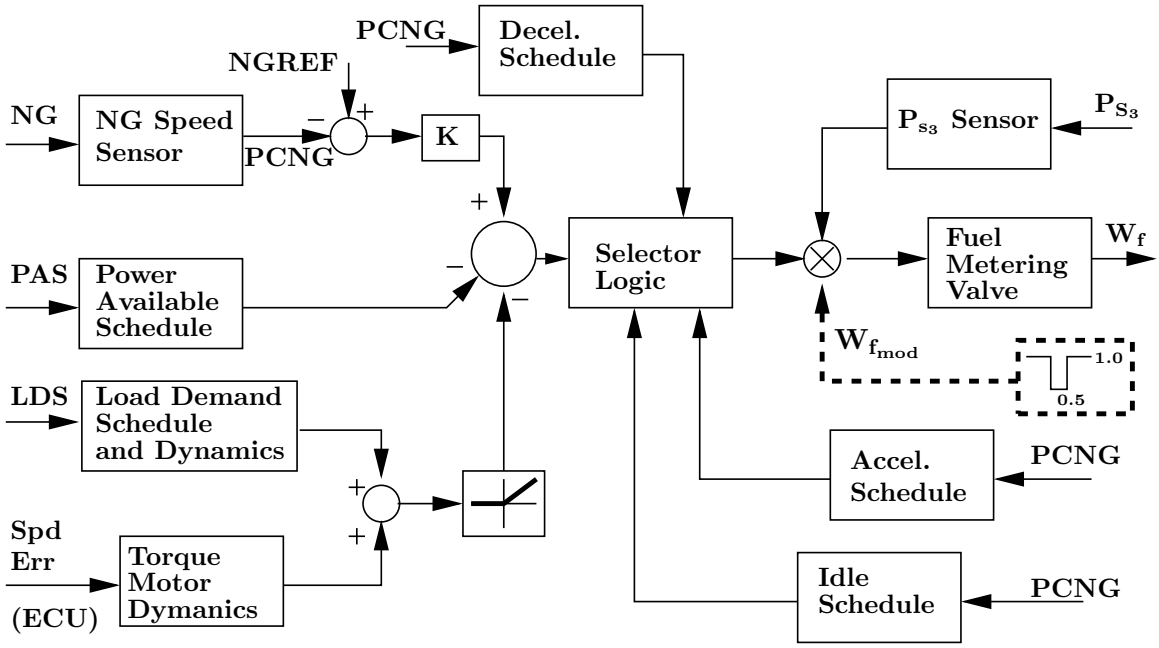

Figure 3: A schematic of the hydro-mechanical unit, adapted from Ballin [3]. The illustration also shows the interface to the electrical control unit and the limit avoidance controller ($\mathbf{W_{f_{mod}}}$).

is still subject to these transport phenomena. The additional block can be identified by its dashed outline in Figure 3.

The objectives of the current work are different from that of Ballin [3]. The original work was geared towards a real-time, pilot-in-the loop simulation. In the interests of simulation performance, the Ballin implementation used a quasi-steady representation of certain dynamic states, based on the *volume dynamics approximation*. As part of this approximation, it is assumed that pressures and mass flows within mixing volumes are always in equilibrium. The current work, on the contrary, aims to capture the transient response of the engine in as much detail as possible. Moreover, as the present work does not require a real-time solution of the simulation, the quasi-steady assumptions have been discarded. The dynamic states are thus not neglected, and the respective non-linear governing equations are used. A variable step Runge-Kutta solver is used to solve the resulting system of ordinary differential equations.

The second modification concerns the lack of mass-flow dynamics in the Ballin model. If mass-flow dynamics are absent, the solution cannot exhibit surge oscillations, even when

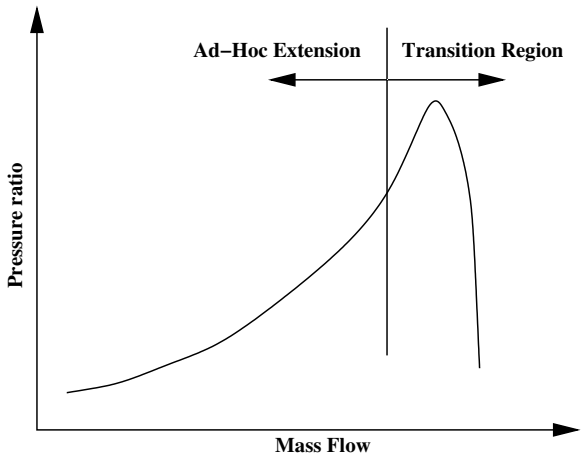

Figure 4: Compressor characteristic extension. A parabolic law is used for the transition region.

the operating point is in the unstable region. Consequently, mass flow dynamics have now been included in the model. These are based on assumptions similar to the Greitzer model of surge in compression systems [22]. In particular, it is assumed that the flow through the compressor is incompressible, and that all compressibility is restricted to the plenum.

Moreover, in the absence of mass-flow dynamics, the Ballin model had no need to include the compressor characteristics beyond the surge line. To make the simulation surge-capable, the compressor characteristics have to be extended beyond the surge line. This extension is accomplished in two zones. The transition zone, illustrated in Figure 4, is the part of compressor characteristic immediately to the left of the peak-pressure point. A reasonable approximation for this zone is critical to current goals. For a given engine transient which brings the compressor operating point to its surge line, the nature of the transition zone determines whether or not surge will occur. To obtain results that reflect reality, this extension has been based on known behavior of stage characteristics. The parabolic nature of the stage characteristics was tempered slightly to account for a mix of stalled and unstalled stages. Beyond the transition region, the characteristics have been extended in an ad-hoc manner. The only goal of this part is to avoid introduction of any numerical artifacts.

It follows that the simulation is expected to be correct only up to surge cycle initiation. It is unlikely to accurately capture the engine dynamics while in surge, may exhibit a single

surge cycle instead of multiple, and generally not applicable for surge recovery investigations. It is, however, considered to be sufficient for surge avoidance studies, which is the goal of this work.

2.3 Stability Management and Engine Operability

The engine simulation can be used to illustrate system level benefits of compressor stability management. In particular, it has been used to demonstrate the improvements in engine dynamic response. As the simulation models a turbo-shaft engine, requirements are expressed in terms of shaft power. The response of the engine to a step command in torque has been analyzed, with and without active stability management. The results of this case study show that while both passive and active management can keep the engine safe, active management allows for an improved dynamic response. Similar studies can be performed using turbo-fan or turbo-jet engines, with engine thrust as the commanded parameter. For this study, it is assumed that a detection algorithm accurately provides an early stall warning at a selected stability margin. Such an algorithm, which has been implemented under real-time constraints, has been developed as part of this work. Moreover, control actuation is performed using mechanisms routinely available on production engines. No improvements to available actuator technology have been assumed.

2.3.1 Passive Management

A helicopter rotor is designed to be run over a narrow range of RPM for its entire operational regime. For the rotor RPM to remain nearly constant, any variation in aerodynamic loads has to be matched by the engine. The aerodynamic torque loading is a function of flight conditions and pilot controls. If an increase in torque required, e.g. due to increased collective, is not met by the engine, the rotor RPM would go down. This decrease is often referred to as the RPM droop. The transient performance of a helicopter propulsion system can thus be benchmarked in terms of its ability to minimize RPM droop.

The conventional stall prevention during acceleration transients, takes the form of a scheduler. This acceleration scheduler, restricts the maximum allowable fuel flow, as a predetermined function of the compressor state and its inlet conditions. In order to illustrate

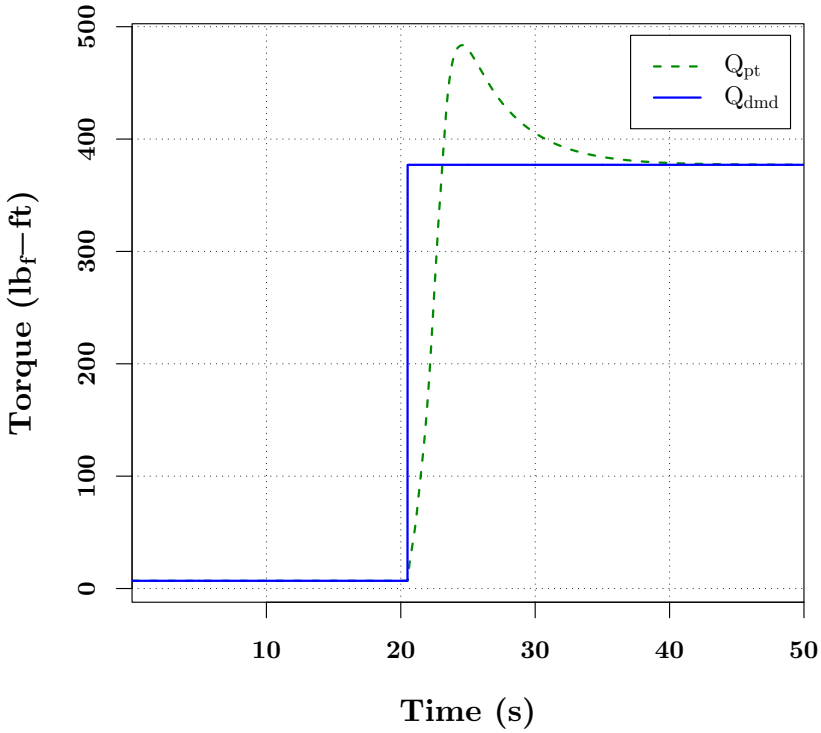

Figure 5: Variations of demanded and available torque with time for the nominal case.

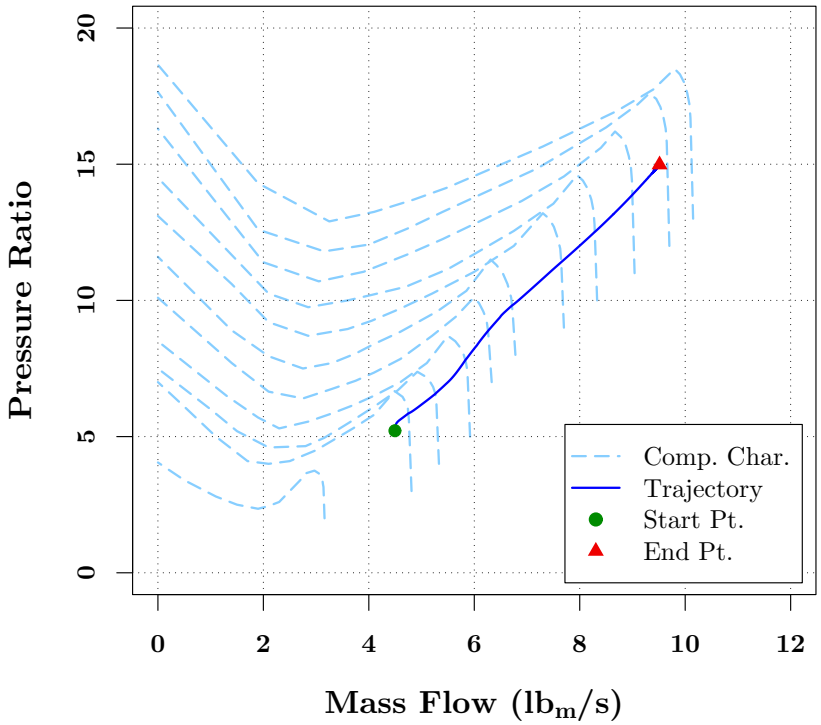

Figure 6: The trajectory for the nominal engine with acceleration scheduler (nominal case).

the impact of the acceleration scheduler, and implicitly compressor stall, on engine transient response, the autorotation recovery maneuver has been analyzed. This specific case has been chosen to illustrate both the need for the scheduler and the increased performance for the ideal case when it is bypassed. The maneuver involves a stop-to-stop step command in collective, switching it from the lower to the upper stop. This collective command translates to a step change in the torque demanded from the engine. The response of the nominal engine along with the torque demanded are graphed in Figure 5. The corresponding variations in compressor pressure ratio and inlet mass flow rate are shown as a trajectory plot superimposed on the compressor map in Figure 6. As expected, the acceleration scheduler protects the system from surge. This protection, however, comes at the cost of a significant droop in power turbine RPM, and in turn a large droop in the rotor RPM, as seen in Figure 7 (nominal case). This RPM droop is attributed to the lag in the engine torque response. The undesirable consequences of the RPM droop are two fold. The loss in rotor RPM means a loss of thrust, which is especially undesirable given the requirements of the maneuver. Moreover, the loss of main rotor RPM is also accompanied by a proportional loss in tail rotor RPM. This reduces the pilot's rudder authority, sometimes leading to the incorrect inference of a tail rotor failure. Together, or even individually, these factors seriously impact the safety of flight.

If the acceleration scheduler is bypassed, there is a significant reduction in the RPM droop for the same pilot command. This can be seen in Figure 7, which compares the power turbine RPM for the two cases. Moreover, due to a sufficient available surge margin, the compressor remains free of surge for the entire transient, as seen in Figure 8.

The results so far show an incomplete picture. This dramatic gain in engine performance is valid only for nominal inlet and compressor characteristics. Several factors, including inlet distortion, deterioration with age, and ambient conditions could degrade the compressor performance. To capture this deterioration, the compressor characteristics have been scaled down. The pressure-ratio at a given mass-flow rate and speed is multiplied by a factor of 0.94. This roughly reduces the surge margin for a given operating point by 7%. This degree of degradation is normal, and by no means exaggerated.

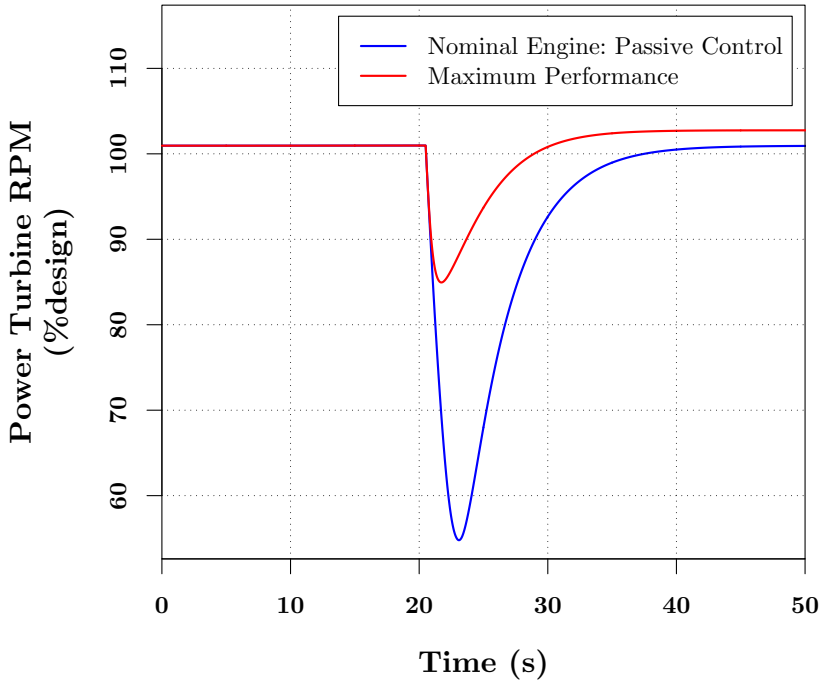

Figure 7: Power turbine RPM variation with time.

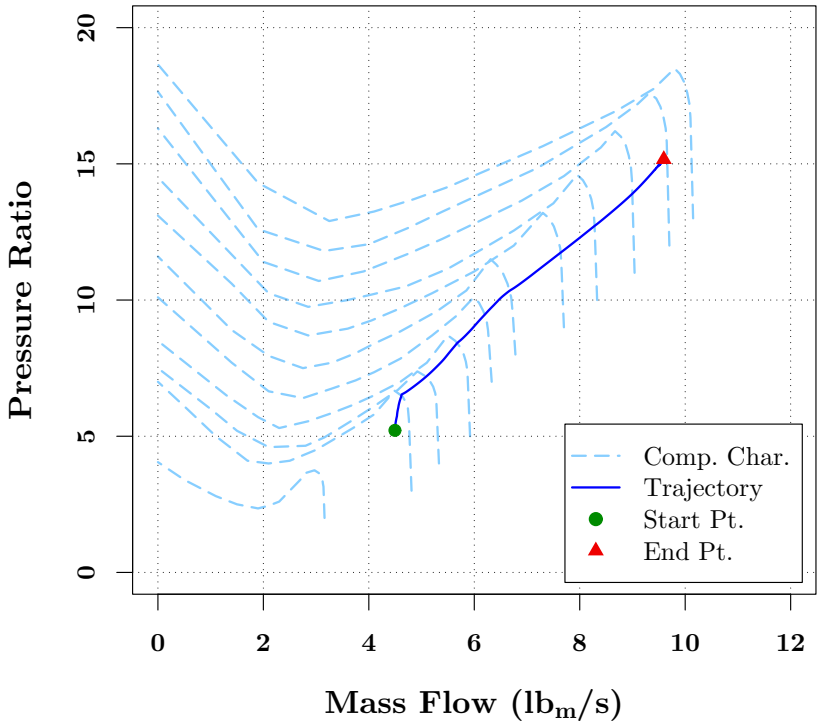

Figure 8: The trajectory for the nominal engine without acceleration scheduler.

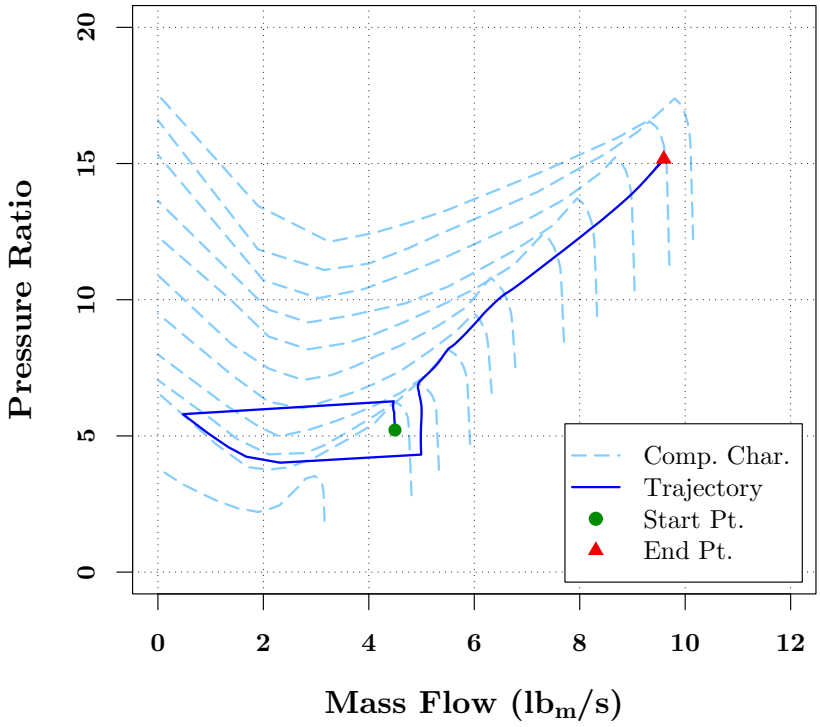

Figure 9: Trajectory for the degraded engine without acceleration scheduler.

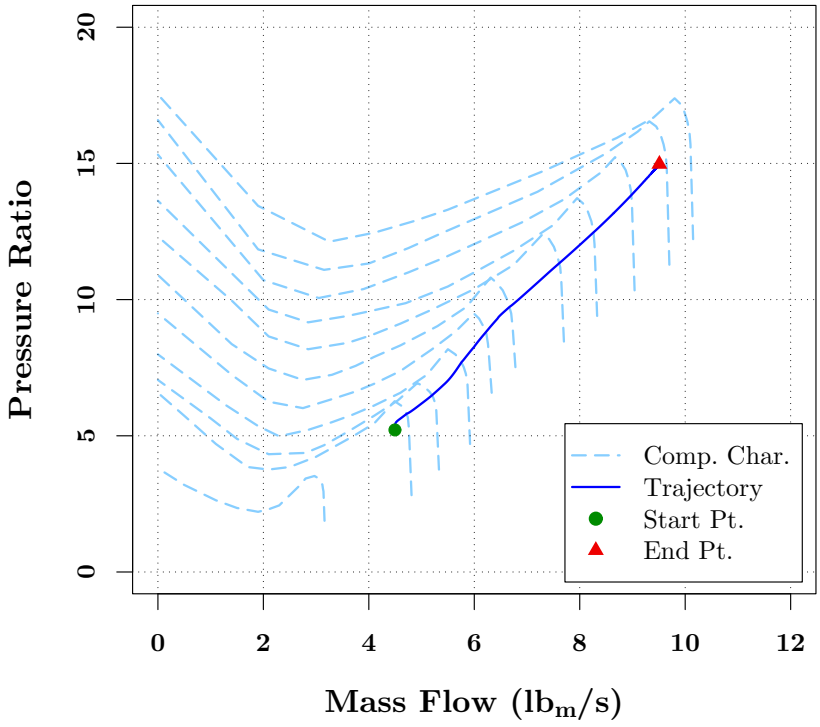

Figure 10: Trajectory for the degraded engine with acceleration scheduler.

If this slightly degraded engine is subjected to the same step change in torque demand, and the scheduler is bypassed, the compressor enters a surge cycle. This can be seen in Figure 9, where the trajectory is superimposed on the compressor map. On the other hand, when the acceleration scheduler is retained, as with the nominal engine, the degraded engine is free of any compressor instability for the duration of the transient (Figure 10). In fact, as seen in Figure 11, the degraded engine replicates the original performance.

Clearly some form of surge prevention is required as a part of the engine control system. A passive, predetermined scheduler severely impacts the engine transient response. An active stability management alternative is hence sought, which can save the engine during a degraded scenario, while improving its transient response.

2.3.2 Active Management via Fuel Modulation

As briefly discussed in the beginning of this section, the actuation mechanisms for this study are restricted to the pre-existing ones. There are three main possibilities: variable geometry of the compressor, bleed valve, and fuel actuation. As a first step, fuel modulation can be used to move the operating point on the compressor map. While the introduction of fuel modulation into a simulation can be done in various ways, the stress here is on practical implementation on a flight system. As the simulation contains a model for the fuel valve, along with the delay due to transportation in fuel lines, the additional fuel modulation is introduced prior to the fuel valve (Figure 3), ensuring realistic results.

Numerical experiments have been carried out to demonstrate the benefits of active compressor stability management. These experiments study the engine response to a step change in commanded torque, identical to the passive control scenerio detailed above, and use the deteriorated compressor map. In these experiments, a limit proximity alarm is generated whenever the stall margin falls below a preselected trigger value, SM_{trig}. As a response to each alarm, the limit avoidance control cuts back fuel. This is achieved via a fuel modulation pulse, $\mathbf{W_{f_{mod}}}$, as shown in Figure 3. The pulse is $10\,ms$ wide and, while active, cuts the fuel flow rate to half of that determined by the nominal fuel control system.

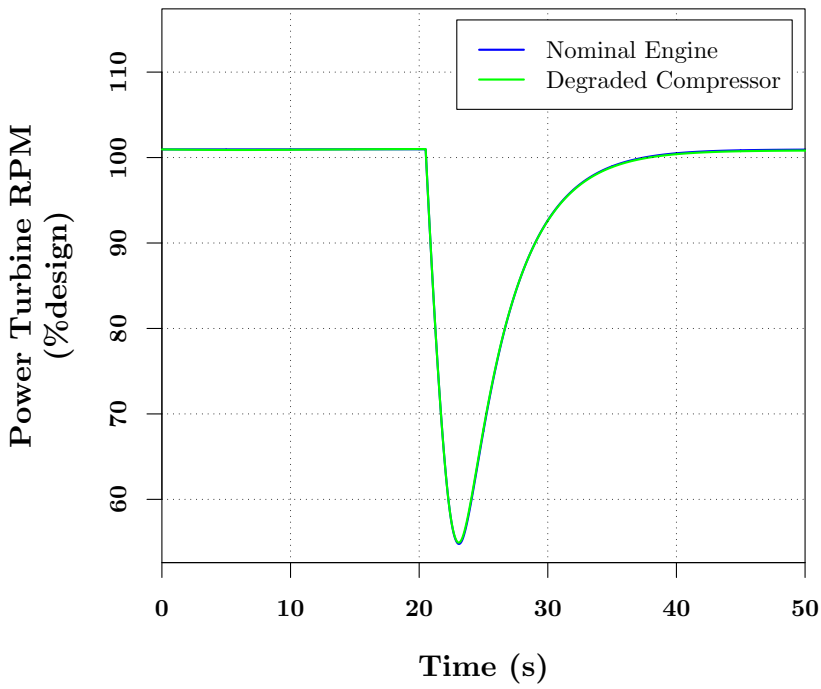

Figure 11: Comparison of the RPM response of the nominal and degraded engines with acceleration scheduler.

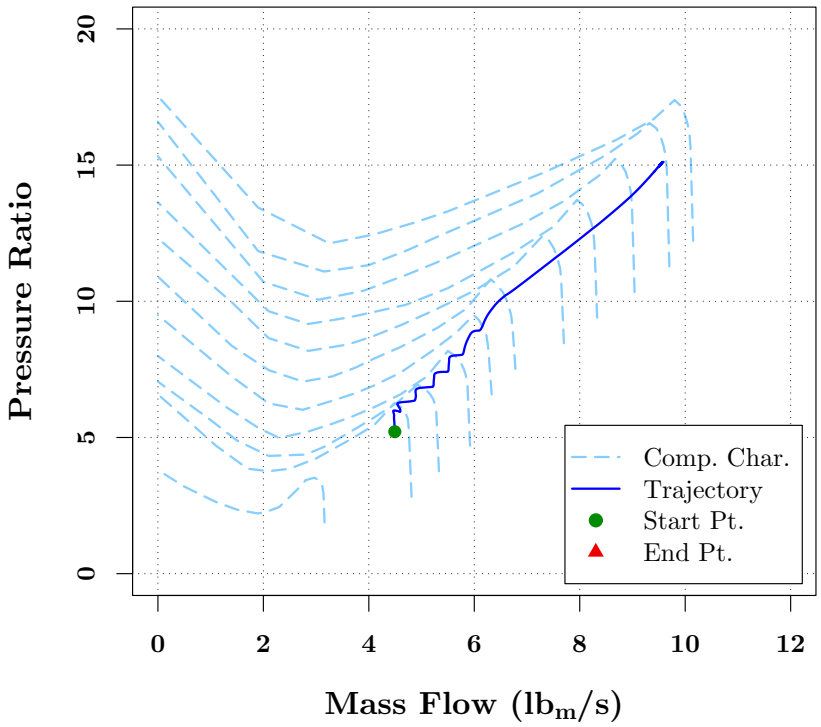

Figure 12: The trajectory for the degraded engine without acceleration scheduler, with active fuel modulation. $SM_{trig} = 3\%$.

The results for a particular numerical experiment are shown in Figure 12, where the pressure versus mass flow trace illustrates the effectiveness of this actuation. In this experiment, the preset trigger point was set at 3% surge margin. However, similar results were observed when SM_{trig} was varied from 1% to 6%. This yields some insight into the requirements of a stall margin estimator. In particular, as far as safety of operation is concerned, a continuous estimation of stall margin is not required. Although this study is conceptual in nature, the results indicate that even if a "stall-limit approaching warning" is obtained fairly close to the surge boundary, conventional actuation can keep the system inside the stable regime. Besides keeping the system safe, active margin management leads to an improvement in the transient response, as shown in Figure 13. It is important to note that the active stability management delivers a near maximal level of performance, even with a degraded compressor.

An inspection of Figure 12 shows small oscillations in the compressor trajectory. These oscillations are a direct consequence of the oscillations in the fuel flow rate, graphed in Figure 14, which arise due to the simplistic control laws used. The specific control law used cuts back fuel when stall margin is less than SM_{trig}, waits for $10\,ms$ then opens fuel back to its commanded value. This simple control law can easily lead to chattering of the actuator. This aspect of the result underscores the importance of an integrated, from the ground up, approach for controller design.

2.4 Compressor Efficiency Aspects

Another benefit of compressor stability management relates to compressor efficiency. If the peak compressor efficiency point does not nominally coincide with design point, active stability management can be used to raise the operating line. This would deliver peak efficiency at the design point, as suggested by Figure 1. However, with the current state of compressor design, it is very unlikely that the peak efficiency point does not lie on the operating line.

Stability management can however, still contribute to higher compressor efficiency. Some efficiency is traded off to satisfy the stall margin requirement as part of compressor design.

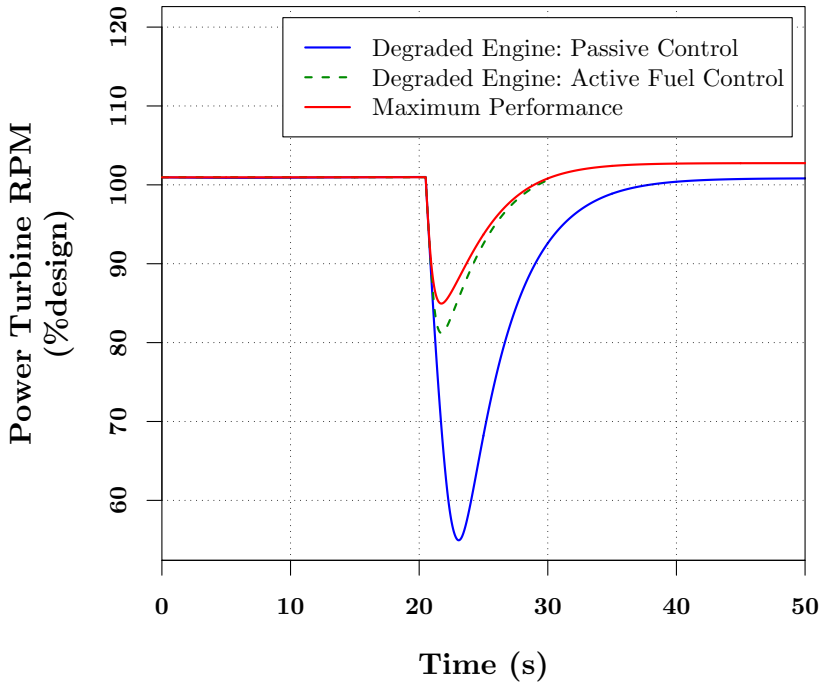

Figure 13: The comparison of RPM variations in the degraded engine between the acceleration scheduler and active fuel modulation for surge avoidance.

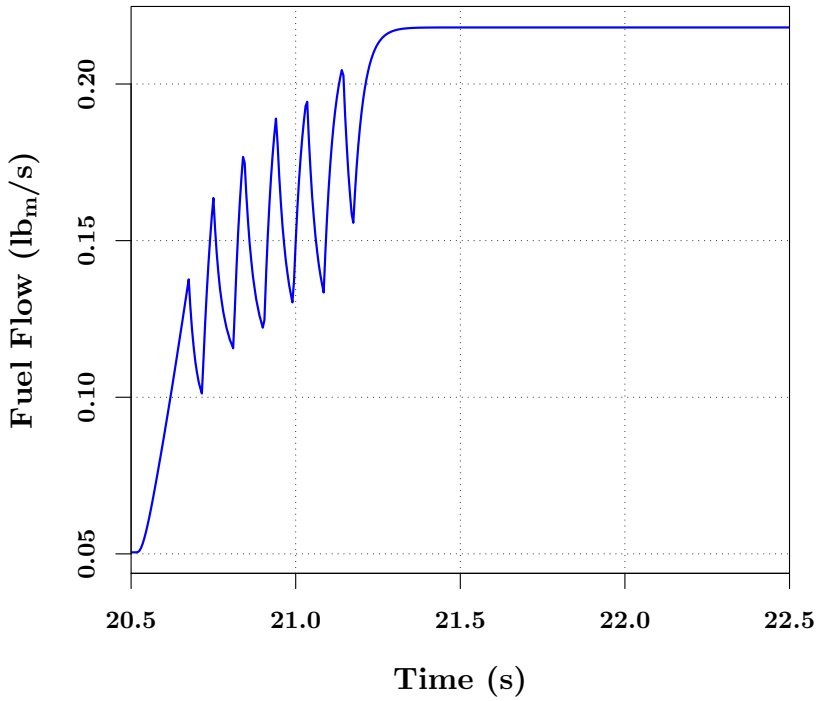

Figure 14: Fuel modulation for surge avoidance.

This trade-off is made via the choice of blade solidity and aspect ratio. As per Cumpsty [10], "The evidence suggests that for a good compressor near the design point, efficiency tends to be slightly lower if solidity is on the high side (and aspect ratio low) but the pressure rise and operating range are greater." Here, the operating range is defined as the ratio of the difference between the maximum and the minimum mass flow rate to its design value. Both pressure rise capability and operating range relate directly to stall margin by its very definition. The reduced stall margin requirement thus enables a higher peak efficiency, as well as a reduction in stage mass through a small reduction in solidity.

The benefit of increased solidity to operating range can be explained once it is realized that the limiting feature of the flow is the boundary layer on the end-walls and not blade loading. The increased chord length reduces the severity of the pressure gradient on the end-wall, which in turn delays end-wall boundary layer separation. Consequently the stalling mass flow rate is lowered. To see the increase in stalling pressure rise due to an increase in solidity, it is beneficial to use the straight diffuser analogy. The pressure ratio across diffuser passages is known to be related to its length-to-width ratio, the larger this ratio, the higher the pressure ratio that can be sustained prior to separation. The compressor solidity, defined as chord-to-pitch ratio is analogous to the length-to-width ratio of a diffuser passage. Thus it is not surprising that higher solidity allows for a higher stage loading prior to stall.

With regards to efficiency, solidity affects the compressor losses in a multitude of ways. For one, the loss production is an integral along the surface in flow direction, so for lower losses lower surface area is desirable. This at least unequivocally favors a low solidity and high aspect ratio. The situation gets compounded, however, when entropy generation is taken into account. The entropy generated in a surface boundary layer is proportional to the cube of velocity over the surface in question. Hence the decrease in losses with solidity is only valid as long as the surface velocity remains fixed. In practice, the reduction in solidity is accompanied by an increase in the suction surface velocity and thus increase in boundary layer losses. These contradicting contributions lead to an optimum value of solidity where the two are balanced.

Besides contributing to profile losses, solidity via the blade aspect ratio, also impacts the end-wall losses. The term end-wall losses encompasses contributions due to various inter-related factors. These include, entropy generation in end-wall boundary layer, entropy generation due to mixing, separation of end-wall flows, and the interaction of the tip leakage flows with the end-wall boundary layer. In general, all these sources of end-wall loss produce a loss coefficient inversely proportional to the blade aspect ratio.

The higher efficiency benefits for new designs can be achieved via any method of stall margin requirement reduction. However, as partly seen in the brief discussion of loss generation above, efficiency is very sensitive to changes in design parameters. The stability management approach outlined previously, has an inherent advantage that it does not alter the internal flow through the compressor. It is thus quite incapable of deteriorating efficiency.

To summarize, while the phenomena relating solidity, efficiency and stall margin are complex, a reduction in stall margin requirement can be translated into a lower solidity, which in turn would yield a larger peak compressor efficiency.

2.5 Summary

The philosophy followed here stresses compressor stability management over extension of its stable operating regime. It further emphasizes system level benefits of efficiency and performance. The strategy includes the development of a method for real-time compressor stability detection. This development, detailed in the following chapters, utilizes four compressors in three experimental facilities. The approach is demonstrated experimentally in a laboratory facility and evaluated for engine applications through a numerical simulation. It has also been demonstrated on a gas turbine engine at GE Aircraft Engines [8].

CHAPTER III

STABILITY LIMIT DETECTION

The success of compressor stability management is contingent upon the detection of stability boundary and the nature of such detection. In general, any method that waits for stall inception detection is unlikely to be successful in practice. Typically, the time scales involved in the growth of stall inception into fully developed stall are extremely short. This is especially true for modern high speed compressors, as evidenced earlier in the review of available literature. Consequently, it is very unlikely that reasonable control authority would keep a compressor free from instabilities, if such control is actuated at stall inception. The difficulties are further accentuated when transient engine operation is taken into consideration. Stall inception essentially signifies that the compressor stability boundary has been reached. If brought about by engine transients, the boundary is likely to be breached by the time stall inception is detected.

The expectation from a stability measure is that it should detect proximity to the compressor stability limit, before the limit is reached. A practically applicable detection method should quantify qualitative observations like, "boundary approaching", "near limit", and "limit breached". The last is for completeness, for it can be trivially achieved given the nature of compressor aerodynamic instabilities, and has little relevance for stability management. The previous chapter illustrated the benefits of compressor stability management to engine transient performance. Implicit in this illustration is an assumption that reliable limit detection was available to the engine controller. The current chapter documents the development of a measure that can be used for compressor stability limit detection. This measure was developed and first reported by Dhingra et al.[17] in 2003. It is essentially truncated auto-correlation and is hereafter called the correlation measure. Although this measure has been heuristically arrived at, its behavior can be related to the fundamental properties of unsteady flow over a compressor rotor. Statistical analysis of correlation

measure obtained on different compressors has been performed. The analysis reveals a consistent trend and the measure appears to be applicable to the compressors studied. This is followed by the development of a control oriented stochastic model, built around the correlation measure. The chapter concludes with the validation of this stochastic model and a discussion of its implications.

3.1 Correlation Measure

The correlation measure was motivated by the features observed in the signal from a pressure sensor located over the rotor. It is an attempt to quantify the proximity of compressor surge limit and fulfill the limit detection requirements of the stability management approach. The measure is defined on the basis of the repeatability of the pressure time-trace obtained with a sensor located over the rotor. This pressure signal is mostly periodic when the compressor is operating away from the surge line. However, as the boundary of stable operation is approached, the periodicity is progressively disrupted. This situation is illustrated via pressure signals obtained on the GTAxial Rig. A representative trace of the pressure signal with the compressor operating in a safe region, away from the stall line, is shown in Figure 15(a). As evident in the overlay on the right, the current pressure trace is very similar to one from the previous rotation. The turbulence present in the tip region ensures that the signals would not be exactly alike. Any measurement noise will also contribute to these differences. In contrast, when the compressor operates close to its stall boundary, the pressure traces are significantly different from one cycle to another. This can be observed in Figure 15(b) where, as before, traces from two consecutive cycles are overlaid.

The correlation measure, essentially a modified form of auto-correlation, quantifies any loss in periodicity. It is mathematically expressed as,

$$C(t) = \frac{\sum_{i=t-wnd}^{t} (P_i \cdot P_{i-shaft})}{\sqrt{\left(\sum_{i=t-wnd}^{t} P_i^2\right) \cdot \left(\sum_{i=t-wnd}^{t} P_{i-shaft}^2\right)}} \tag{8}$$

where,

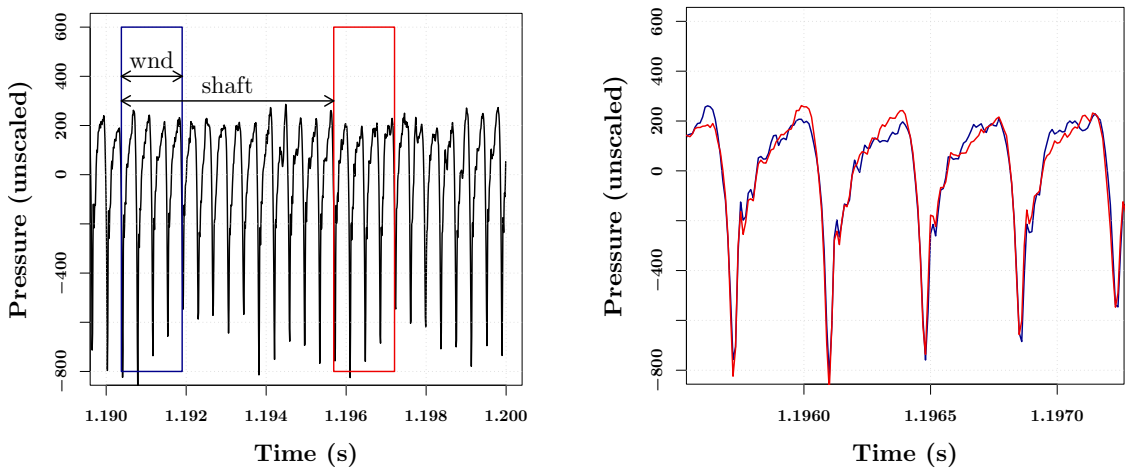

(a) Away from Stall

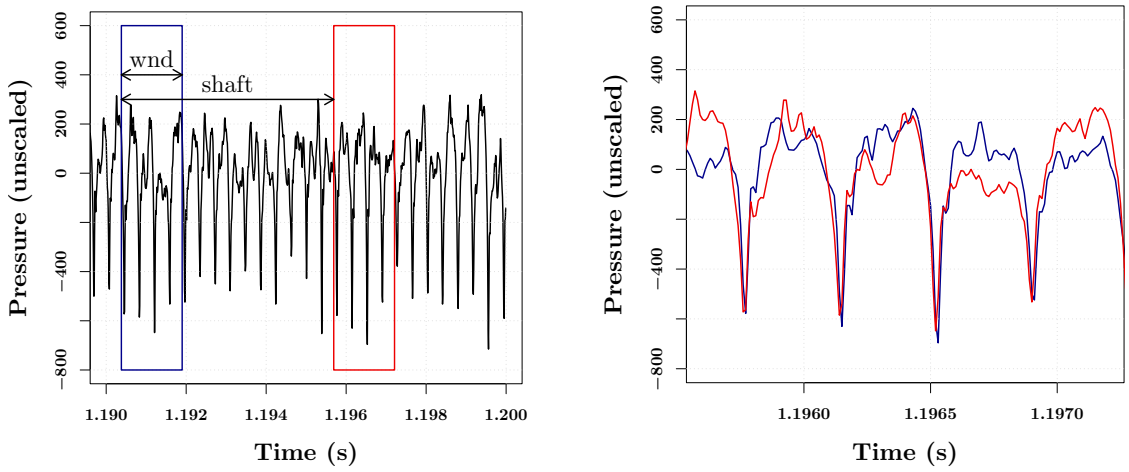

(b) Close to Stall

Figure 15: An illustration of the loss of periodicity

$C(t)$	Correlation Measure
P	Pressure signal
i	Index
$shaft$	Number of samples in one shaft revolution
t	Time, Current sample time
wnd	Correlation window size in number of samples

As per this definition, the size of the moving window, wnd, can take any value. While the number of samples in one shaft rotation forms a natural upper bound, one blade passage is a sensible lower bound. A wider window averages out the differences, yielding a smoother time evolution of the measure. However, more than necessary averaging could mask valuable information, which suggests that the window size should not be too large. Experience to date is that a value which spans 3 to 4 blade passages is a good choice. By its very mathematical definition, the magnitude of the correlation measure is bound by one, i.e. $C(t) \in [-1, 1]$. The negative values of the correlation imply that the two windows being correlated are "out of phase". Even when the compressor is operating close to its stability limit, there is relatively strong periodicity with blade passage, and negative values are not very likely. Further, a correlation with value 1 signifies perfectly repeating signal, and is not expected with real pressure data. Following these observations, the measure is usually contained in the interval from zero to one, i.e. $C(t) \in (0, 1)$, except when the compression system is operating with aerodynamic instabilities. Under the influence of instabilities, blade level flow field can be significantly distorted, and correlation measure can attain negative values.

3.1.1 Representative Properties

Prior to studying the different compressors through correlation measure, it may be beneficial to develop a basic understanding of correlation measure, and relate features observed in it back to the pressure signal. To this end, a raw pressure signal obtained on the GTAxial Rig along with its periodogram are presented in Figure 16. The dataset has been sampled at $100\,KHz$ with an anti-aliasing filter set at $30\,KHz$. Only a part of the dataset used to calculate the periodogram has been included in the figure. The fundamental frequency

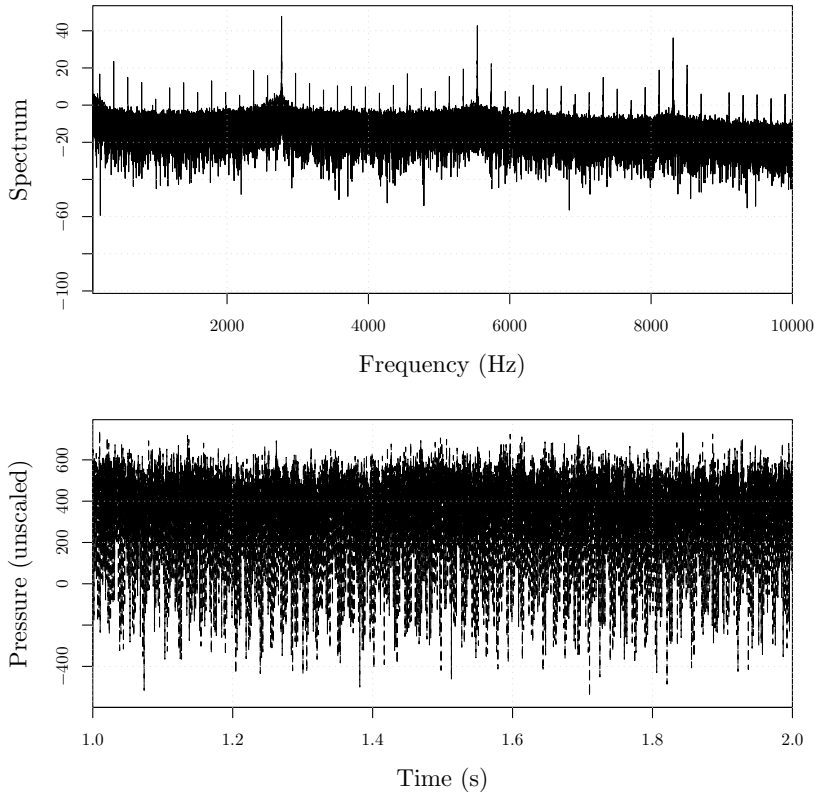

Figure 16: A representative pressure signal and its periodogram. This signal has been obtained on the GTAxial-Rig.

related to blade-passing is around $2.8\,KHz$. This is evident in the periodogram, which also shows higher harmonics present in the signal. Figure 17 contains the correlation measure calculated using this dataset and a periodogram of the calculated measure. The lack of any predominant periodicity and a relatively broad spectrum of the correlation measure are visible in this figure.

The lack of periodicity is in agreement with the time-trace of the correlation measure, where the intermittent drops in the measure lack an apparent pattern. As expected by its definition, these drops are due to distortions in the blade-passing periodicity. Figure 18 serves to emphasize this point. The upper chart shows two traces, both part of the same raw pressure data, where one is simply delayed by one shaft time-period. The lower chart shows the calculated correlation measure, synchronized with the nominal pressure data. The one-to-one correspondence between dips in the correlation measure and pressure distortion can be clearly observed in this figure. In particular, the dip between 1.076 and 1.078

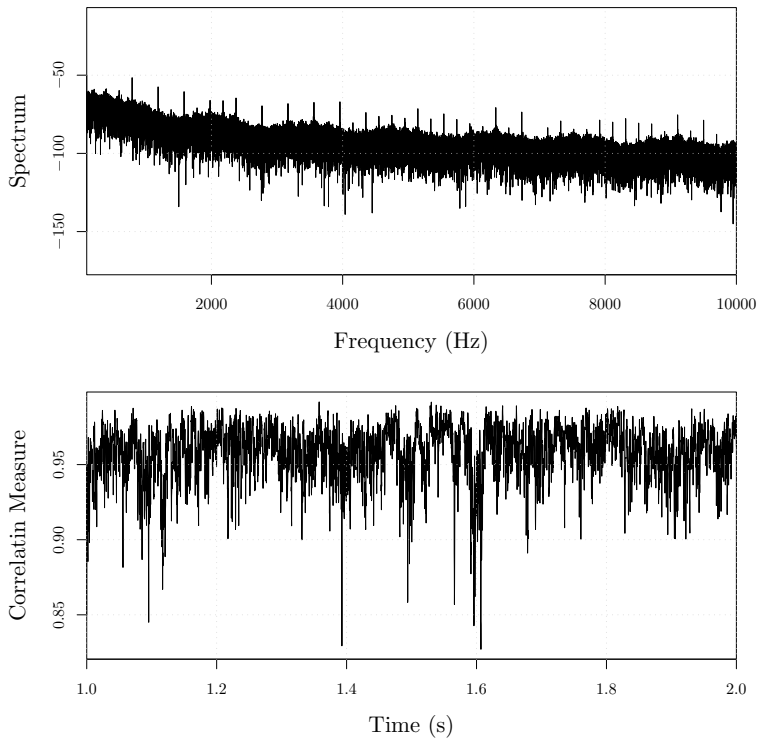

Figure 17: A representative correlation measure time-trace and its periodogram. The correlation measure has been calculated used data obtained on the GTAxial-Rig.

seconds corresponds to a somewhat larger difference in the two pressure traces. On the other hand the peak between 1.072 and 1.074 seconds is associated with higher similarity between the two traces in that region. It is important to realize that correlation measure, in its present form, captures differences in pressure over the same blade passage. Any passage to passage differences do not directly affect its value. This too can be observed in Figure 18 when the pressure, and corresponding correlation measure, at 1.070 and 1.072 are compared. However, the correlation measure would be affected if a particular passage is more susceptible to pressure distortions.

As noted above, the time evolution of the correlation measure drops sharply from time-to-time, where its value falls much lower than the average for the given case. These impulse-like drops do not significantly lower the average value of the measure because of their narrow width and integral nature of an average. Observations suggest that the importance of these dips is more than their contribution to the average value. While this will be expanded upon later, it is sufficient to state that analyzing compressor data in terms of average values will

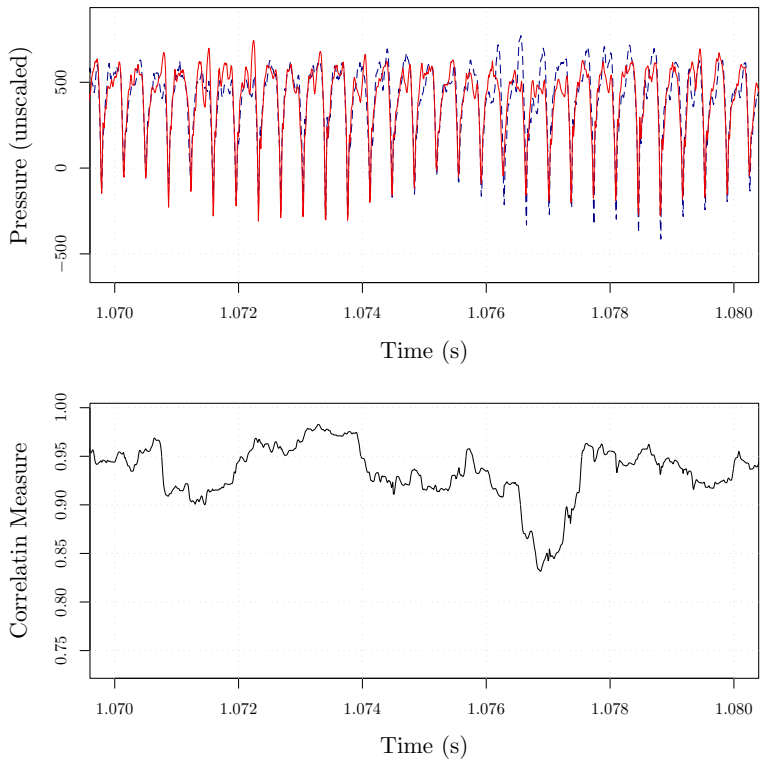

Figure 18: The drops in correlation measure quantify distortions in the pressure periodicity.

necessarily lead to loss of information. Consequently, the *distribution* of the correlation measure has been used to emphasize finer differences, and average as well as standard deviation have been used to show general trends.

3.1.2 Application to Experimental Data

Correlation measure technique has been applied to two low speed compressors and two builds of a high speed compressor. In the various cases, correlation measure has been found to decrease with decreasing stall margin. Recall that stall margin is a measure of the distance of a given operating point to the stall line. For these data the point of stall is known *ex post facto* and thus stall margin is in fact the true stall margin. One definition for stall margin is based on the compressor inlet mass-flow and overall pressure ratio across the compressor. This is expressed as,

$$SM = \left[1 - \frac{PR_{op} \cdot \dot{m}_{stall}}{PR_{stall} \cdot \dot{m}_{op}}\right] * 100 \tag{9}$$

where SM is the percentage stall margin, PR is the pressure ratio, $\dot{m}$ is the mass-flow rate, the subscript *stall* refers to the values at stall, and subscript *op* pertains to the values at the given operating point. However, the GTAxial facility is not equipped with a mass-flow sensor. A modified definition has been employed for data obtained on this facility, and is given by,

$$SM = \left[1 - \frac{PR_{op}}{PR_{stall}}\right] * 100 \tag{10}$$

where the symbols are as defined above. This difference is not significant as long as only qualitative comparisons are made across the different compressors. However, the compressors studied are so diverse, that this restriction is not as severe as it may appear initially.

A comprehensive picture of the behavior of average correlation measure is available in Figure 19, which shows its average value as a function of stall margin for the four cases. In all four cases, data has been acquired via pressure sensors located over the rotor blade row. In particular, the sensor is located at 54% chord along the axial direction on the third stage of HSC-A and at 81% chord on the fourth stage of LSRC for results presented in Figures 19(c) and 19(b) respectively.

In each case the average correlation measure decreases with stall margin. This is true for three different speeds analyzed in each case. In results from the GTAxial Rig, shown in Figure 19(a), the curves pertaining to the three speeds occupy a narrow band. On its own, this would suggest that the relationship between stall margin and correlation measure is relatively independent of the compressor speed. This is not well supported by the results from the other compressors. However, GTAxial Rig is the only single stage machine, the other three being multi-stage compressors. In multi-stage compressors the loading distribution usually varies with speed. The respective stages in these multi-stage compressors, for which data are available, may not be the most loaded stages at the speeds analyzed. Consequently, the difference in curves may not be attributed to changes in speed.

Analogous results for the standard deviation of the correlation measure are presented in Figure 20. In every case, standard deviation of the correlation measure increases when the stall margin is reduced. The standard deviation results mirror that of the average correlation measure. A comparison of Figures 19(b) and 20(b) shows that for LSRC, while

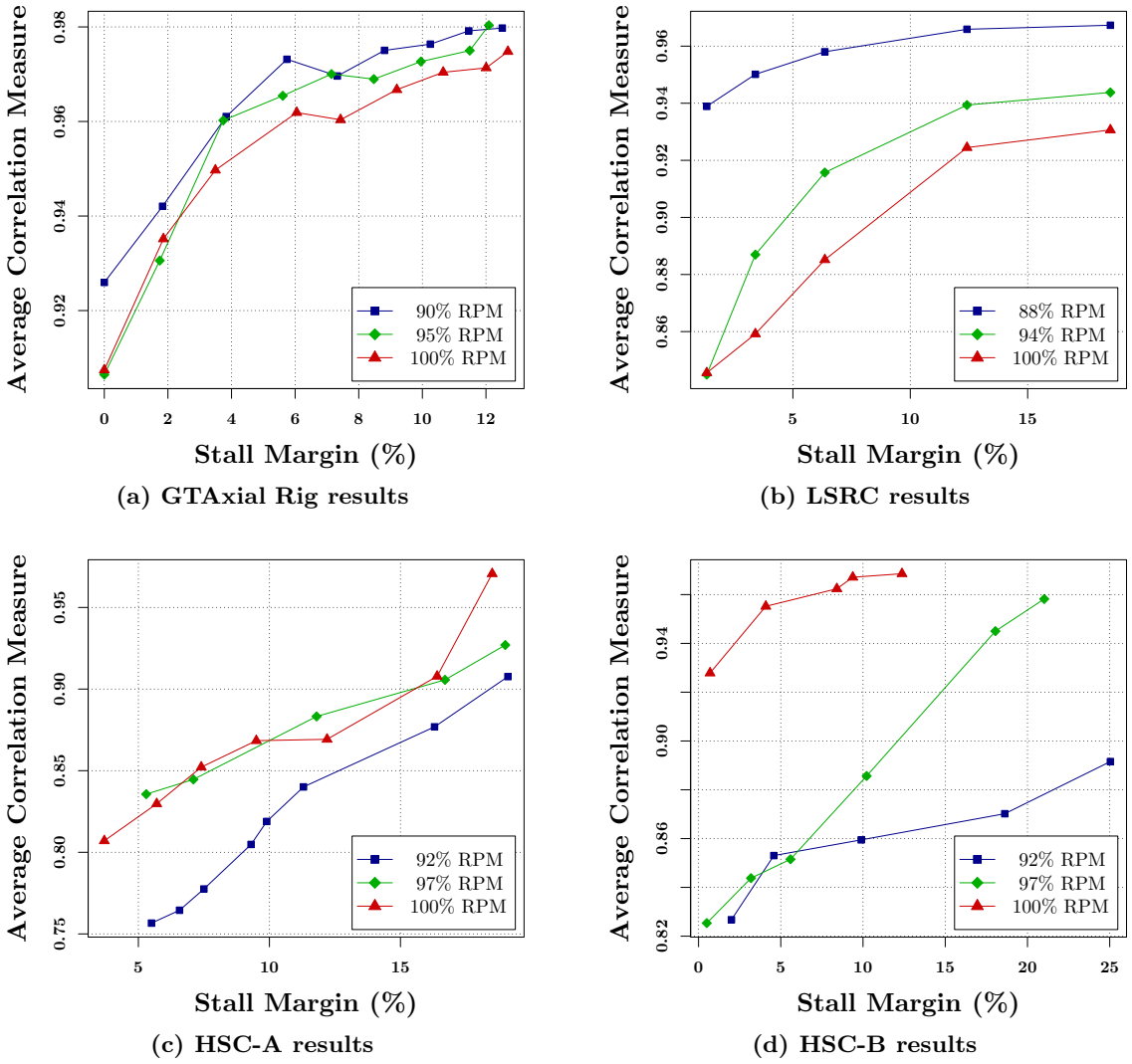

(a) GTAxial Rig results

(b) LSRC results

(c) HSC-A results

(d) HSC-B results

Figure 19: Average correlation measure as a function of stall margin. Results are for four compressors, each with three speeds.

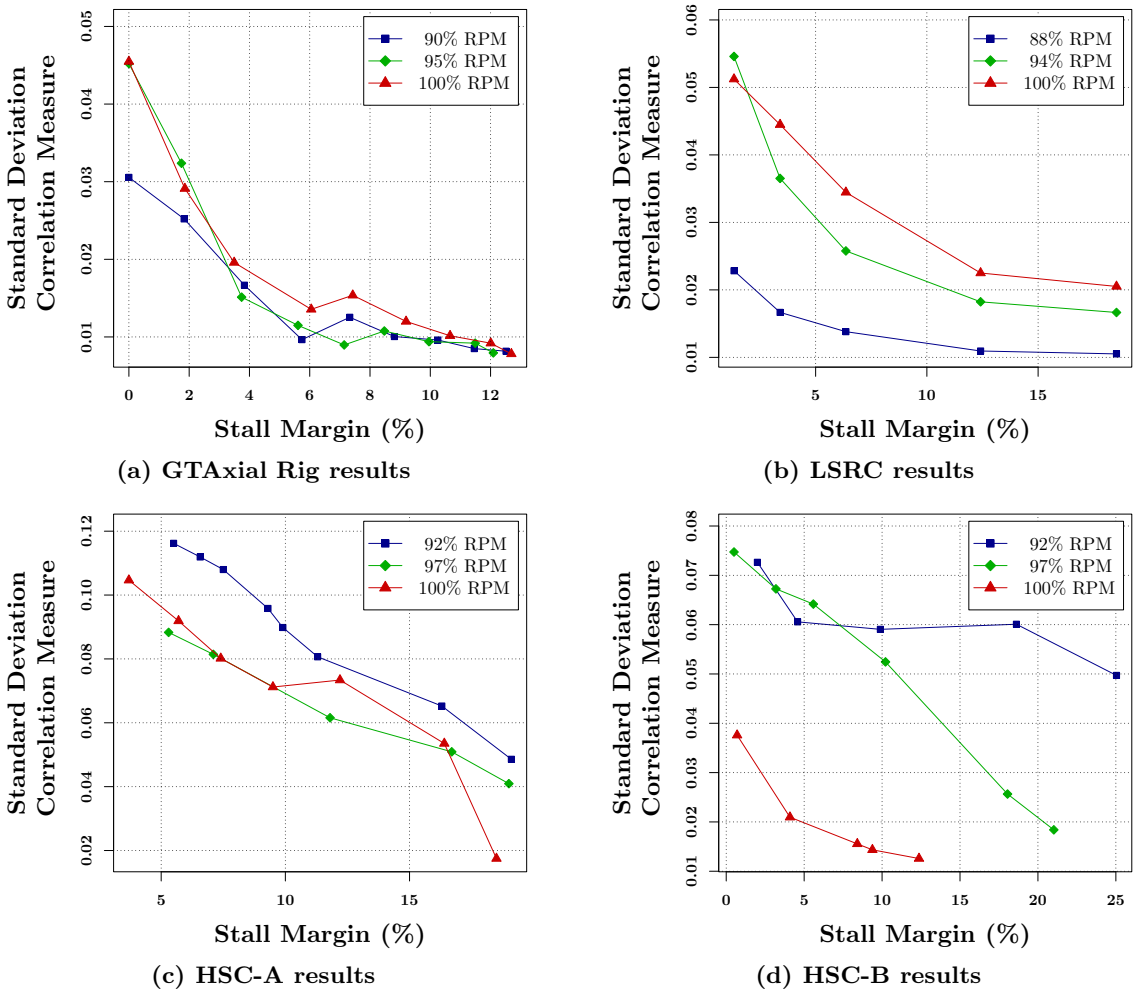

(a) GTAxial Rig results **(b) LSRC results**

(c) HSC-A results **(d) HSC-B results**

Figure 20: Standard deviation of correlation measure and its dependence on stall margin. Results are for four compressors, each with three speeds.

Table 2: Variations in stalling pressure ratio on GTAxial Rig observed over a period of three weeks.

Dataset YYYYMMDD	**Pressure Ratio At Stall** Normalized to the 20030418 dataset	**Ambient Temperature** $^{\circ}C$
20030418	100.00	NA
20050715	99.72	27.2
20050721	99.72	29.3
20050801	100.23	24.5-25.9
20050805	99.47	26.4-27.0
20050808	100.23	22.2-24.7

the average correlation measure for the 88% is larger than both 94% and 100% speeds, the correponding standard deviation is lower.

The results presented so far show that the stall margin to correlation measure relationship is qualitatively similar for different compressors. In fact, for a fixed speed, this relationship is a characteristic of a given machine and has been found to be independent of day to day variations. To illustrate this point, five sets of data, spread over three weeks and with varying ambient conditions, have been acquired on the GTAxial Rig. The average correlation results from these data are compared to a baseline case acquired more than two years ago. The comparison results are shown in Figure 21 and Table 2 lists the corresponding stalling pressure ratio and ambient temperature. The pressure values have been normalized to that from the 20030418 dataset. The temperature range reflects the change in temperature reading before and after an entire data acquisition run. There is a minimal scatter in the stalling pressure ratio across the different datasets. The curves relating to the different datasets are confined within a narrow band, despite a gap of over two years between the baseline dataset and the rest. The correlation measure is a time-invariant function of stall margin and this relationship is a characteristic of a compressor.

Both the mean and standard deviation of the correlation measure exhibit consistent trends across different speeds and for different compressors. In particular, the correlation measure falls in an average sense and the variation around its average increases as the compressor is loaded. The distribution of the measure further elucidates this trend. Either

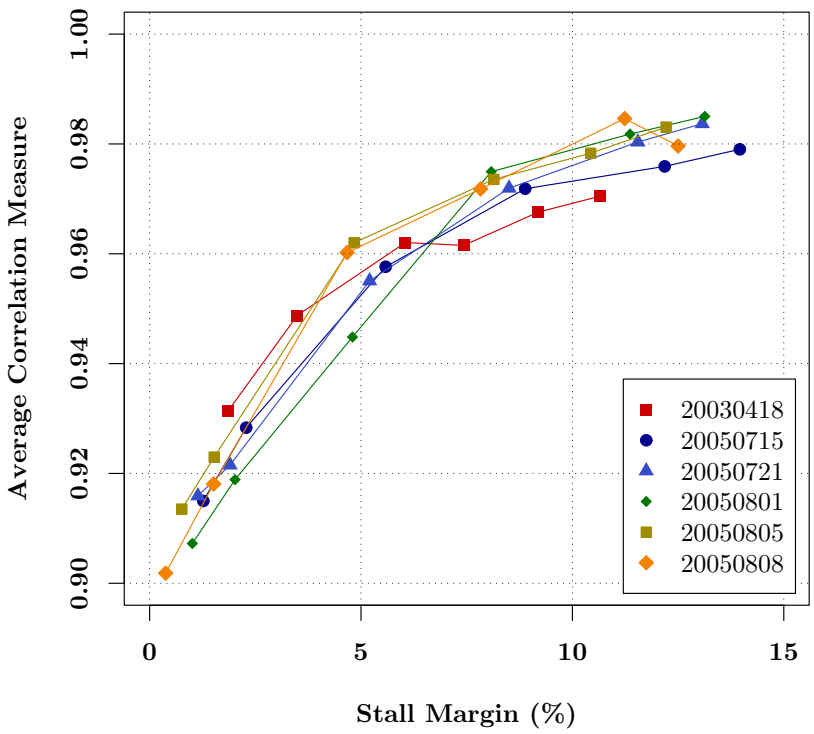

Figure 21: Correlation measure - stall margin relationship is unchanged over a period of two years on the GTAxial Rig. Data sets are labeled by year, month and day

the cumulative distribution function or the probability density function can be used for this purpose. The empirical probability density function (EPDF) is in fact the normalized data histogram, whereas the empirical cumulative distribution function (ECDF) can be expressed as,

$$F(y) = n^{-1} \sum I_{(-\infty,y]}(Y_i), \tag{11}$$

where the indicator function $I_A(x)$ equals 1 when $x \in A$ and 0 otherwise.

The probability density and cumulative distribution functions for the four compressors are presented in Figures 22 and 23. The data are for $100\%RPM$ in each case. As in the previous results, data from a sensor on the third stage of HSC-A at an axial location of 54% chord and from a sensor located at 81% chord on the fourth stage of LSRC have been used for respective results. Although the EPDF has an advantage in that the trends in the mean and variance are visually apparent, it can be more sensitive to the statistical sample size. Further, probability can be directly read from an ECDF plot. As an illustration, the decrease in correlation measure for the GTAxial rig with stall margin can be observed by

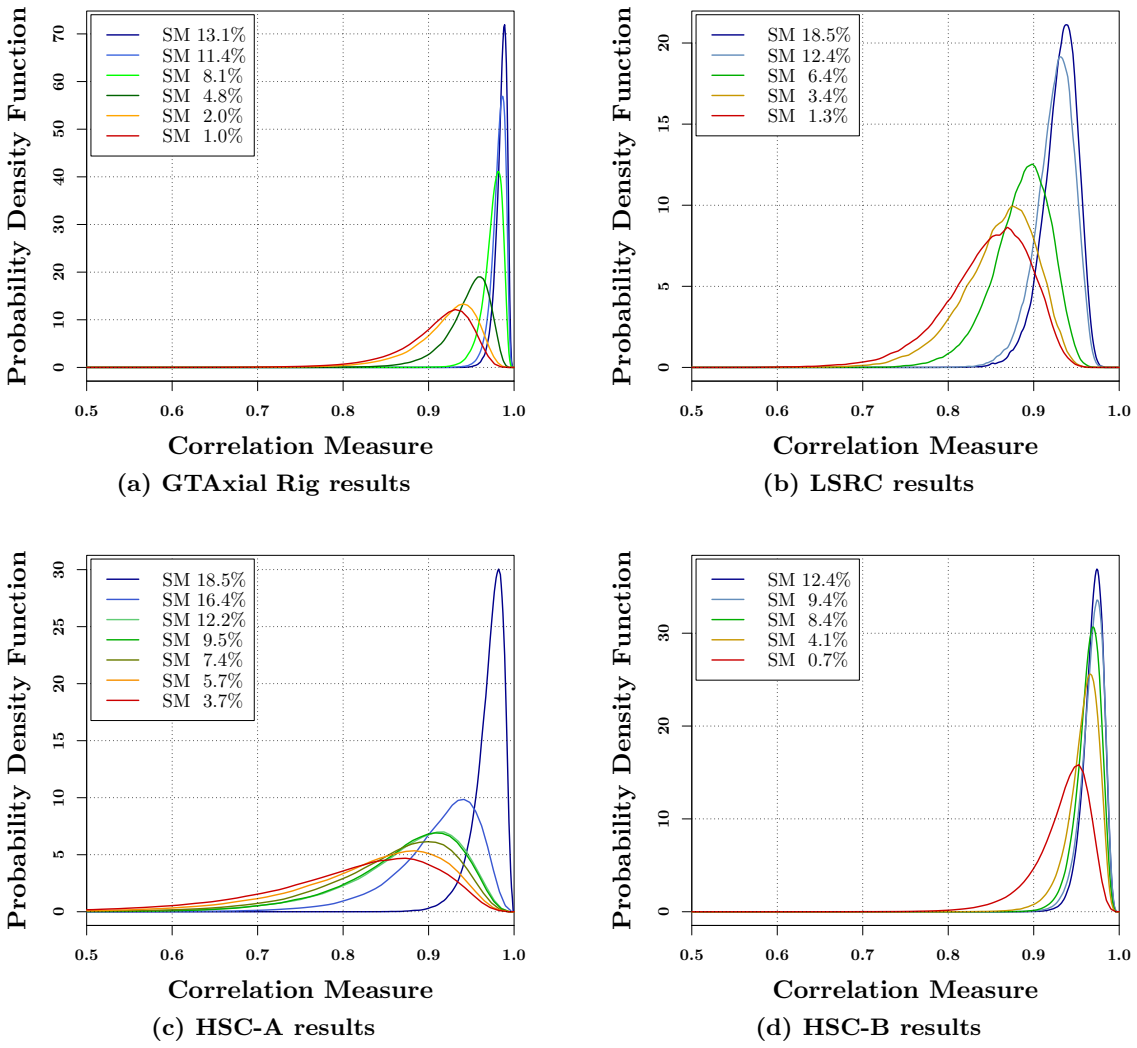

Figure 22: Correlation measure behavior with respect to stall margin captured via changes in its Probability Density Function. Results for all four compressors are presented.

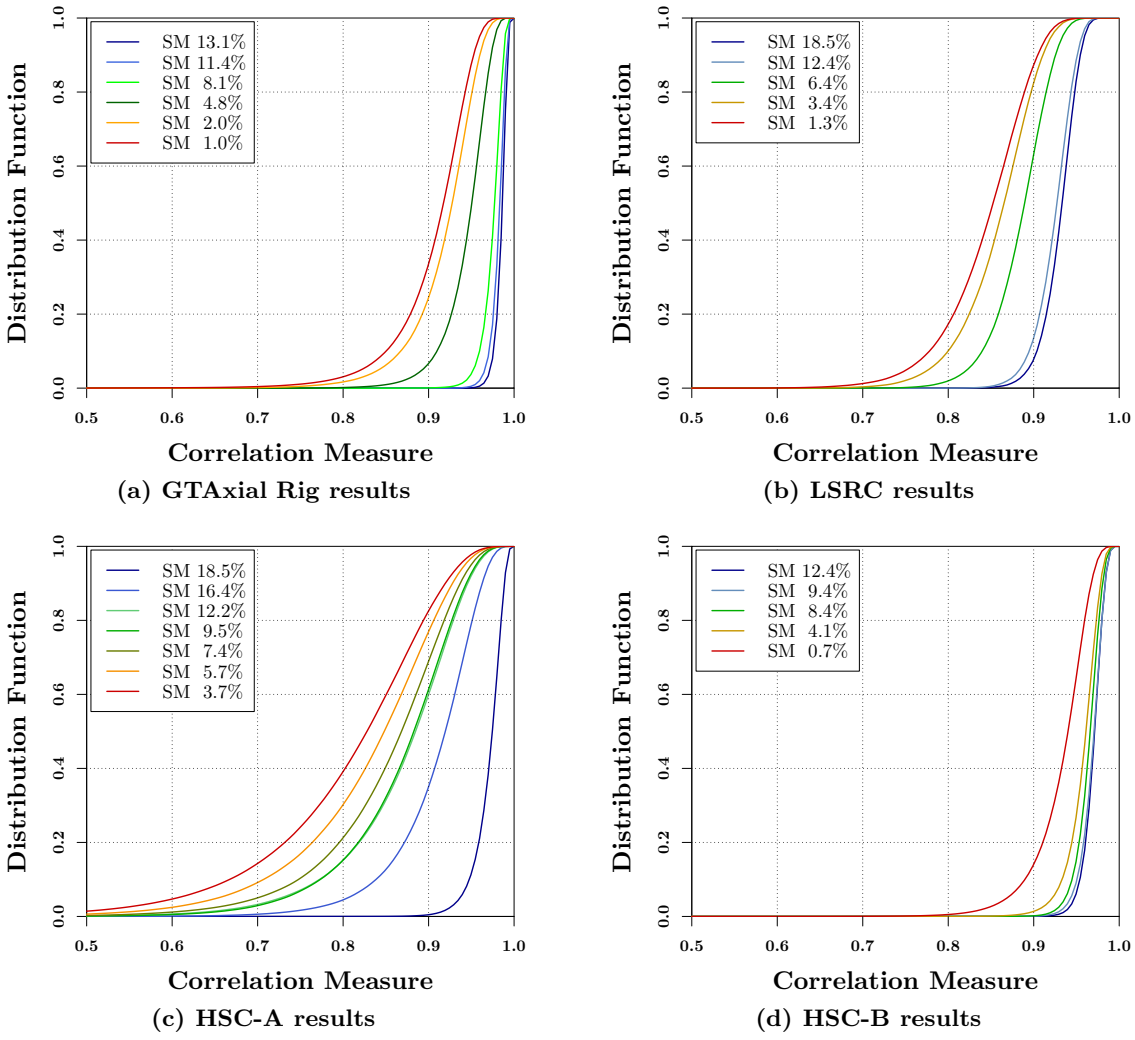

Figure 23: Correlation measure behavior with respect to stall margin captured via changes in its Cumulative Distribution Function. Results for all four compressors are presented.

the peaks moving left in Figure 22(a). The increased variance is apparent from the wider curves. On the other hand, as observed in Figure 23(a), there is negligible probability for the correlation measure to fall below 0.9 when the compressor operates with larger than 2% stall margin. The skewed nature of the EPDF curves is due to the sharp drops observed in the time trace of correlation measure. Though these drops have a small contribution to the average, they are responsible for the tailing to the left of the peak, as observed in the EPDF. Both EPDF and ECDF show that the change in correlation measure with stall margin is larger than that visible via its average value. For example, when the results for HSC-B in Figure 23(d) are considered, the correlation measure in the 4.1% stall margin case has a significantly low probability of dropping below 0.9 compared to the 0.7% stall margin case. This can be exploited by setting a threshold value and observing how many times, or how much time, the correlation measure was below it. It may also be noted that the average correlation for the respective cases does not differentiate them to the same extent. Specifically, the difference in the average value of correlation measure for the two cases is about 0.025 (Figure 19(d)), whereas the difference in above mentioned probability is greater than 0.15.

3.1.3 Importance of Sensor Location

Sensor location plays a vital role in the behavior of the correlation measure. Initial analysis determined that a sensor located around the mid-chord location is suitable for the correlation measure technique. In general, a sensor located at the leading edge had a high correlation measure, whereas one at the trailing edge had a low value, irrespective of the compressor loading. Analysis of all the data available shows that while this is not the entire picture, it is essentially correct.

The impact of sensor location is apparent in the ECDF results presented as Figure 24. For these results, data from a series of sensors on the third stage of HSC-A have been used, with the compressor operating at 100% RPM. In particular, the results from sensors at -32%, 3%, 37% 54% 88% and 106% chord along the axial direction, are shown in Figures 24(a) to 24(f). Sensor location is measured in terms of the axial projection of rotor

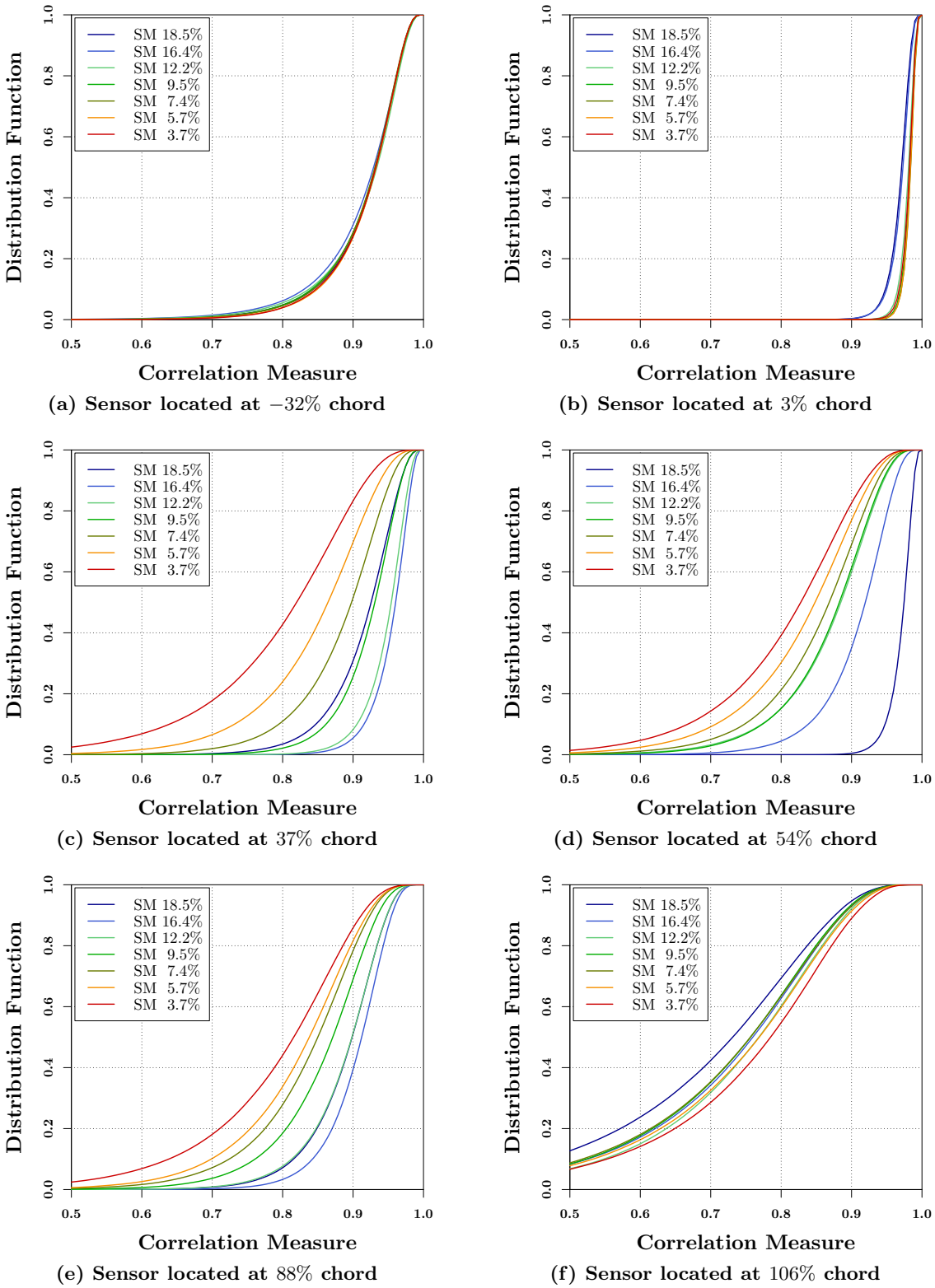

(a) Sensor located at −32% chord

(b) Sensor located at 3% chord

(c) Sensor located at 37% chord

(d) Sensor located at 54% chord

(e) Sensor located at 88% chord

(f) Sensor located at 106% chord

Figure 24: Impact of the sensor location on correlation measure. These results utilize six sensors on the third stage of HSC-A, with the compressor running at 100% design speed.

tip chord, with leading edge as the origin. In particular, 0% chord location designates the leading edge, while 100% chord location refers to the rotor tip trailing edge. As observed in Figure 24(a), the correlation measure calculated using data from a sensor located in front of rotor leading edge is relatively high and is nearly independent of the stall margin. A sensor on the leading edge shows an even higher correlation measure (Figure 24(b)), still independent of the compressor operating condition. When sensors at axial locations 37%, 54% and 88% are used (Figures 24(c) to 24(e)), the cumulative distribution of correlation measure is dependent on the stall margin and its behavior is similar to one discussed earlier. The trends observed via 37% as well as 88% chord location are not always monotonic. In particular, correlation measure corresponding to the 18.5% stall margin (SM) has a lower value than its 16.4% counterpart. Infact, in Figure 24(e) the 18.5% SM results are hidden by those pertaining to 12.2% SM. The results obtained via the sensor at near mid-chord location are consistent with initial observations. The correlation measure decreases monotonically with increase in compressor loading. It may be noted that curves for 12.2% SM and 9.5% SM overlap (Figure 24(d)) and thus the relationship is not strictly monotonic.

The situation is very different when data from a sensor aft of the trailing edge are analyzed for trends in correlation measure. The results presented in Figure 24(f) show that correlation measure is typically low for this case. This is true for various steady state operating conditions, each with a different stall margin. While the correlation measure is not entirely independent of compressor stall margin, its behavior is contrary to that observed via over the rotor sensors. A small increase in the measure can be observed as the stall margin is reduced.

Similar analysis on LSRC reveals a slightly different picture. The results for six sensor locations on the fourth stage, with the compressor operating at 100% RPM are presented in Figure 25. The sensor location trends are similar to those observed through HSC-A, i.e. correlation measure is low in front of the rotor, high over the rotor passage, and low again at the rotor trailing edge. However, the change, or lack thereof, in correlation measure with stall margin is unlike the HSC-A case. The sensor in from of the rotor (-26% chord location shown in Figure 25(a)) shows an increasing correlation level with decreasing stall margin.

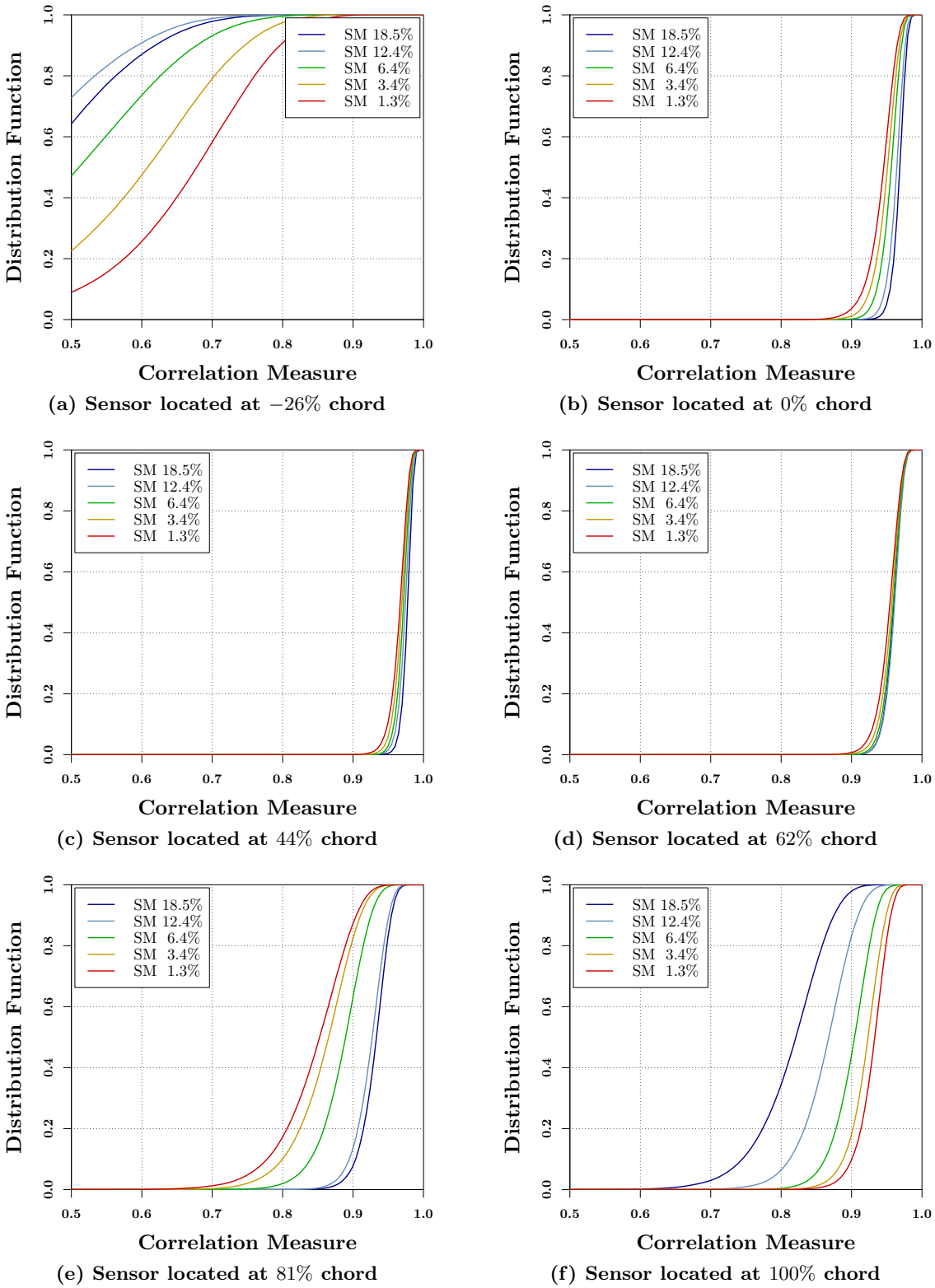

(a) Sensor located at −26% chord

(b) Sensor located at 0% chord

(c) Sensor located at 44% chord

(d) Sensor located at 62% chord

(e) Sensor located at 81% chord

(f) Sensor located at 100% chord

Figure 25: Impact of the sensor location on correlation measure. These results utilize six sensors on the fourth stage of LSRC, with the compressor running at 100% speed.

A careful examination of Figures 25(c) and 25(d) shows that while correlation measure does decrease prior to stall, the change is quite small. In fact 81% chord sensor location seems to be the only usable location for this set. Finally, the correlation measure of the pressure signal from the sensor at the trailing edge (100% chord, Figure 25(f)) exhibits a reverse trend. The correlation measure increases as compressor loading is increased.

The unusual results presented above can be attributed to the particular nature of LSRC data. The objective of this test was performance evaluation of a specific stator geometry with embedded air injection. This stator belongs to the third stage of the compressor, and is thus upstream of the fourth stage rotor. Further, the data used for the results presented here corresponds to the baseline case, where injection system was off. Ancillary data suggests that there was significant separation in the third stage stator passages in these conditions, which in turn leads to an unloading of the front portion of fourth stage rotor[29].

In all the compressors analyzed, at least one location over the rotor tip has been found that yields exploitable trends in correlation measure. A near mid-chord location has been found to be acceptable for most of the compressors studied. LSRC data represents an unusual case, and serves to emphasize that sensor location should be carefully evaluated for unusual designs.

3.1.4 Physical Interpretation

The observed behavior of the correlation measure can be related to unsteady flow phenomena in the compressor, in particular the tip leakage flow. Pressure differences between the suction and pressure surfaces of a rotor blade cause the flow to leak over the blade tip. The leakage flow typically separates at the corner between the pressure side and the blade tip. The separated flow forms a vena-contracta in which the flow is confined to an area less than the tip clearance. The leakage jet then becomes turbulent and expands to fill the entire clearance gap. When the clearance flow clears the tip on the suction side of the blade, it is not aligned with the main flow there. This difference in direction requires a vortex sheet with high vorticity to exist between the two. The vortex sheet rolls up near the maximum pressure difference location to form the tip leakage vortex. Further details

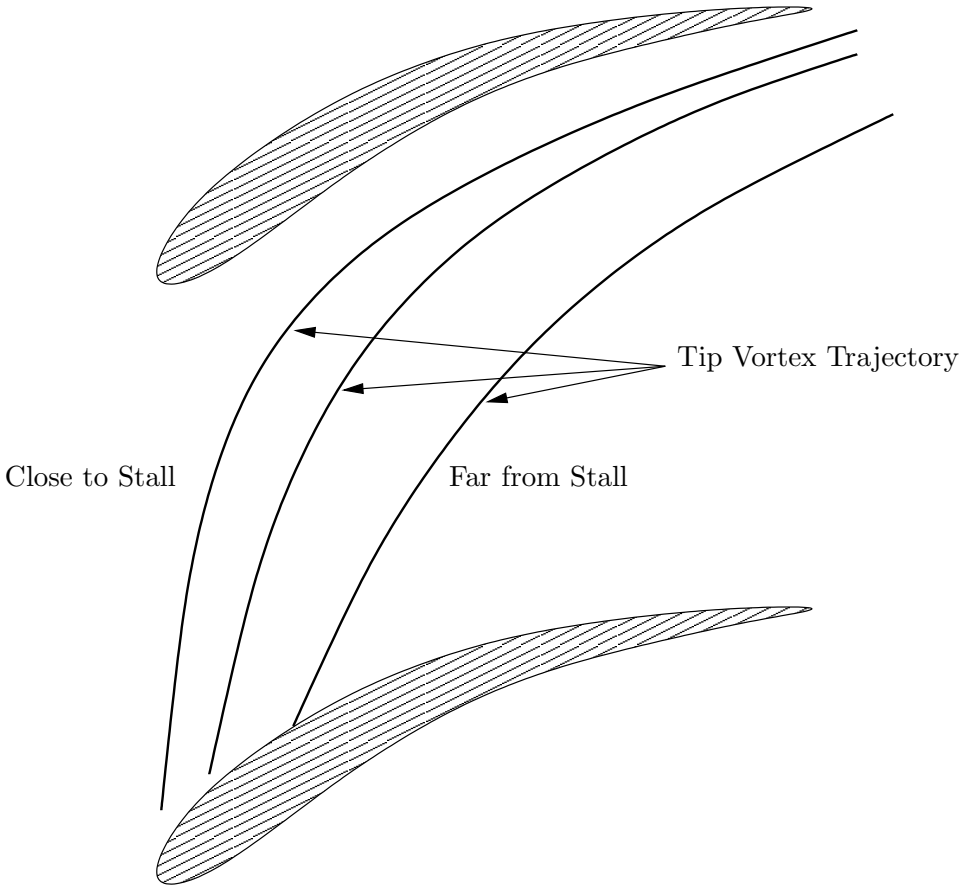

Figure 26: Impact of compressor loading on the trajectory of the tip vortex. Adapted from Hoying et al. [25]

of this phenomena can be found in Inoue and Kuroumaru [26] as well as Storer and Cumpsty [42]. Bindon [4] has studied losses in the tip clearance flows in turbine cascades. Even in compressors, the tip leakage flow has a significant contribution to the end-wall losses. Denton [15] provides formulae for estimating its contribution.

The trajectory of the tip vortex has been associated with compressor stage loading. Chen et al.[7] state that the tip vortex moves further from the suction surface as mass flow through the compressor decreases because the convection time and the shed vortex strength both increase. Hoying et al.[25] have employed numerical simulations to understand the relationship between blade passage flow and compressor stall inception. On the basis of their results, the researchers postulate that the tip vortex trajectory moves forward as the stage is progressively loaded and the mass flow reduced. Figure 26 which has been adapted

from their results, illustrates this behavior. Hoying et al. further state that the trajectory is perpendicular to the axial direction at stall inception.

Recently, Wisler et al.[49] have used a low speed experimental facility to investigate the tip vortex flow. They confirm that the vortex trajectory indeed moves forward as the compressor is loaded. Wisler and co-workers observed this phenomenon in two different blade designs as well as different amounts of tip clearance.

It follows that the variation of the vortex trajectory with compressor loading is predicted in simulations and verified by experimental observations. The turbulent nature of the tip vortex formation suggests unsteadiness in its trajectory. Together, these ideas provide an explanation for the observed aspects of correlation measure. A sensor located around rotor mid-chord is relatively free of the turbulence associated with the tip leakage flow at low loading. Not only the vortex is weaker, its trajectory is more aft in this case. Consequently the pressure signal from this sensor at low loading is expected to be periodic and yield a high correlation measure. As the loading is increased, the vortex gets stronger and its trajectory moves forward, increasing the level of chaos at the sensor. Thus, the value of the correlation measure would decrease as the loading is increased. The sharp drops in the correlation measure can be attributed to any fluctuations in the vortex strength and trajectory. The increased unsteadiness and strength with an increase in compressor loading translates into the drops increasing in magnitude and becoming more frequent.

A sensor located at and/or in front of the rotor leading edge is unlikely to see any effects of the leakage vortex till the onset of stall. Consequently, the correlation measure calculated using pressure signals from such a sensor is going to have a high value. This high value is maintained till stall inception, at which point every location will show poor shaft to shaft periodicity. A sensor at the trailing edge, or close to it, will always be subjected to effects of the leakage vortex. Further, the turbulence level is expected to be higher at the blade trailing edge. It is not surprising then, that the correlation measure of pressure signals from this location has a low value, indicating poor periodicity.

A correlation measure of unity corresponds to perfect periodicity, an idealization unlikely to exist in real flows. In practice if the measure is ever observed to be unity, it would

probably be due to a failed sensor or related instrumentation.

Correlation measure in its present formulation captures unsteady flow phenomena in compressor blade passages. These phenomena are fundamental to axial compressors as evidenced by the consistent trends observed on the different compressors studied. As per the current hypothesis, the phenomena in question are related to tip leakage flow.

3.2 Stochastic Model

3.2.1 Events

It has been established that average value of the correlation measure decreases monotonically with stall margin. Although important in its own right, average value is not a good basis for active stability management. An average value is slow to respond by definition, and would be unreliable during transients with rapid variations in stall margin. Moreover, averaging obscures the importance of impulse-like drops observed from time to time in the correlation measure. The tail-like features present in the probability distribution curves suggest that these drops have a greater significance than average values. One way to capture the contribution of these impulsive drops, as alluded to earlier, is to track when correlation measure falls below a specified threshold. To facilitate this, downward crossing of the threshold by the correlation measure is defined as an event. This idea is illustrated in Figure 27, which shows a time trace of correlation measure obtained on the GTAxial Rig. The apparent randomness of the dips in the correlation measure leads to events that are randomly distributed in time. In a likely implementation, a controller would react to these events by initiating suitable preventive actuation.

Initial observations suggested that magnitude as well as frequency of the impulsive drops in correlation measure increase as the compressor is progressively loaded. This can be captured via the average number of events for a given *steady-state* operating condition, μ, which is defined as,

$$\mu = \lim_{T \to \infty} \frac{N(0,T)}{T} \tag{12}$$

where N is the number of events in time period $(0,T)$. In practice, $(0,T)$ is a finite time period, sufficiently large for the average to be statistically meaningful. The results

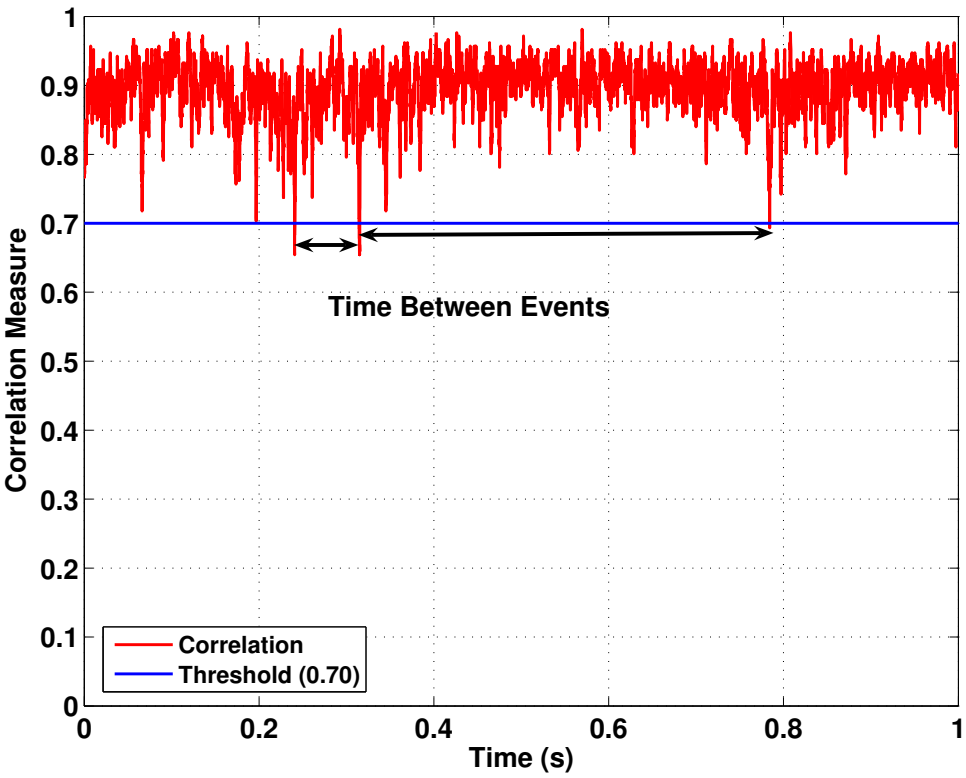

Figure 27: An illustration of the random occurrence of events. An event is defined as downwards crossing of a threshold by correlation measure.

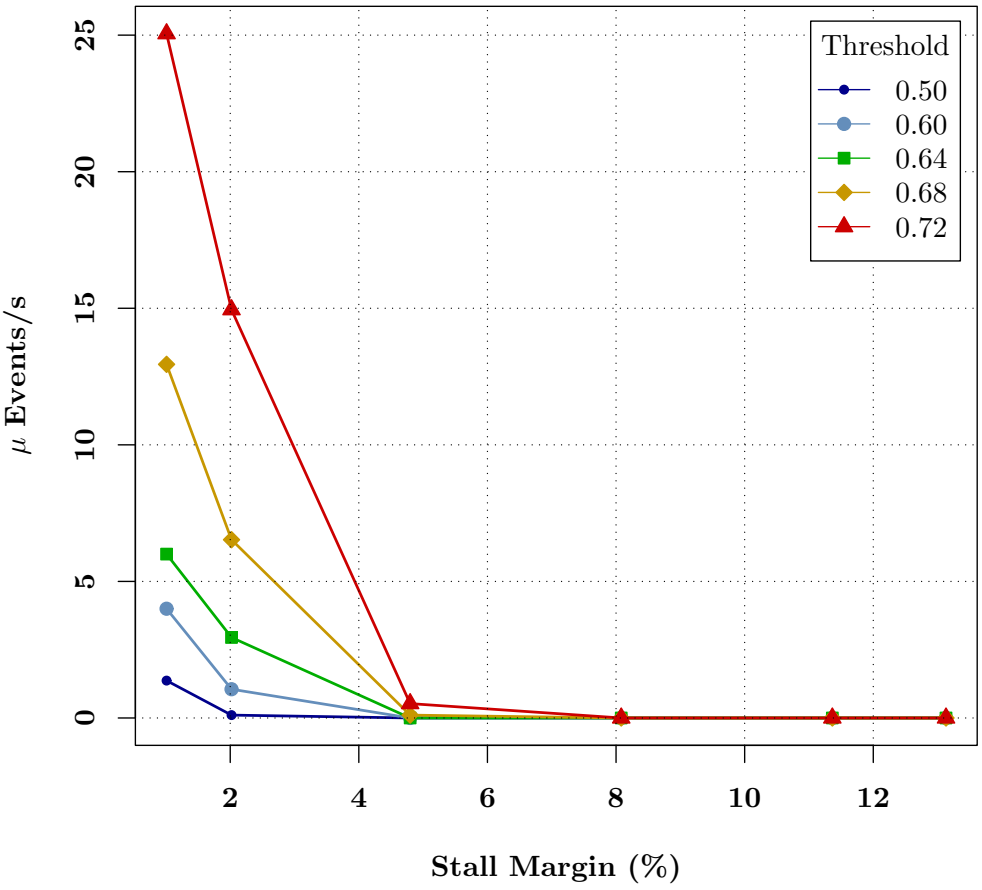

Figure 28: The relationship of average number of events to stall margin. The choice of threshold value plays a dominant role in this relationship.

pertaining to μ obtained on the GTAxial Rig are presented in Figure 28. The figure shows variations in μ with stall margin for a variety of threshold values, C_{th}. The results show that for a given C_{th}, μ increases with decreasing stall margin. In other words, events occur at a higher rate at lower stall margins. On the other hand, μ decreases as the threshold C_{th} is lowered, i.e. fewer events are observed, at a given stall margin. Events cannot be observed for the higher stall margins. More significantly, the first appearance of an event shifts to lower stall margins as C_{th} is lowered. For example, some events can be observed at 4.8% stall margin when C_{th} is set at 0.72. If it is lowered to 0.64, events only appear when the compressor stall margin is reduced to 2%. Thus even though dips in correlation measure are present at all stall margins, their magnitude is larger for lower stall margin.

Average number of events can be used to estimate stall margin close to the compressor stability limit. This is demonstrated via Figure 29, which shows results for several datasets

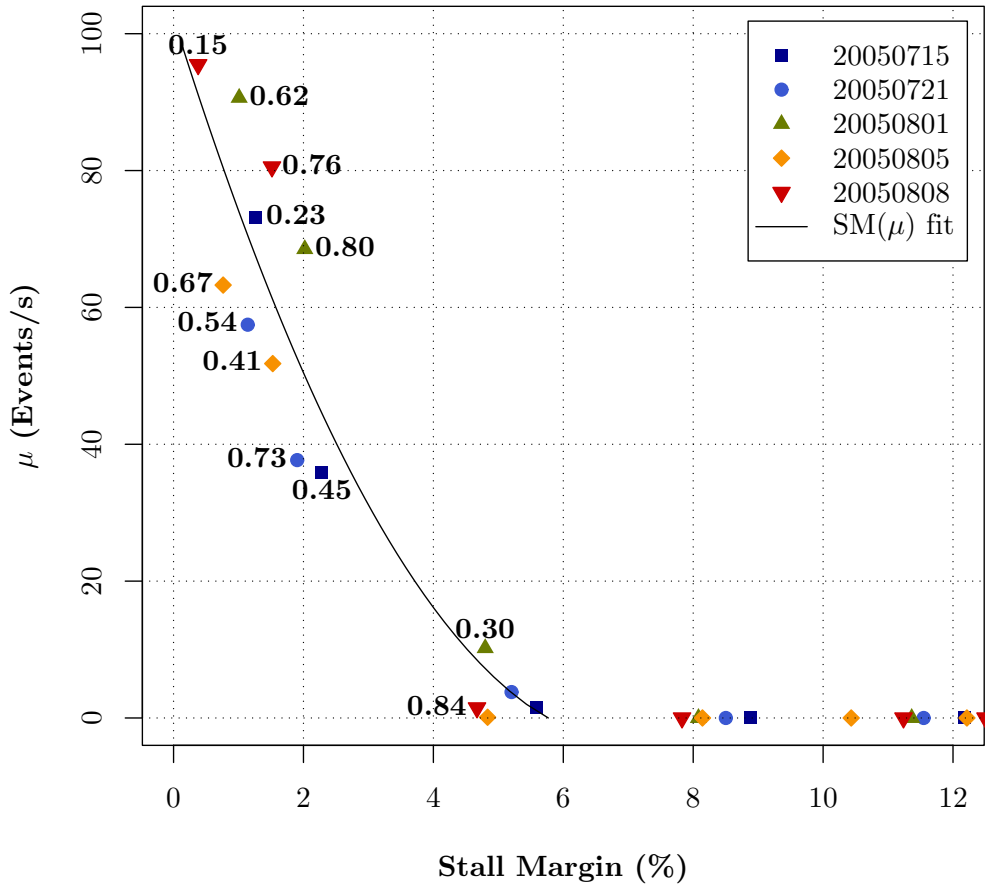

Figure 29: Estimation of compressor stall margin via average number of events. The labels next to each marker designate the error in stall margin as estimated via least-square error curve fit.

obtained on the GTAxial Rig. The different markers correspond to observed μ values, each with a different stall margin and part of the respective runs. A least square fit has been used to obtain μ as a function of stall margin (SM). The one-to-one part of this curve has then been inverted to yield a function of the form $SM(\mu)$. The labels next to each marker identify the horizontal distance between it and the $SM(\mu)$ curve shown. This distance in essence is the error in stall margin that would be predicted through observed μ. For example, about 38 events/s have been observed for the 2% stall margin case, a part of the 20050721 dataset. On the basis of the fitted $SM(\mu)$ curve, 38 events/s would correspond to about 2.7% SM, leading to an error of about 0.7% SM (actual error 0.73% SM). The nature of $SM(\mu)$ is such that higher stall margins cannot be distinguished from each other.

Two very important points can be made following these results. Tracking events generated by correlation measure can only be used to detect proximity to compressor surge line. This method is not applicable as a general stall margin estimator. For example, in the GTAxial case, average number of events cannot differentiate between 8% and 12% stall margin. The other observation pertains to accuracy of the stall margin estimation. For GTAxial Rig results presented here, the estimation error is less than 0.85% stall margin. It can be intuitively stated that estimation error depends not only on the scatter in experimental observation, but also on the slope of the μ-SM curve. Regardless, it is important to note that, in general, stall margin cannot be precisely determined. A real-time estimation of compressor stall margin, accurate to the order of 1%, is a significant improvement over the state of the art.

The observed behavior of average number of events, μ, is not specific to the GTAxial-Rig. Instead it is common to all four compressors studied. An illustration for this is provided by Figure 30, which shows μ-SM curves for three speeds of each compressor. The HSC-A results correspond to data from its second stage, with the sensor located at 48% chord. In every case, μ increases monotonically as stall margin is reduced. In these results, threshold values used are different for each compressor, and in two cases are also dependent on its speed. In particular, a threshold of 0.84 has been used for GTAxial Rig (Figure 30(a)), whereas it is set at 0.50 for the HSC-A results (Figure 30(c)). In either case, threshold setting is independent of compressor speed. For LSRC, threshold is set at 0.88 for its 88% speed and 0.72 for 94% as well as 100% speed cases (Figure 30(b)). In case of HSC-B (Figure 30(d)), thresholds are set at 0.54 for 92% as well as 97% speeds, but at 0.74 for 100% speed.

A single threshold is advantageous as it would simplify practical controller implementation. Although slightly more involved, it is possible to account for different thresholds, if required. Moreover, the dependence of threshold on speed in the multistage compressors could in fact be an artifact of loading distribution. Typically, guide vane angles are prescribed as a function of compressor speed, scheduled to balance the loading across different stages. Such a balance may not always be attained, and a difference in load distribution

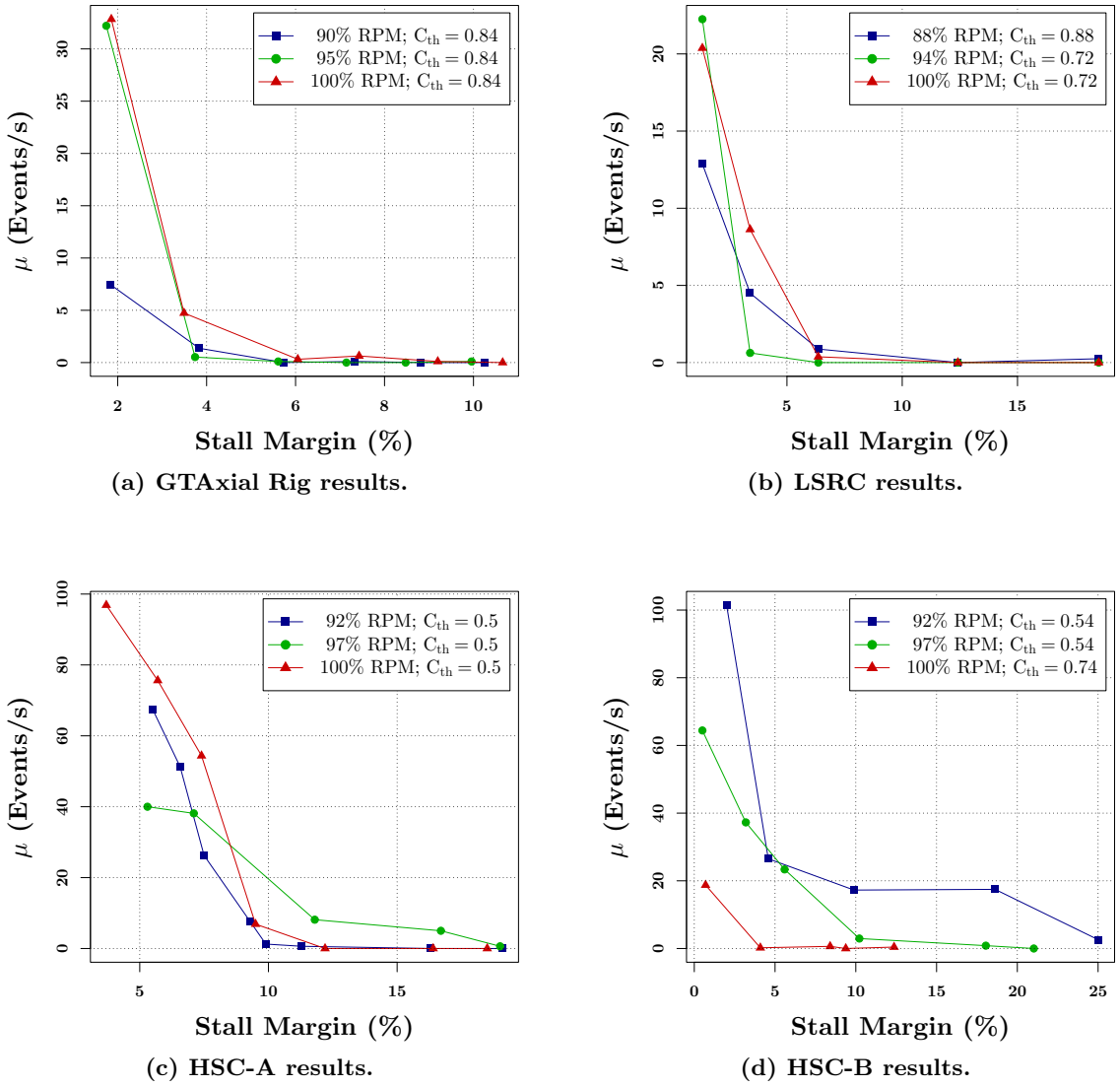

(a) GTAxial Rig results. **(b) LSRC results.**

(c) HSC-A results. **(d) HSC-B results.**

Figure 30: Average number of events are inversely related to stall margin. Results include three speeds each for four compressors

would account for different thresholds. Finally, results presented in Figure 30 are aimed at illustrating a common trend, and thresholds have been selected accordingly. The similarity in the μ-SM results across the different compressors is not surprising, given the similarity in correlation measure behavior observed earlier.

3.2.2 Modeling Time Between Events

Threshold selection plays an important role in the present approach to compressor stability management. Given the existing relationship between μ, C_{th} and stall margin, it is possible

to select a value of C_{th} such that events do not occur unless stall margin is close to zero, i.e. the compressor is about to stall. As outlined in earlier, this is not necessarily desirable. During transient engine operation, the compressor operating point can move rapidly towards the stall line. In order to be effective, any preventive actuation should be executed with sufficient lead time. The required lead time is a function of the system as well as actuator dynamics. An acceptable C_{th} is in turn dependent on this lead time and the trajectory under consideration. As an illustration, consider a hypothetical example where a $100\,ms$ lead time is required. Further, consider a transient where stall margin changes linearly from 10% at time $t = 0$, to 0 at $t = 200\,ms$. Then stall avoidance control has to be initiated prior to $t = 100\,ms$, when the stall margin would be 5%. Now if the true stall margin were available *a priori*, control could be initiated just before 5% stall margin is reached. Clearly, if a threshold is selected such that μ is zero up to 2% stall margin, lead time requirements cannot be met and stall avoidance would fail. Not only that, selecting a threshold such that $\mu > 0$ for stall margin less than 5% and zero otherwise, may also be insufficient. As events are randomly spaced, it is not certain that one would occur just as compressor stall margin reduces to 5%, even when μ is greater than zero. To this end it is necessary to establish an upper bound on the time to next event for a given value of μ, the average number of events.

The discussion above shows that the time between consecutive events (TBE), as identified in Figure 27, is an important metric. A stochastic model is thus sought which captures the time distribution of events and its relationship to the stall margin. In order to show that such a model exists, it may be beneficial to demonstrate that sharp drops in correlation measure possess a characteristic structure. The invariance of underlying processes is apparent when particular threshold settings are used and the resulting TBE statistics are analyzed. Specifically, if the threshold value in each case is related to its average correlation measure, the TBE distribution becomes independent of compressor stall margin. This has been found to be true for all four compressors analyzed. An illustration is provided by Figure 31, where in each case, threshold has been set at 3σ below respective average correlation measure values. Similar results have been obtained when threshold is set at any multiple of σ below the average. In particular, the TBE distribution remains independent

of stall margin when average correlation measure is used as the threshold in each case. Here σ refers to the standard deviation of correlation measure.

It is important to note that TBE distribution is not unconditionally independent of compressor stall margin. As the average correlation measure has been found to be a function of stall margin, for the results shown in Figure 31, threshold values are in turn dependent on the stall margin. Thus, these results are limited to the dynamics governing crossing of a set threshold by correlation measure. A strong similarity among the results of all four compressors is visible in Figure 31. This suggests that the processes characterizing the time evolution of correlation measure, during steady compressor operating conditions, possess a fixed structure. Consequently, it would be feasible to model TBE distribution.

A stochastic model for correlation measure based events has been obtained as an application of the theory of stochastic processes. Of particular interest are *point processes* which are a class of stochastic processes where a point event occurs successively in time, in a more or less random manner. An everyday example of a point process is the arrival of customers in a bank. Recall that in the current scenario, an event is generated whenever correlation measure crosses a set threshold in the downward direction. In other words, events are downward crossings of a specified level. Cramer and Leadbetter [9] have extensively studied level-crossings by stochastic processes. They have shown that several random variables are associated with such level-crossings, including the number of upcrossings, downcrossings and time spent above a level. Cramer and Leadbetter have provided formulae for statistical properties of several random variables expected to be useful in applications. In particular, they have obtained results for the "distribution function of the length of the interval between an arbitrarily chosen upcrossing and the next upcrossing." In this context, there is little difference between an upcrossing and a downcrossing, and as such this is the required result. Then, following Cramer and Leadbetter, the distribution of time between successive events, with events defined as before, is given by,

$$F(\tau) = 1 + \mu^{-1} D^{+} u_0(\tau) \tag{13}$$

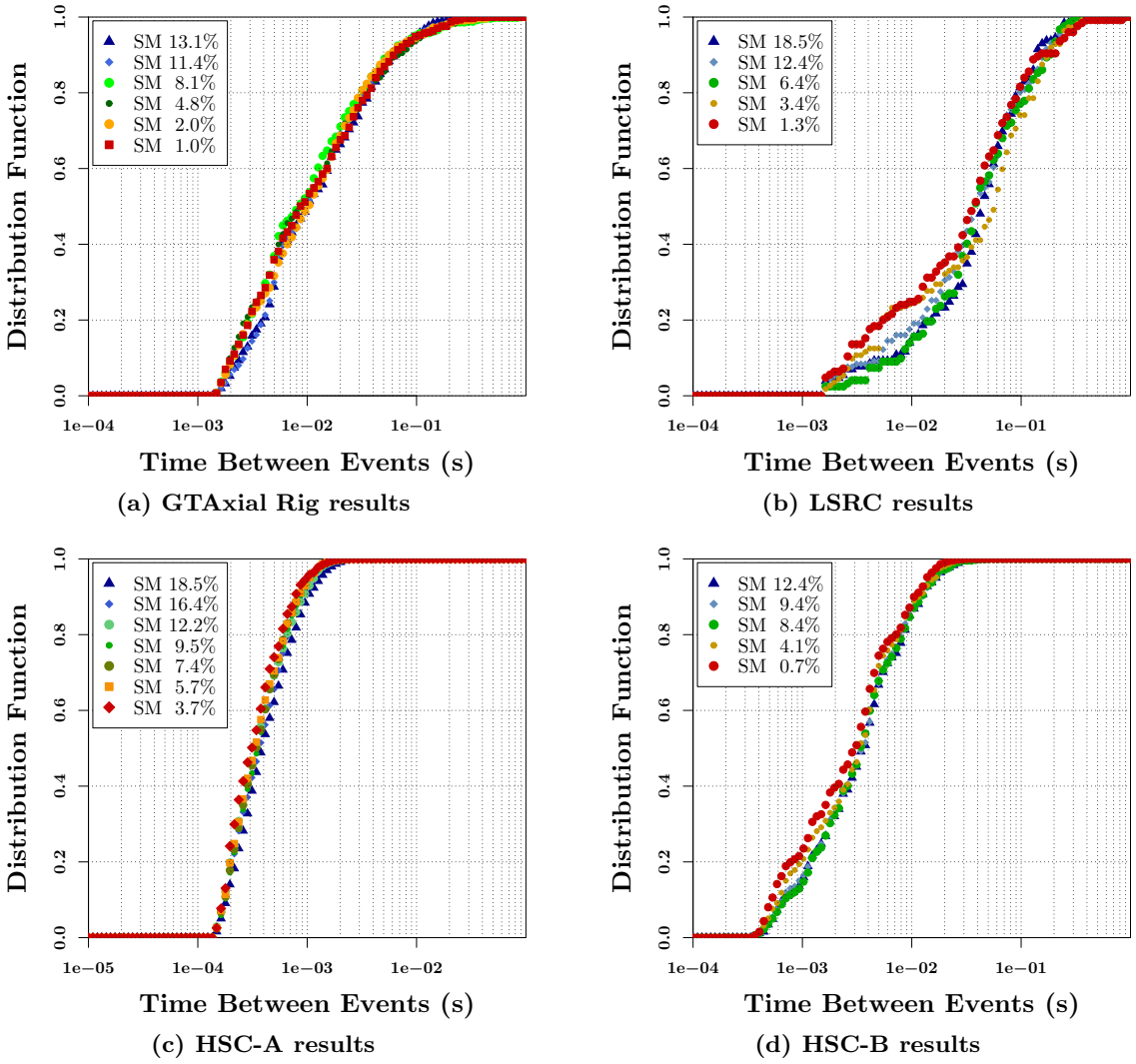

Figure 31: An illustration of the invariance of processes driving correlation measure. The cumulative distribution of Time Between Events is independent of the stall margin when the event defining threshold is set three sigma below average correlation measure for each case.

with

$$u_0(t) = P(N(0,t) = 0) \tag{14}$$

where τ is the time between consecutive events, D^+ is the right hand derivative, $P(x)$ is the probability that x is true, and variables $N(0,t)$ and μ are as defined previously.

Now $u_0(t)$ is the probability that no event shall occur in time interval $(0,t)$. For the events generated due to threshold crossing by correlation measure, it may be reasonable to assume this probability decays exponentially with time, i.e.,

$$u_0(\tau) = e^{-\mu\tau} \tag{15}$$

When this is substituted in Equation 13, the distribution function $F(.)$ reduces to,

$$F(\tau) = 1 - e^{-\mu\tau} \tag{16}$$

It is proposed that Equation 16 gives the cumulative distribution of Time Between successive Events (TBE), where an event is the downward crossing of a specified threshold by the correlation measure. The distribution has a single parameter μ, the average number of events. This is the exponential distribution function and is applicable to *P*oisson processes, which is the simplest class of point processes.

The impact of average number of events on the exponential TBE distribution is illustrated by Figure 32, where the distribution function has been traced for three values of μ. It can be observed that a higher value of μ leads to a higher probability of encountering an event in a given time interval. As an example, the probability of observing an event in an interval of $100\,s$ with $\mu = 1$, 10 and 100 are close to 0.1, 0.63 and 1 respectively. Alternatively, for a fixed chance of event occurrence, smaller values of μ translate into longer time intervals.

Consider a case with $\mu = 50$, i.e., on average fifty events occur in an interval of one second. If these events were equally spaced in time, at least one event would be guaranteed to occur in $21\,ms$. As a contrast, when events are exponentially distributed in time, the probability for the same time interval is about 0.65, i.e., there is a 35% chance of an event failing to occur. In fact, the time interval required for a reasonable probability of success is

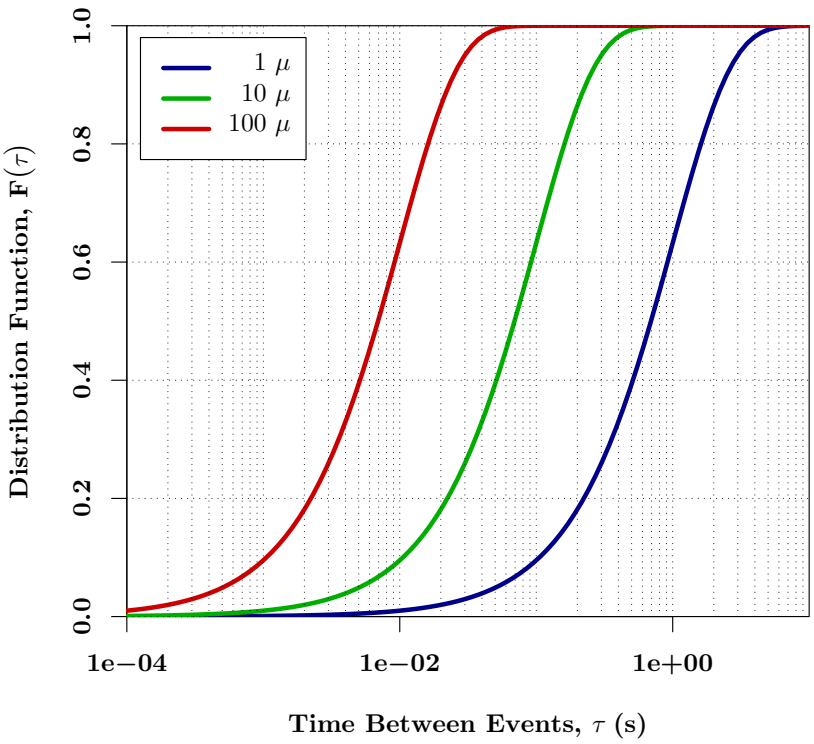

Figure 32: A visualization of the relationship between average number of events (μ) and time between consecutive events

about ten times as long, at $200\,ms$. It follows that the distribution of time between events is important to the success of correlation measure based compressor stability management.

3.3 Model Validation

Two significant assumptions have been made in the development of the stochastic model. It has been explicitly assumed that the probability of zero events in a time interval decays exponentially with the length of the time interval. Given a non-zero average for events, this assumption has the appropriate form, i.e., this probability should decrease with the length of interval in question. Another assumption, implicitly made, is that correlation measure is a stochastic process. Although not explicitly shown, the stochastic nature of correlation measure is alluded to by its frequency content, as well as its cumulative distribution. The experimentally observed distribution of TBE has justified these assumptions after the fact.

The model validity is assessed by comparing the predicted distributions to those obtained experimentally. Typical results for all four compressors are presented in Figure 33.

In each case, the predicted curves utilize the experimentally observed values for μ, the average number of events. In the results presented, the experimental distribution is omitted whenever less than ten events are observed under given conditions. In these circumstances the number of data points is not enough for meaningful statistical description. The number ten is somewhat ad-hoc but has been found to work well.

Of the four compressors, in general, results of the GT-Axial Rig show the poorest fit. However, even for this compressor, for larger values of τ, there is a fairly reasonable agreement of prediction with reality. Both facts can be observed in Figure 33(a), which compares predicted and experimental distributions for a 0.70 threshold value.

The TBE distribution results for LSRC shown in Figure 33(b) have been obtained with compressor operating at 94% speed. Data from 81% chord location has been used, and threshold value is set at 0.82. Only three stall margin cases yielded non-zero μ values for these settings. There is an excellent agreement between the predicted and observed TBE distribution. Similar levels of agreement are also observed in the results for HSC-A and HSC-B (Figures 33(c) and 33(d)). The HSC-A results utilize a sensor mounted over the third stage rotor, at 54% chord aft of its leading edge. Both HSC-A and HSC-B results are for compressors operating at their respective 97% design speeds, with threshold set at 0.60.

Similar analysis with different threshold levels and for different sets of data shows that TBE distribution for lower stall margins is consistently and adequately captured by the proposed model. The distribution corresponding to higher stall margins is sometimes not as well captured. The 16.7% stall margin case in Figure 33(c) is a good example of this fact. However, as the following observations show, any possible undesirable implications of this limitation of the proposed model are not severe.

First of all, the average number of events observed for higher stall margin operation of the compressor typically have a low numerical value. The low absolute numbers would translate into a low confidence level of the experimentally observed TBE distribution. Consequently the mismatch between prediction and observation cannot be strictly attributed to modeling limitations. Then, as evident in Figure 33(c) as well as Figure 33(d), the predicted and experimental distributions are nearly identical, even for the high stall margin cases, when

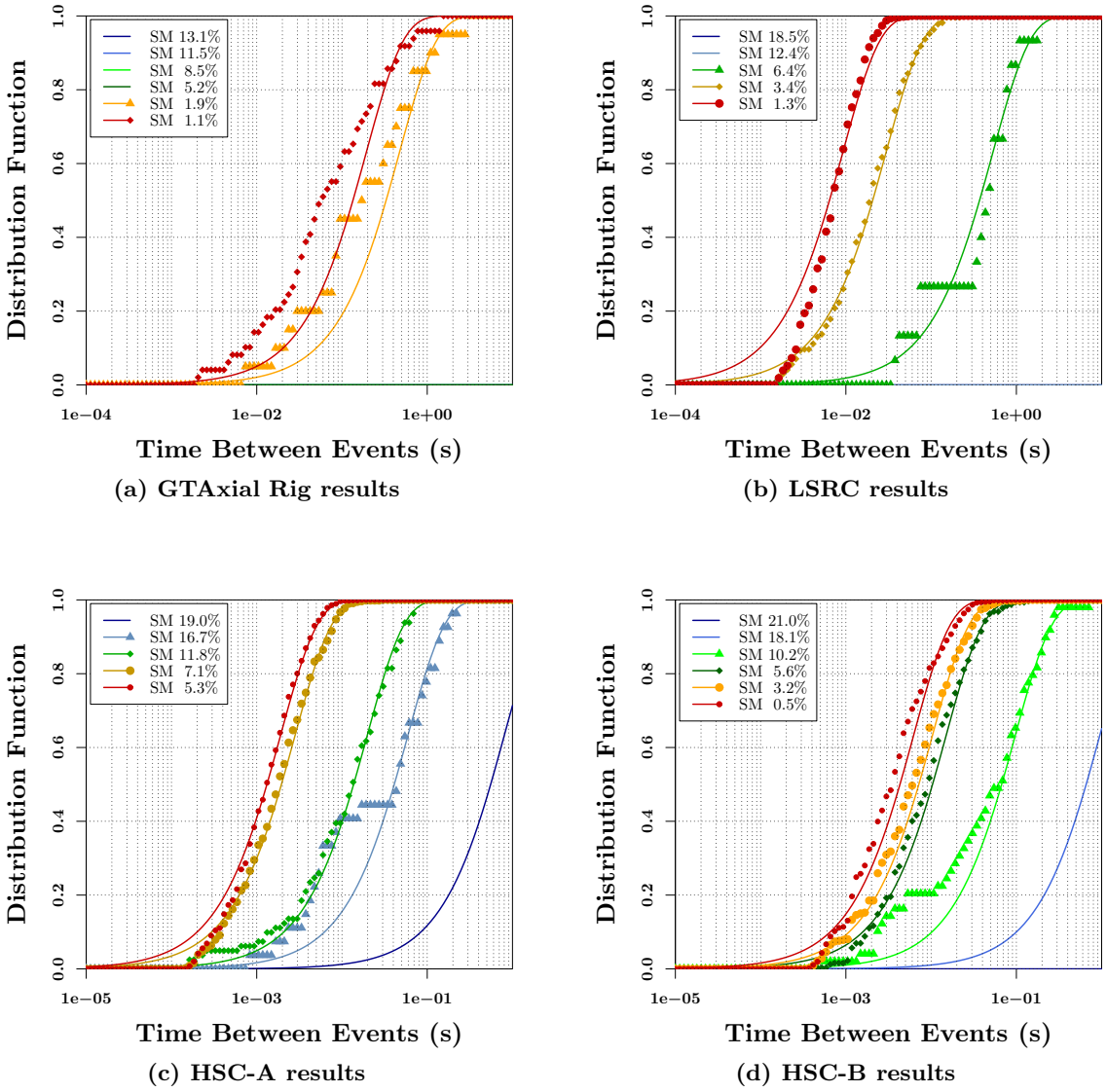

(a) GTAxial Rig results

(b) LSRC results

(c) HSC-A results

(d) HSC-B results

Figure 33: Comparison of predicted distribution and experimentally observed distribution of Time Between successive Events.

restricted to the upper part of the respective curves. Now the value of $F(\tau)$ is, by definition, the fraction of observed TBE less than τ. As a consequence, the proposed model adequately captures the worst case scenarios for all stall margins.

Next, the intended objective of this effort is to enable compressor stability limit detection. As such, accurate modeling of the TBE characteristics when the compressor is operating near its stability limit is of higher importance. Results show that this requirement is fulfilled by the proposed model. Finally, it should be noted that the stochastic model has been used to understand the importance of parameters such as threshold level on successful active stability managment. This model is not directly embedded in the control law and thus its limitations have a minimal impact.

In conclusion, a comparison with experimental results shows that the exponential distribution function adequately models the distribution of time between successive events, where events are defined as the downward crossing of a preset threshold by the correlation measure. It should be realized that the model underpredicts in some cases, leading to theoretical results which could be more pessimistic than reality. As this would introduce conservatism in the stability management approach, pushing it towards the safer side, this underprediction is not a cause for any significant concern.

The experimental results of the TBE distribution sometimes contain a stair-step feature, usually at higher stall margins. An example of this is visible in the 16.7% stall margin case in Figure 33(c). This step signifies that few events are spaced with the corresponding time interval, $20\,ms$ in this case. In other words, for the 16.7% stall margin, very few events could be observed that were $20\,ms$ apart. Moreover, in this case, events with shorter TBE values have a much higher probability than predicted. It is possible that more than one process, perhaps not all stochastic, drive the correlation measure and hence the events. The overall comparison suggests that the developed model captures the effects of the dominant process, and hence yields acceptable results. However, this aspect of the stochastic model warrants further investigation.

3.4 Sensor Location Revisited

The importance of sensor location has been demonstrated via its impact on the cumulative distribution of correlation measure. Analysis shows that a sensor located over the rotor, about mid-chord axial projection is suitable for the current approach. Given the intent to use events generated via threshold crossing of correlation measure, this topic is now re-evaluated, in terms of average number of events. Recall that the correlation measure is high for a sensor in front of the leading edge, higher for one at the leading edge, and typically low for sensors at or aft of the trailing edge. Results obtained on HSC-A and presented in Figure 34, show the same trend, albeit in terms of events. For a given threshold, say 0.64, average events for -32% sensor location are of the order of 100 events/s, none are observed for sensor at the leading edge (3% chord), and results from a sensor at 106% chord location show about 2500 events/s. The results for the other three locations, 37%, 54% and 88% of chord axial projection aft of leading edge, are very similar. In each case, average number of events, μ, increases as the stall margin is decreased. The flow in the respective regions is turning more chaotic as the compressor is increasingly loaded

As mentioned earlier, due to intermittent drops in correlation measure, tracking threshold generated events can highlight differences that are too subtle to be captured via average, or even distribution functions. A comparison of cumulative distribution results and the average number of events for the sensor located at 32% chord in front of the leading edge highlights this point. Differences in correlation measure for different stall margins which are barely perceptible in the cumulative distribution (Figure 24(a)), are accentuated by μ for the same case (Figure 34(a)). It is interesting to note that μ decreases as compressor is loaded in this case, signifying that flow in front of the leading edge is becoming less chaotic.

As evidenced earlier, analysis of LSRC data shows that, as far as application of correlation measure is concerned, mid-chord location is not the optimum choice for this compressor. This has been further explored using μ as a metric, with a focus on the over the rotor locations. Specifically, results using data from 44%, 63%, and 81% chord locations and for three compressors speeds are presented here.

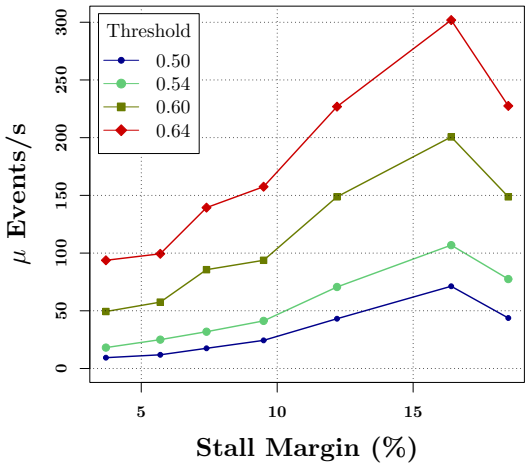

(a) Sensor located at −32% chord

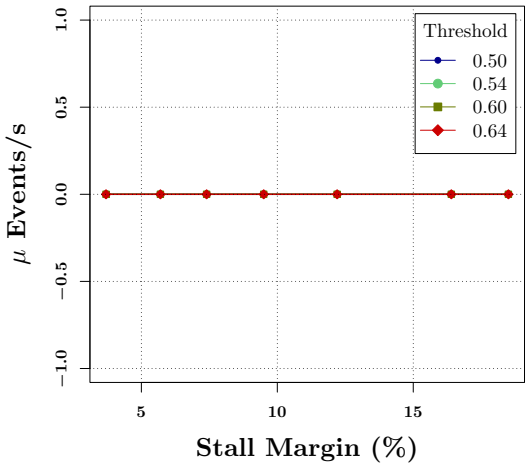

(b) Sensor located at 3% chord

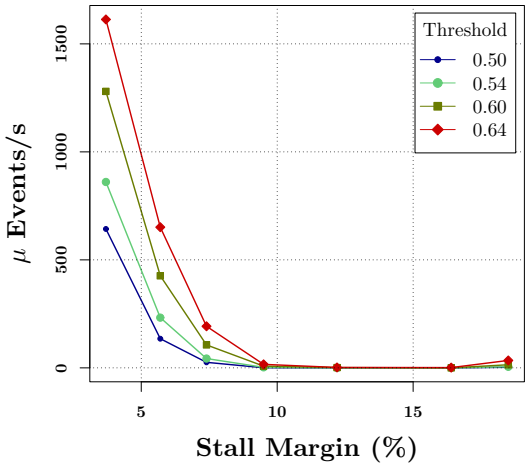

(c) Sensor located at 37% chord

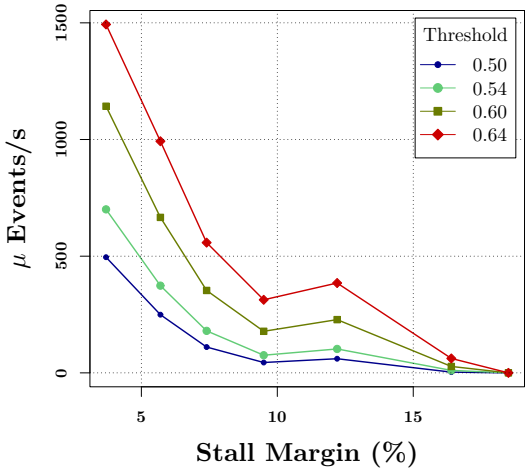

(d) Sensor located at 54% chord

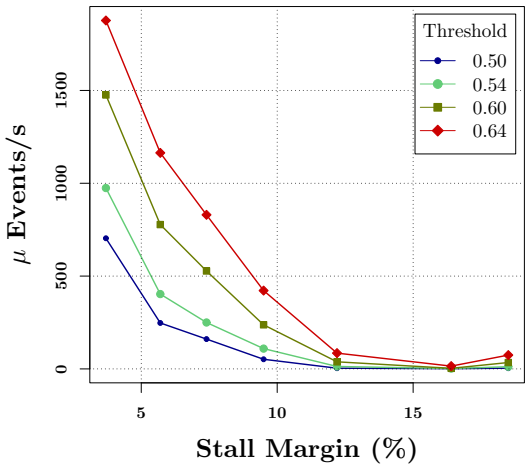

(e) Sensor located at 88% chord

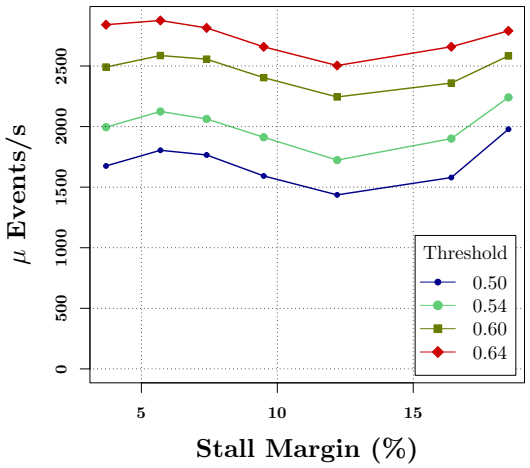

(f) Sensor located at 106% chord

Figure 34: Impact of the sensor location on correlation measure, elucidated via average number of events. These results utilize six sensors on the third stage of HSC-A, with the compressor running at 100% design speed.

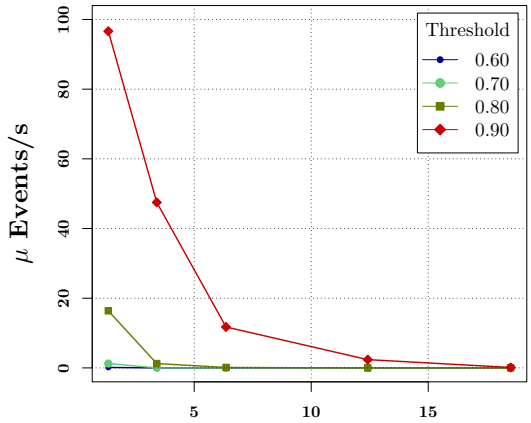

(a) Sensor located at 44% chord

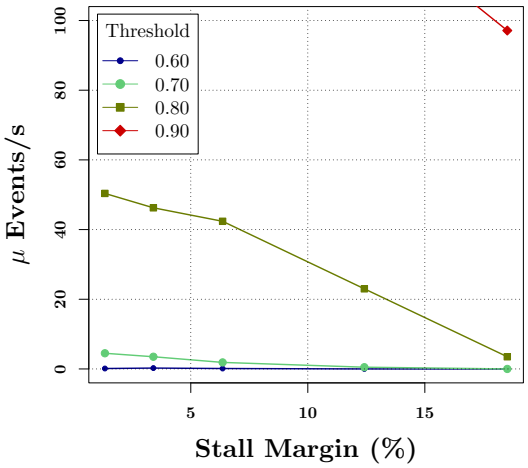

(b) Sensor located at 63% chord

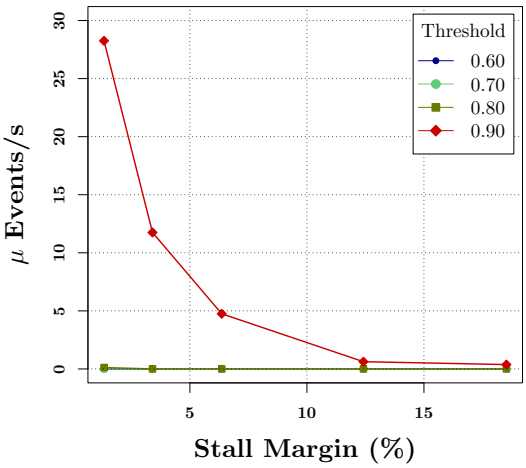

(c) Sensor located at 81% chord

Figure 35: Sensor location results for LSRC evaluated through average number of events, with the compressor running at 88% design speed.

The results for the 88% speed in Figure 35 show that all three locations exhibit a viable trend. Results are deemed viable for compressor stability management application, if μ increases with compressor loading. The 44% and 81% locations are better, as the μ-SM curves have an exponential-like relationship for these locations. Thus as the compressor moves closer to its stability limits, a multitude of events would be observed, making it easier to detect an approaching limit. In results of the 94% speed case, all three locations exhibit trends that are qualitatively similar. However, the growth of μ is much more pronounced in results from 63% and 81% locations when compared to the 44% location. For the 81% location, when threshold is set at 0.90, number of events observed drops as the stall margin

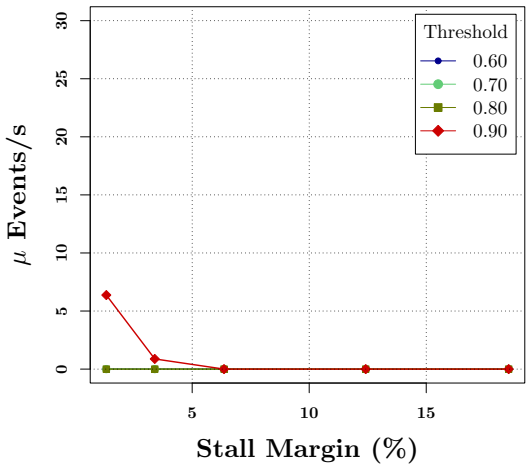

(a) Sensor located at 44% chord

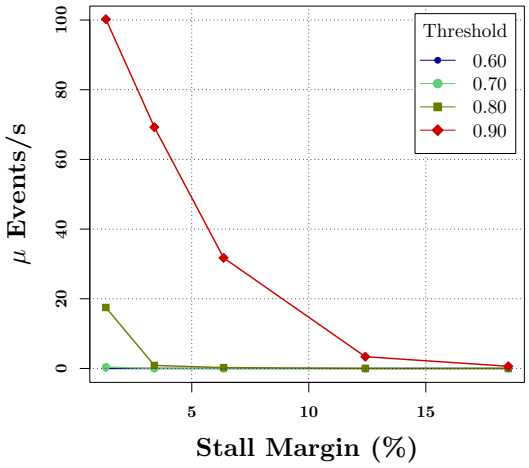

(b) Sensor located at 63% chord

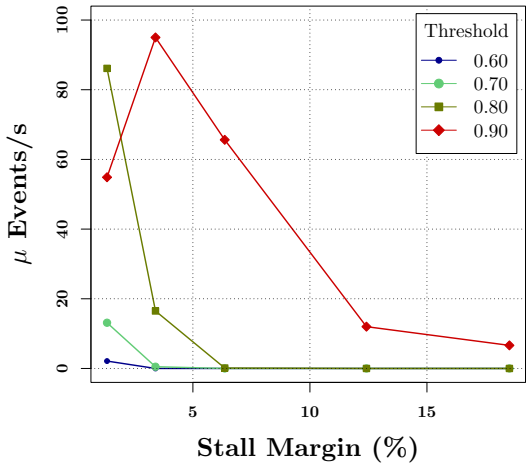

(c) Sensor located at 81% chord

Figure 36: Sensor location results for LSRC evaluated through average number of events, with the compressor running at 94% design speed.

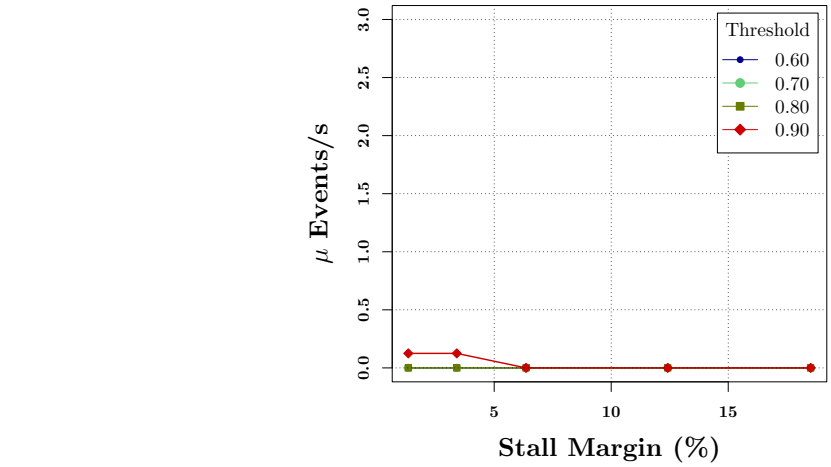

(a) Sensor located at 44% chord

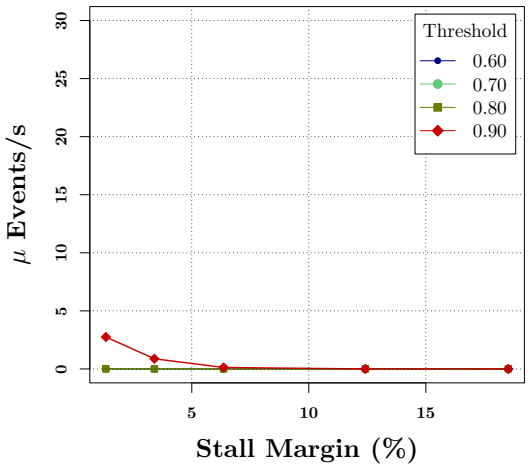

(b) Sensor located at 63% chord

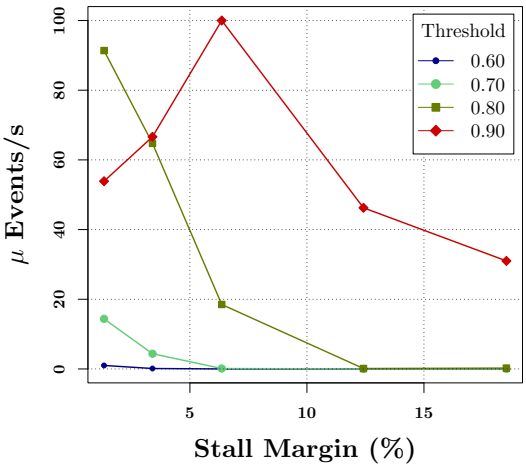

(c) Sensor located at 81% chord

Figure 37: Sensor location results for LSRC evaluated through average number of events, with the compressor running at 100% design speed.

falls to about 1% (Figure 36(c)). This is simply due to the fact that average correlation measure is less than 0.90 for this combination of location and stall margin.

To complete the picture of sensor location on LSRC, Figure 37 shows the results for the 100% speed case. As with the 94% speed case, all three sensor locations exhibit qualitatively similar trends for the average number of events. However, the 81% chord location is the only one which shows a quantitatively reasonable variation of μ with stall margin, as illustrated by Figure 37(c). While it is possible to tune threshold values and obtain quantitatively substantial μ values using pressure signals from 41% and 63% chord locations, overall results favor use of 81% location for correlation measure application.

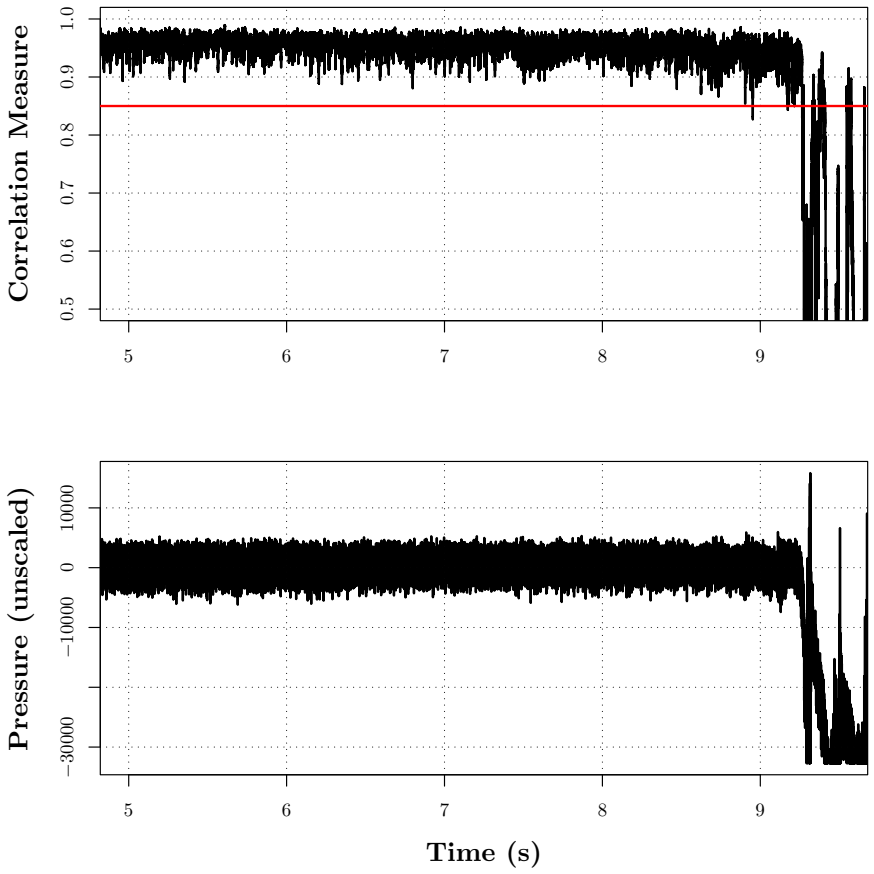

Figure 38: Correlation measure evolution as LSRC is throttled to stall while the compressor is operating at 100% RPM. The results utilize a sensor located at 63% chord.

It is perhaps necessary to distinguish between usable and desirable sensor locations. Towards this end, transient throttle operation of LSRC has been analyzed. In this test, the throttle is continuously closed from its fully open position, till the compressor stalls, while the compressor speed is maintained at a given value. For the case analyzed, the compressor was operating at 100% RPM, and stall could be observed $9.5\,s$ into the transient. The correlation measure depicted in Figure 38 has been calculated using data from the 63% chord location. For this location, if a threshold level of 0.85 is used, impending stall can be detected slightly prior to $9\,s$. This translates into a $500\,ms$ advanced stall warning. In the light of this and previous results, while the 63% chord location may not be desirable with regards to the correlation measure technique, it may still be used to provide stability limit detection.

As mentioned previously, the results pertaining to sensor location on LSRC are unusual. The HSC-A results favor the near mid-chord location, and both GTAxial Rig and HSC-B results utilize a sensor mounted over the rotor, near their respective mid-chord axial projections. As discussed earlier, this discrepancy may be attributed to the unusual operating conditions characterizing the available LSRC data. To summarize, a mid-chord location for an over the rotor sensor should be sufficient for correlation measure application. This location would generally yield results suitable for compressor stability limit detection.

3.5 Summary

The correlation measure approach is a new technique to gauge the aerodynamic stability of the compressor. The phenomena captured by the correlation measure are local to flow over the rotor. Consequently, correct placement of a sensor is important for success of this technique. A mid-chord location is a good starting point for most cases,. However as the LSRC results show, unusual situations may require a survey of different locations. The threshold crossing of correlation measure allows one to retain the significance of sharp dips in the measure that can be observed from time to time. The events generated by these dips have been found to possess an exponential distribution in time. This distribution has been successfully modeled by making intuitive assumptions and application of general theory of

stochastic processes. The relationship of the threshold crossings to compressor stall margin reiterates the fact that this scheme should only be used to detect the proximity of stability limits. In particular, it is not applicable as a general stall margin estimator.

The correlation measure technique was first developed and reported by Dhingra et al.[17] in 2003. The stochastic model of events has been developed in 2005 [16]. Tahara et al.[44], in 2004, reported a stall index which is alomost identical to the correlation measure. However, this stall index was intended to provide a stall warning in advance of spike inception. Persumably, a warning generated by this stall index would imply that that compressor is going to stall. The correlation measure, on the other hand, is simply used to detect the proximity to the compressor stability limit. This subtle difference between the two approaches is quite significant. Moreover, in contrast to the mid-chord sensor location prefered in the current work, Tahara et al. suggested that a sensor location near the rotor leading edge yielded better results.

CHAPTER IV

ACTIVE STABILITY MANAGEMENT

It has been established that correlation measure, computed using a pressure signal from an over the rotor sensor and fixed to the compressor casing, can be used to detect proximity to the surge line. It remains to show that limit detection can be used in closed loop compressor control for active stability management scheme. The current chapter focuses on these aspects. The viability of limit detection based compressor stability management is demonstrated here, both via simulation and experimental results.

4.1 Stability Management via Engine Simulation

4.1.1 Model Implementation

The events defined by the downward crossing of a threshold are exponentially distributed in time. The mean value of time between consecutive events is a function of compressor stability margin, and is likely to be a time varying parameter. To generate random sequences of given distribution, any of the numerous available algorithms can be utilized. However, typical algorithms are not designed to generate sequences with time-varying distribution parameters.

A natural and efficient implementation has been obtained by detecting threshold crossings of a computer generated random sequence. The generated sequence does attempt to replicate correlation measure directly, it is only used to simulate the threshold crossing behavior. To understand why this works, it is necessary to realize that the results embodied by Equation 13 are valid for level crossings by *a*ny suitable stochastic process. As long as two different processes have identical probabilities for zero event observed in a given time interval, as defined in Equation 14, the resulting distribution for time between successive events would also be identical. This property of stochastic processes has been exploited in the current implementation for the limit detection model.

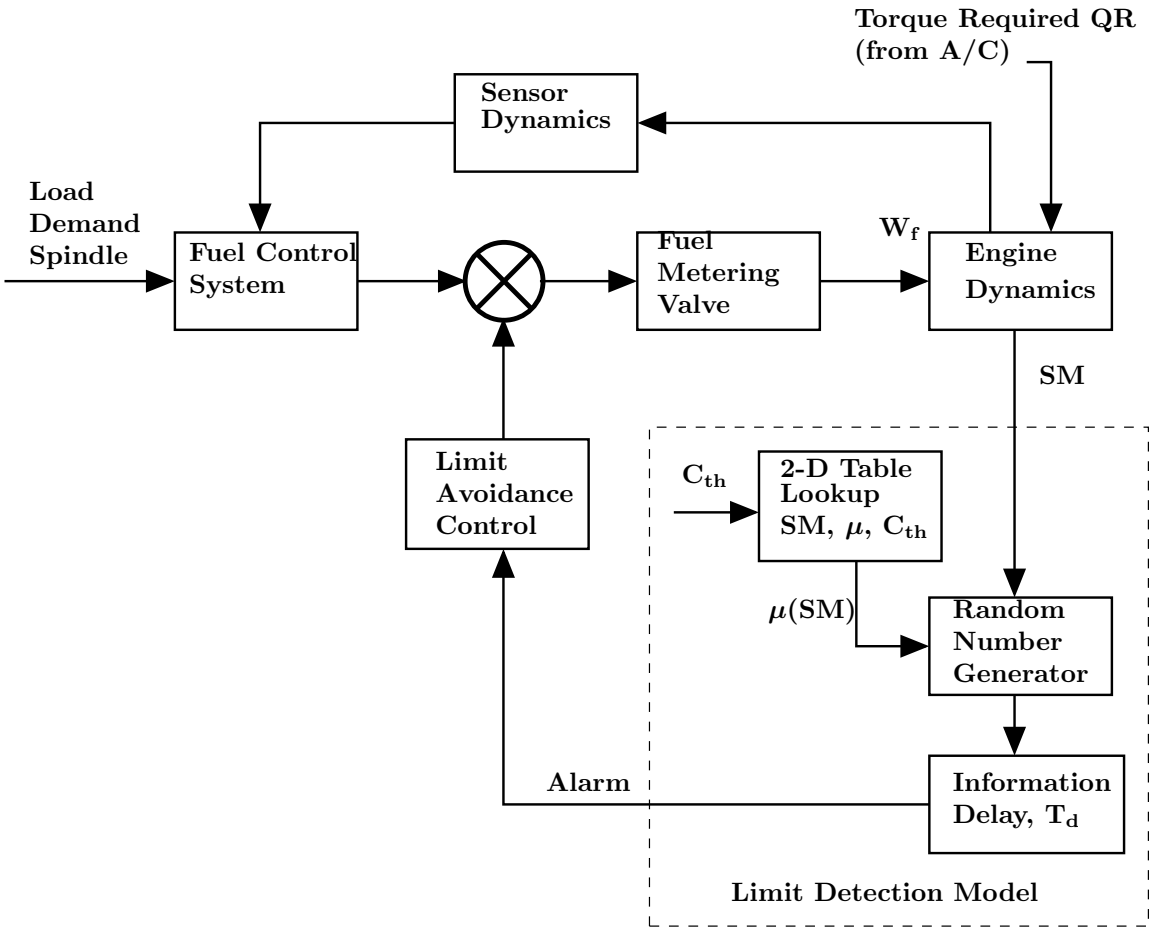

Figure 39: Block diagram representation of the limit detection implementation and its interface with the engine simulation.

The main features of event simulation are detailed in Figure 39. A selectable threshold C_{th} is used to obtain a μ-SM table, via interpolation of experimentally obtained data (Figure 28). This is performed only once, as part of the initialization routine. The core module consists of a Random Number Generator (RNG) proposed by Marsaglia and Tsang [33]. This RNG generates random numbers with an exponential distribution using the ziggurat algorithm, an efficient method that can construct series of random numbers with any desired distribution. At each time step, a new number is generated and compared to a threshold level. This level is updated every time-step, based on current stall margin as available from engine dynamics, and the μ-SM table obtained above.

If a downward crossing is detected, an event is triggered. This event is not directly passed to the limit avoidance controller, but is entered in a first-in-first-out list. The length of the lists corresponds to a information time delay parameter, T_d. This parameter has been introduced to model practical aspects of control implementation. T_d is an addition to the delay of $15\,ms$ due to fuel transport phenomena, modeled into the Fuel Metering Valve. Hence T_d reflects any pure time delay present in a control system due to inevitabilities like loop rates and data transfer rates. The correlation measure algorithm is extremely efficient, and can be calculated at rates upwards of $1\,KHz$ on moderately fast hardware. Thus correlation measure, in itself, does not add significant time delays to the control loop.

The stochastic nature of the events implies that a single run of the simulation cannot be used as an indication of success or failure. In such a situation, a Monte-Carlo simulation is typically performed. This involves repeating a given simulation run with a different set of random numbers. As is usually true for algorithmic random number generators, the RNG used needs a seed or starting value. If a fixed seed value is used, the RNG reproduces the same sequence of random numbers, contrary to the requirements of Monte-Carlo simulation. Consequently, in the current implementation, the RNG is seeded with a random number obtained via the UNIX facility */dev/random* on initialization. This ensures that the RNG generates a different sequence of random numbers with every run of the simulation program.

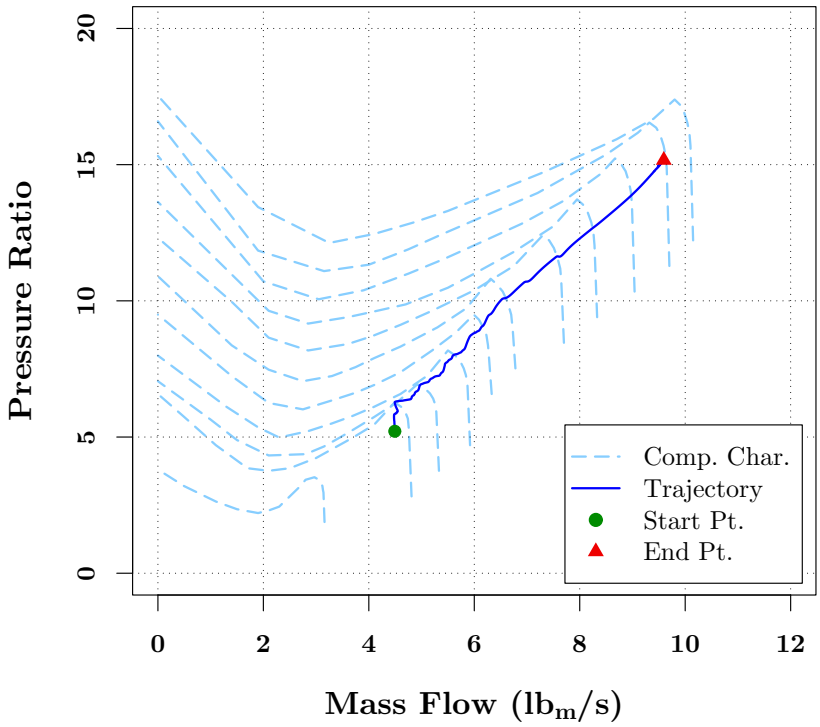

Figure 40: The trajectory for the degraded engine with active fuel control. The stochastic model parameters are $C_{th} = 0.82$ and $T_d = 10ms$.

4.1.2 Limit Detection and Avoidance via Fuel Modulation

The case study in Chapter 2, Section 2.3 illustrated the benefits of active management over the passive fuel acceleration scheduler, with regards to engine dynamic response. In particular, it was observed that the active approach lead to a faster response to a step command in torque, a difference quantified by the RPM droop parameter. In those results, control actuation was triggered on the basis of compressor stall margin. The results presented here also analyze the same step change in torque required. However, in this case, the controller is triggered by stochastic alarms generated by the limit detection model. The stochastic nature of events implies that for a fixed simulation scenario, surge may not be successfully avoided in every run.

The results presented in Figures 40 and 42, which show a successful run, demonstrate the viability of limit avoidance approach. As before, a simple fuel control law is used here, which cuts down the fuel when an alarm is raised by the limit detection module, waits for $10\,ms$, and opens the fuel back to the commanded value. This is achieved via a fuel

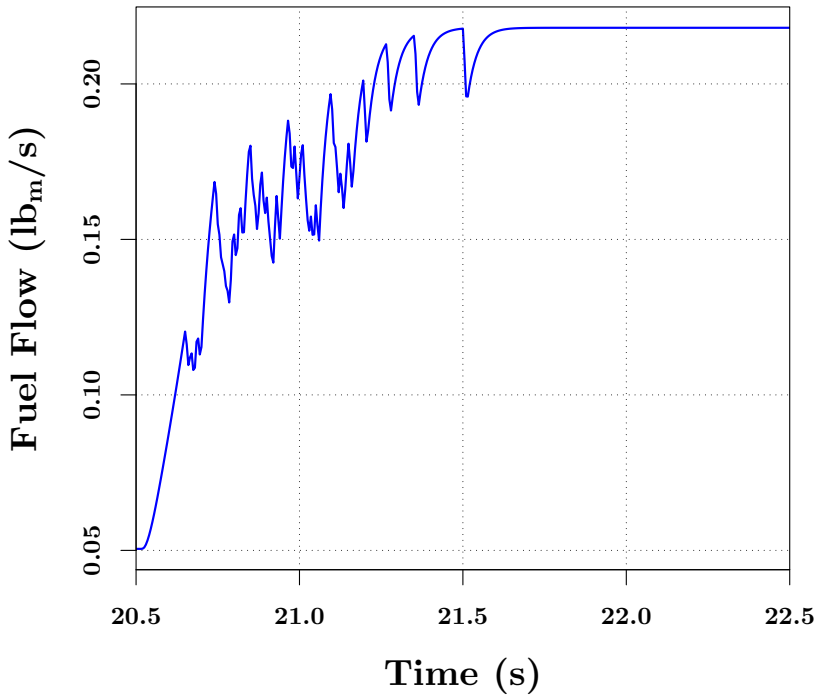

Figure 41: Fuel modulation for surge avoidance using the stochastic model for limit detection.

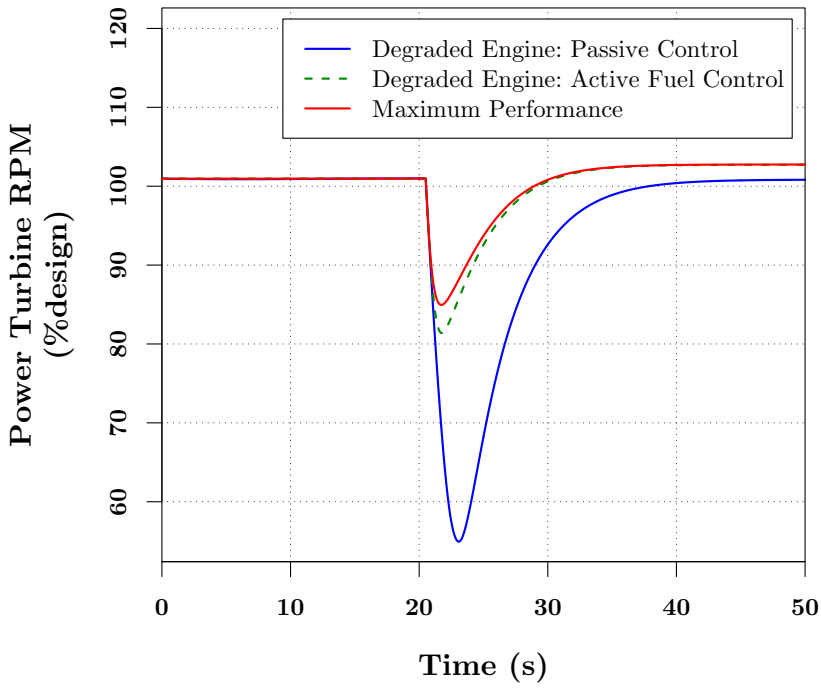

Figure 42: The comparison of RPM variations in the degraded engine between the open-loop acceleration scheduler and active fuel control for surge avoidance.

modulation pulse, $\mathbf{W_{f_{mod}}}$, as shown in Figure 3. The pulse is $10\,ms$ wide and, while active, cuts the fuel flow rate to half of that determined by the nominal fuel control system. The resulting fuel flow rate, which enters the engine through the fuel metering valve, is traced in Figure 41. Note that only a small part of the run, where fuel control is active, has been shown. The threshold has been set at 0.80 and an information related pure time delay of $10\,ms$ has been used for these results. A trace of the engine trajectory on the pressure rise, mass flow rate state-space is shown in Figure 40. When the compressor gets close to the surge line, active fuel control keeps it within the safe region. A comparison of RPM droop in the active control case to that in the nominal case, presented in Figure 42, shows that limit avoidance control achieves significant improvements in the engine dynamic response. Moreover, a comparison to the unrestricted case shows that active avoidance attains nearly maximum level of performance. The maximum level is delivered using the nominal compressor map and without any restrictions on fuel flow rates by the control system. It is interesting to note that the active avoidance matches this level of performance with a degraded compressor.

Once the performance benefits and the feasibility of limit avoidance have been established, further studies have focused on the impact of the two parameters, namely, the information delay T_d and the threshold C_{th}. As part of a Monte-Carlo simulation, each case, characterized by a pair of C_{th} and T_d values, has been repeated hundred times. The results can be different for each run because a different sequence of random numbers generated is every time. The engine transient corresponds to a step change in torque, as seen in the results presented above. The transient is such that the compressor will enter a surge cycle if some form of stall prevention mechanism is not used. A successful run is one where active control prevents any occurrence of surge during the transient.

Results of the Monte-Carlo simulation are recorded in terms of success-rates as a function of information delay, T_d and threshold levels, and are shown in Figure 43. The success-rates are independent of T_d for its values up to $30\,ms$. As expected, for the same range of T_d, success-rates are strongly dependent on the threshold level, C_{th}. It follows that for short time delays, success-rates are only dependent on the distribution of time between successive

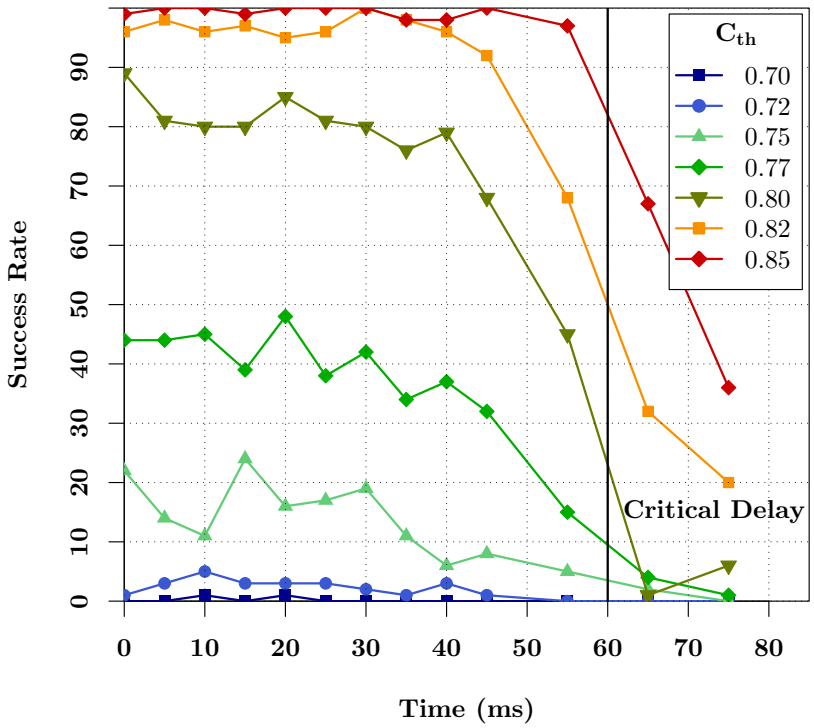

Figure 43: Monte-Carlo Simulation results: Success rate as a function of information delay T_d and threshold C_{th}.

events (TBE). As any implementation would aim to minimize time delays, this part of the regime is relevant to practical control systems.

As T_d is increased beyond $40\,ms$, the success-rates fall sharply with increasing T_d. The probability of success is still dependent on C_{th}, emphasizing that TBE distribution continues to be important. Finally, there exists a critical information delay value, $T_{d\ crit}$, beyond which surge limit avoidance may not be reliably achieved via active control, irrespective of the chosen threshold. It is important to note that this critical value is not only a function of the system in question, but also the particular transient under consideration. Specifically, "fast" transients would tolerate smaller critical values, while in "slow" transients one may be able to get away with larger time delays.

It may be observed in Figure 43 that even with C_{th} at 0.85, and low values of T_d, successful limit avoidance is not achieved in all the runs. In practice, the situation is expected to be better. In fact on the GTAxial Rig it is possible to select a threshold such that stall avoidance is successfully executed every time. With regards to the simulation

results, as mentioned before, the μ-SM relationship used in the simulation is derived using the GTAxial Rig results (Figure 28). The average number of events in HSC-A results is several magnitudes larger, e.g. as shown in Figure 34(d). If the HSC-A numbers were to be used, success-rates would improve.

It follows that the results in Figure 43 show the generic features of the problem, and are not indicative of actual absolute values. In particular, when overall delays in the control loop are kept to a minimum, it is expected that the success of limit avoidance would depend on the selected threshold level.

4.2 Stability Management on a Compressor Rig

In order to demonstrate the effectiveness of correlation measure based stability management, experiments have been performed on the GTAxial Rig. Figure 44 shows a schematic of this facility, when operating in the closed-loop mode. A standalone, portable real-time computer, designated as PXI-RT, calculates the correlation measure using pressure signals from an over the rotor sensor. The sensor is fixed to the compressor casing, and situated above the rotor mid-chord. The PXI-RT computer also tracks any threshold crossings by the correlation measure and raises an alarm signal when one is detected. Another computer, also operating with real-time constraints, implements the surge avoidance logic based only on this alarm signal. A butterfly valve downstream of the plenum provides the only required control input to the entire compression system. The modular setup provides for a flexible operation of the facility. As a side effect, the split architecture contributes time delays in the control loop and ensures that unrealistic results are not achieved in the laboratory environment. further details of the GTAxial compressor facility are included in Appendix A

Two scenarios have been implemented to demonstrate limit detection based compressor stability management, "ride the limit" and surge avoidance under fast throttle transients. The control law used is similar to that used in the engine simulations. Essentially a "open-pause-close" sequence is executed by the control computer for every alarm received. The throttle is opened at a fixed rate for the duration of the alarm. As opening the throttle unloads the compressor, its operating point moves away from the surge line. The controller

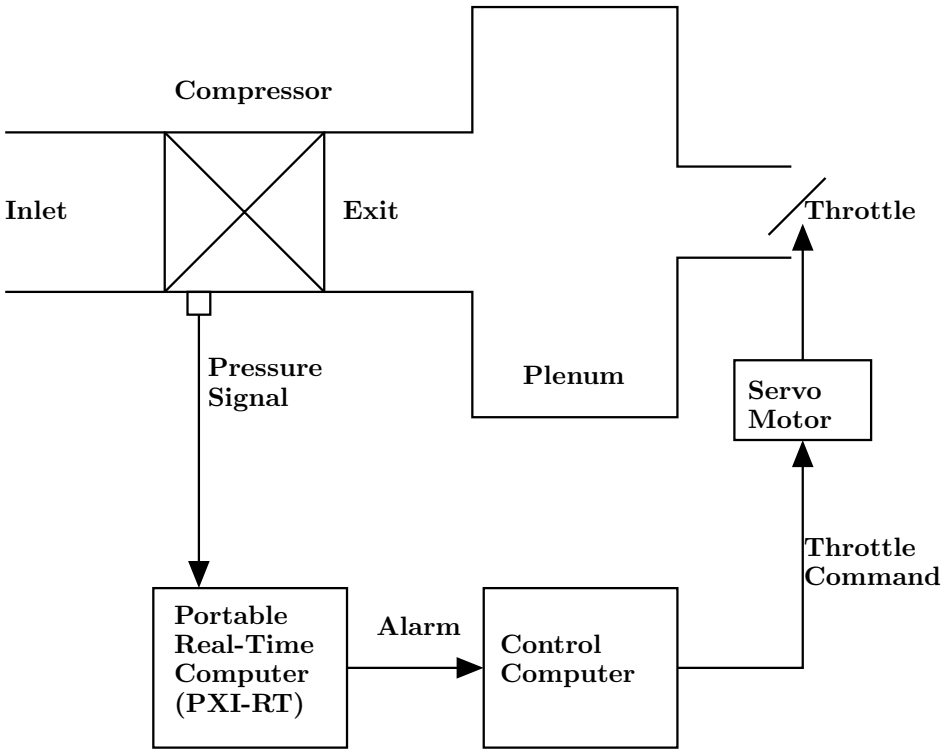

Figure 44: Block diagram representation of the control architecture used in the GTAxial Rig.

then waits for a short time interval, and if no further alarms are received, it closes the throttle at a fixed rate up to its operator commanded value.

The objective for the "ride the limit" case is to keep the plenum pressure as close to the maximum deliverable by the compressor as possible, without crossing the stall boundary. Typical results for "ride the limit" have been presented in Figure 45. A $25\,s$ segment shows the pressure ratio, commanded and controlled throttle values, and the alarms. An alarm value of two corresponds to the open-throttle phase, one to hold, and zero to the close-throttle phase. The pressure ratio is shown as a percentage of the maximum attainable. The system is held at $4-5\%$ stall margin by the stall avoidance controller. The operator command is set deep into the unstable region. This ensures that even small deficiencies in the controller will be manifested as surge cycles of the compression system. As far as "ride the limit" is concerned, the simple control law has been found to be adequate and can hold the system close to the stall line indefinitely. In a practical application, a more sophisticated control law may be designed to eliminate the chattering which can be observed

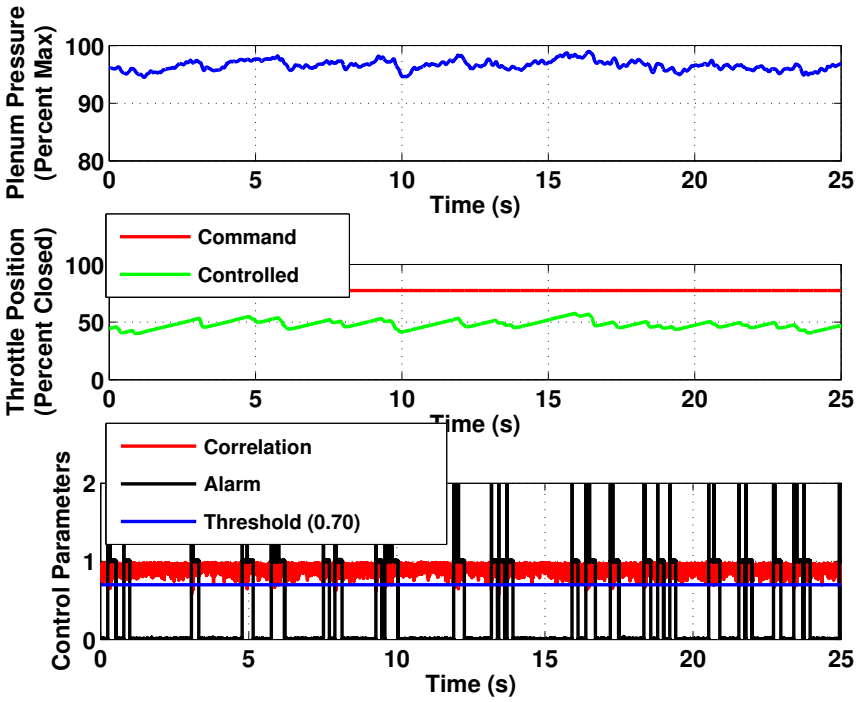

Figure 45: GT-Axial Rig Results. The simple open-pause-close control law keeps the system close to its maximum pressure operation.

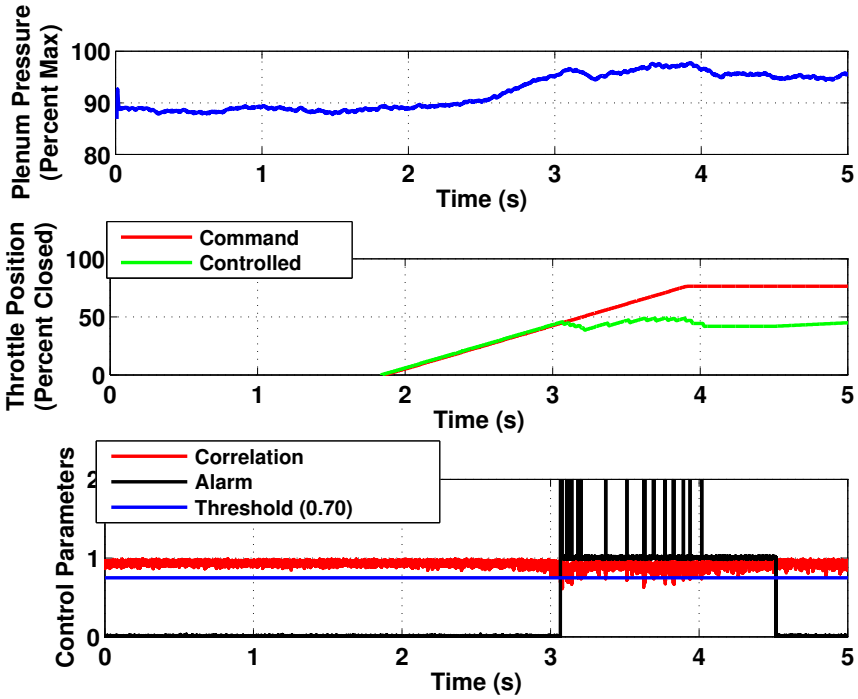

Figure 46: GT-Axial Rig Results. The open-pause-close controller is able to avoid surge under throttle transients.

in Figure 45. As discussed before, the dips in correlation measure occur intermittently. This is also evident in the time trace of alarms shown in the lower chart of this figure. As noted, the threshold level for the correlation measure has been set at 0.70 in this case.

The next scenario involves rapid changes in commanded throttle position. A ramp command profile is executed, where the throttle is closed from its fully open setting to one corresponding to deep stall in two seconds. Incidentally, the system reaches the limit of its stable operation in about one second after the command is initiated. The situation is analogous to engine acceleration transients analyzed in simulations earlier. The objective here is to track the commanded throttle as long as it is safe to do so, while keeping the compression system free from surge. Typical results are presented in Figure 46. For these results, the threshold level has been set at 0.75. The transient was initiated slightly before $t = 2\,s$, the controlled throttle value tracks the commanded value up to a little over $t = 3\,s$. The occurrence of alarms, as observable in the lower chart, causes the controller to deviate from the commanded throttle value and prevents the system from entering into surge oscillations. The operation beyond $t = 4\,s$ is identical to the "ride the limit" scenario. The controller actively adjusts the throttle position in an attempt to maximize pressure ratio, while keeping the system safe.

The results of the Monte-Carlo simulation highlighted the importance of selecting threshold levels for achieving acceptable success rates. Analogous experiments have been carried out on the GTAxial Rig. This involves executing a series of ramp throttle transients, similar to the one analyzed above. The results, presented in Figure 47, emphasize the stochastic nature of the correlation measure based alarms. The figure shows roughly ten transients from a sequence of twenty transients. Active surge avoidance failed in two out of the twenty transients performed. This translates into a 90% success rate at the selected threshold level of 0.75. It is possible to achieve a near 100% success rate either by selecting a higher threshold value, or increasing the rate at which throttle is opened. However, this set of parameters has been deliberately selected to illustrate the importance of threshold levels in active stability management.

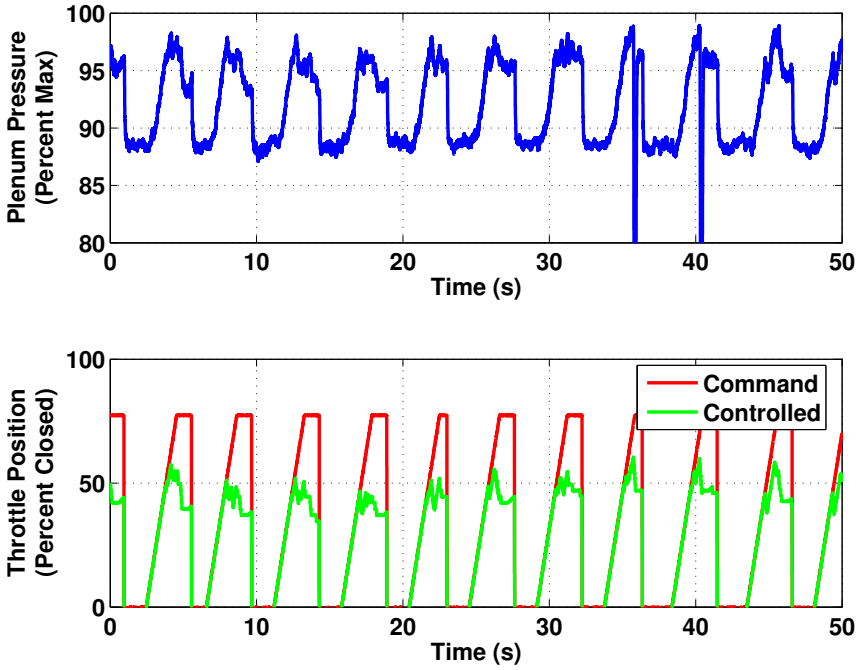

Figure 47: Importance of threshold parameter C_{th} for surge limit avoidance. A poor choice coupled with stochastic nature of alarms can lead to failure of the controller.

4.3 Stability Management on a Gas Turbine Engine

As mentioned above, the GTAxial facility employs a portable computer for a real-time implementation of the correlation measure algorithm. This portable hardware facilitates rapid integration with different experimental platforms. In particular, it has been used to demonstrate the feasibility of correlation measure based stability management in full-scale engine tests conducted by GE Aircraft Engines [8].

The demonstration involved a series of deceleration-acceleration cycles, sometimes referred to as "bodes". Bode tests are frequently performed with fuel enrichment to demonstrate excess stability margins as part of engine certification. In these tests fuel enrichment as well as distortion screens were employed to push the engine into stall. Open loop tests were conducted to validate the limit detection capability of the correlation measure technique. In a series of transients, this technique successfully raised impending stall warning. The open loop tests were followed by a series of closed loop tests. In all cases, correlation measure generated an alarm which triggered a fuel enrichment deactivation routine, preventing engine stalls.

4.4 Summary

Limit detection and avoidance can be used to actively manage the compressor stability margin. Its viability has been established through simulations, and through experimental studies. This approach has the potential to improve the engine dynamic response, without deteriorating design point efficiencies. Further, this approach utilizes routine control devices, available on production engines. The downward crossing of a specified threshold level by correlation measure has been used to detect proximity to compressor stability limit. The threshold level selection plays a critical role in the success of active stability management. This aspect has been highlighted via simulations as well as laboratory experiments.

CHAPTER V

CORRELATION MEASURE: APPLICATIONS BEYOND STABILITY MANAGEMENT

The correlation measure technique is at the core of the compressor stability management approach pursued here. It is understood that correlation measure captures flow phenomena local to the rotor tip region. Irrespective of the particular phenomena involved, the impact of sensor location corroborates their local nature. This characteristic of correlation measure enables its application to problems not directly related to compressor stability. This chapter illustrates two such applications. The first is the so called stage matching problem, where the onus is to equally distribute loading across the different stages in a multistage compressor. The second problem deals with health monitoring. The examples used are admittedly contrived, but still show the potential of correlation measure in this aspect.

5.1 Vane Schedule Optimization

In a multi-stage compressor different stages may not be equally loaded for its entire operating range. In general, the front stages are loaded more than their rear counterparts at low speeds, whereas rear stages are under higher loads at high speeds. In order to attain optimum performance and efficiency, one of the goals in multi-stage compressor design is to match the stages at the design point, i.e., ensure that loads are equally distributed across each stage. The variable features of compressor geometry can be employed to extend stage matching to other operating points. These features include inlet guide vanes and movable stator vanes, typically on the front two or three stages. Although it would be aerodynamically advantageous to have movable vanes on all the stages, this advantage is sacrificed in favor of reducing mechanical complexity.

Vane angles are typically scheduled as a function of compressor speed. The schedule is determined using a combination of past experience, theoretical/numerical predictions and

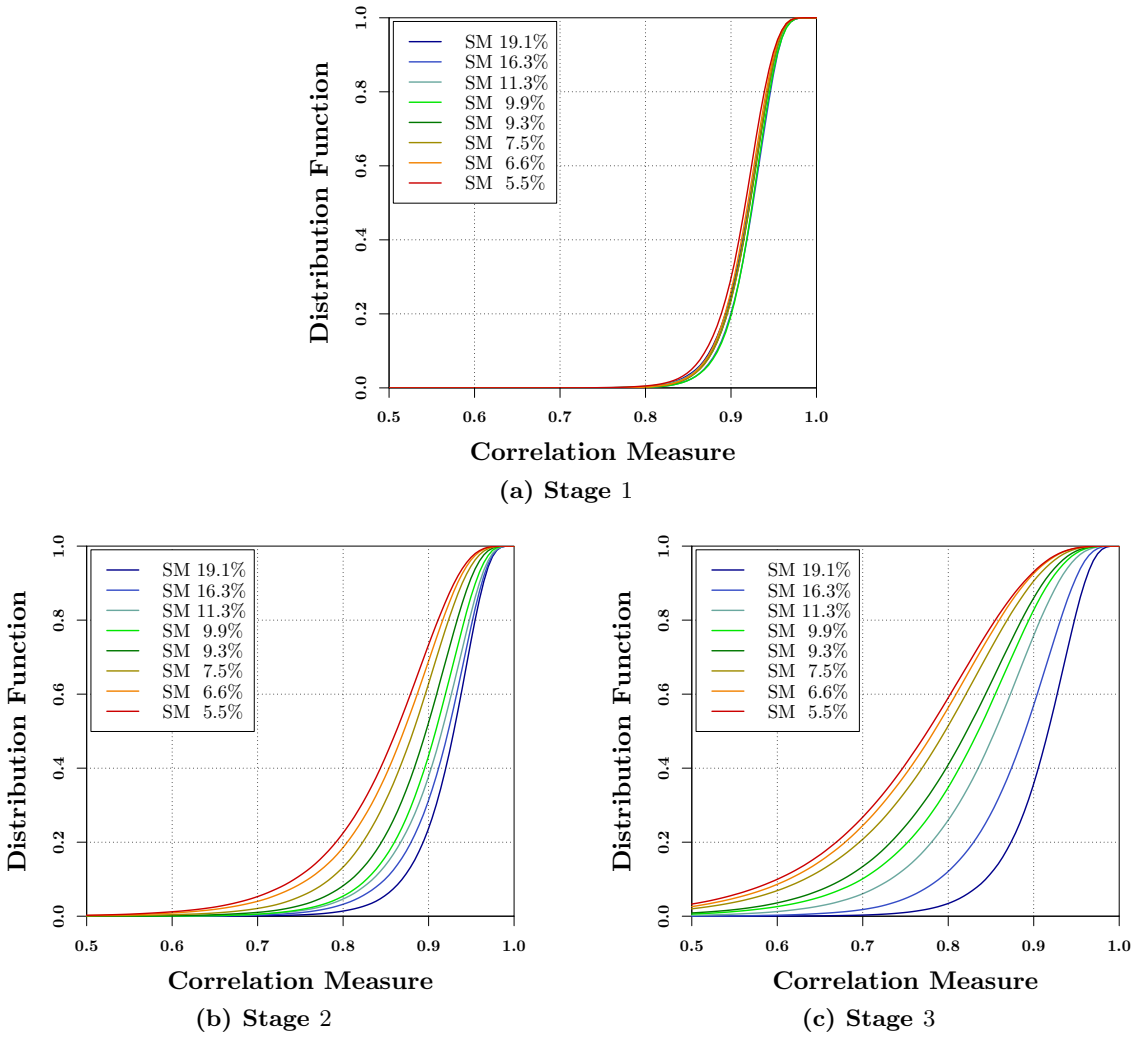

(a) Stage 1

(b) Stage 2

(c) Stage 3

Figure 48: Load distribution across the first three stages of HSC-A, as visualized via correlation measure. The compressor is operating at 92% speed, and data from respective mid-chord sensors has been used.

rig tests. The compressor design process can derive significant benefits from an ability to measure relative stage loading. An online measurement would enable a quick optimization of vane schedule, reducing the number and time of tests required.

Correlation measure can provide a quick assessment of relative stage loading in a multi-stage compressor. The basic concept has been illustrated via results obtained on the HSC-A compressor. The behavior of the correlation measure for the first three stages can be compared in Figure 48. In this case the compressor is operating at 92% speed. At any given compressor stall margin, correlation measure is highest for the first stage, followed by the second and third stages. As chaos in the flow is expected to increase along its path, this

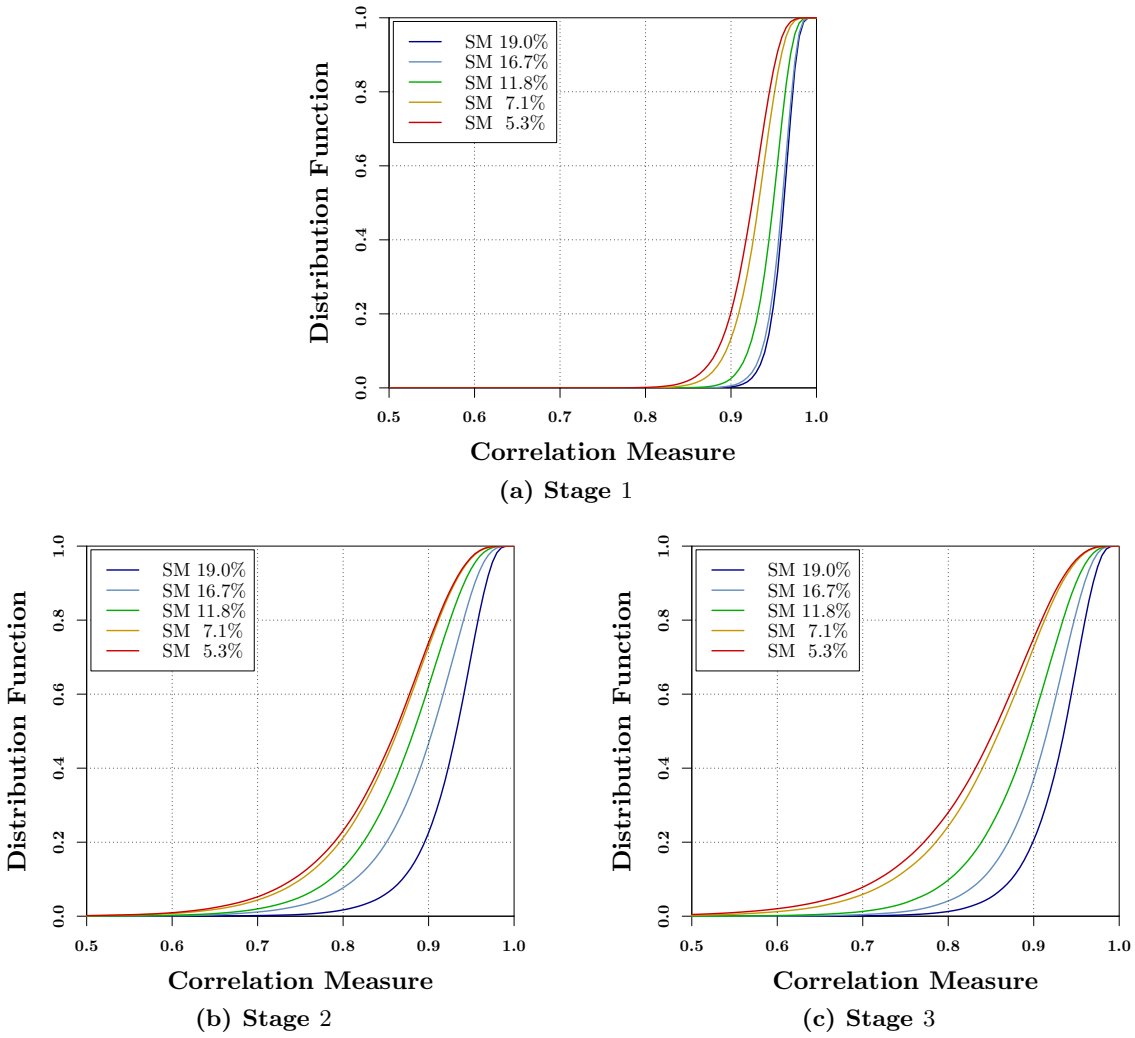

(a) **Stage** 1

(b) **Stage** 2

(c) **Stage** 3

Figure 49: Load distribution across the first three stages of HSC-A, as visualized via correlation measure. The compressor is operating at 97% speed, and data from respective mid-chord sensors has been used.

gradation of correlation measure cannot be inferred as a reflection of relative stage loading. However, the correlation measure values for the first stage exhibit little variation with the overall compressor stall margin. Following this observation, in this case, an increase in compressor loading is not reflected by the first stage.

Analogous results with HSC-A operating at 97% provide a contrasting view. In this case, correlation measure for the first stage decreases as compressor stall margin is reduced (Figure 49(a)), suggesting that the first stage also contributes to the increase in compressor loading. Further, a comparison of Figure 48(c) and 49(c) shows that the third stage sustains larger loading levels at 92% speed. The second stage shows similar levels of loading for the

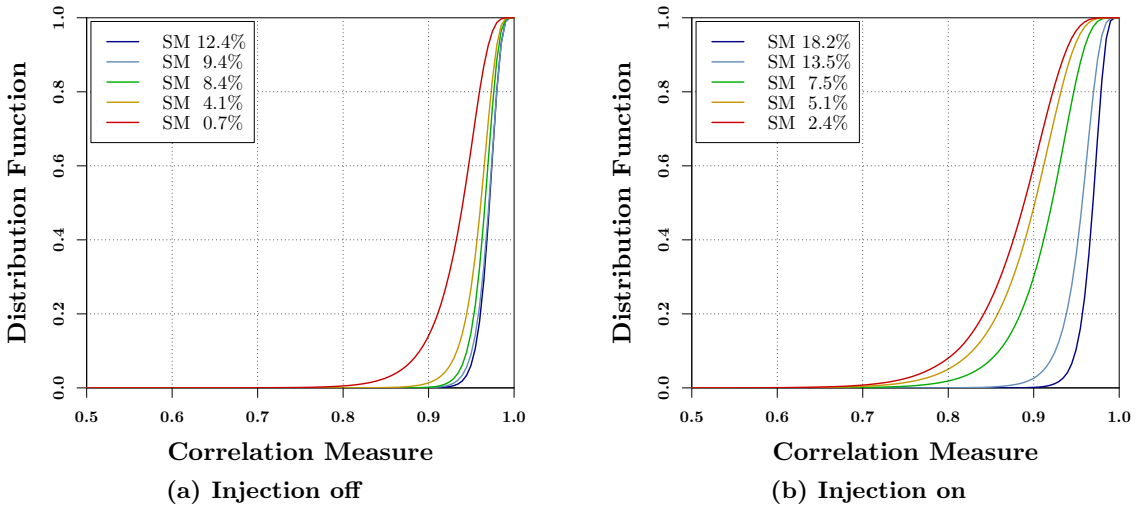

Figure 50: An illustration for the dependence of correlation measure on stage loading. Injection downstream of the second stage increases its loading, lowering the correlation measure values in the "injection on" case. The compressor is operating at design speed.

two speeds. Together, these observations imply that the three stages have been evenly loaded in the 97% speed case.

The suitability of correlation measure for analysis of the stage matching problem is substantiated by results obtained on the HSC-B compressor. In this compressor, external flow can be injected between the second and third stages. As the exit flow is governed by a discharge valve, injecting flow reduces the rate of mass flowing through the stages upstream of the injection point, thus effectively increasing their respective loading. In HSC-B, as the flow is injected at a plane between the second and third stages, second stage loading is expected to increase when injection is turned on. The behavior of correlation measure calculated using a mid-chord sensor on the second stage is consistent with this expectation. This can be observed in Figure 50 which compares the "injection off" and "injection on" cases. In the "injection on" case, with the compressor operating at design speed, the correlation measure exhibits a larger variation with stall margin. Moreover, for comparable stall margin, correlation measure is lower with flow injection, e.g., 4.1% stall margin case in Figure 50(a) has higher correlation measure values than 5.1% case in Figure 50(b).

It follows that correlation measure calculated for a particular stage reacts to its specific loading levels. For a given compressor stall margin, correlation measure for a given stage

is lower if its loading levels are relatively higher. Consequently, correlation measure can be used as an aid to vane schedule optimization.

5.2 Blade Health Monitoring

It has been observed that correlation measure quantifies local flow behavior. So far it has been emphasized that the pertinent flow phenomena are local to the rotor. In fact, the phenomena can be associated with a particular blade on a given rotor, and this can be used to monitor the aerodynamic health of rotor blades. The GTAxial Rig has been used to illustrate this point. Aerodynamic performance of two diametrically opposite blades has been degraded by applying a thin strip of clear tape. This tape has been applied aft of the leading edge and spans half the blade height, starting from the tip.

A comparison of correlation measure results for the nominal and "unhealthy" blades shows that "unhealthy" blades can be identified via correlation measure. This is illustrated via Figure 51, which shows the correlation measure as a function of circumferential angle and rotor revolutions. The two dark regions visible in Figure 51(b), that run parallel to each other, are characterized by fixed circumferential location and identify the tampered blades. These regions are an artifact of the two blades exhibiting correlation measure values that are consistently lower than respective neighbors.

Another perspective of the consistently lower correlation measure can be obtained via the ensemble averaging technique. At each circumferential location, correlation measure is averaged across several rotor revolutions. In essence, random variations at a particular location are smoothed out, and average correlation measure is obtained as a function of circumferential angle. Ensemble averages of the correlation measure depicted in Figure 51 have been calculated and the results are presented in Figure 52. The results show significant drops in average correlation at about 90° and 270° location, corresponding to the"unhealthy" blades. Thus ensemble average highlights the impact of the tampered blades and also provides a method to algorithmically identify them.

Similar results have been obtained on the LSRC facility. In this case a single blade has been tampered along the same lines as the GTAxial Rig. The results for nominal as well

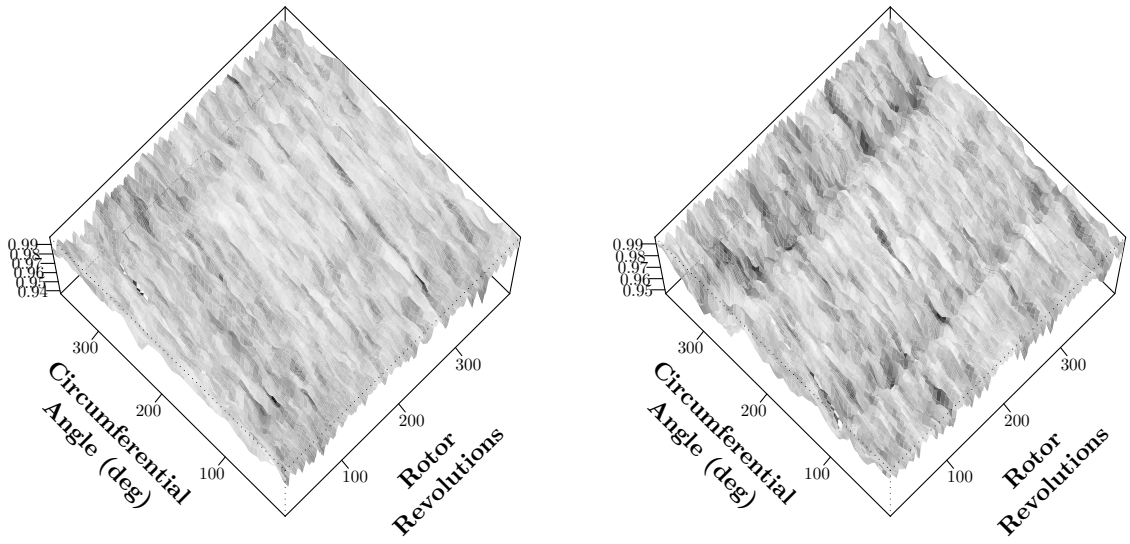

(a) Nominal Blades

(b) Unhealthy Blade Case: Two "unhealthy" blades

Figure 51: Application of the correlation measure to blade aerodynamic health monitoring. These results have been obtained on the GTAxial Rig.

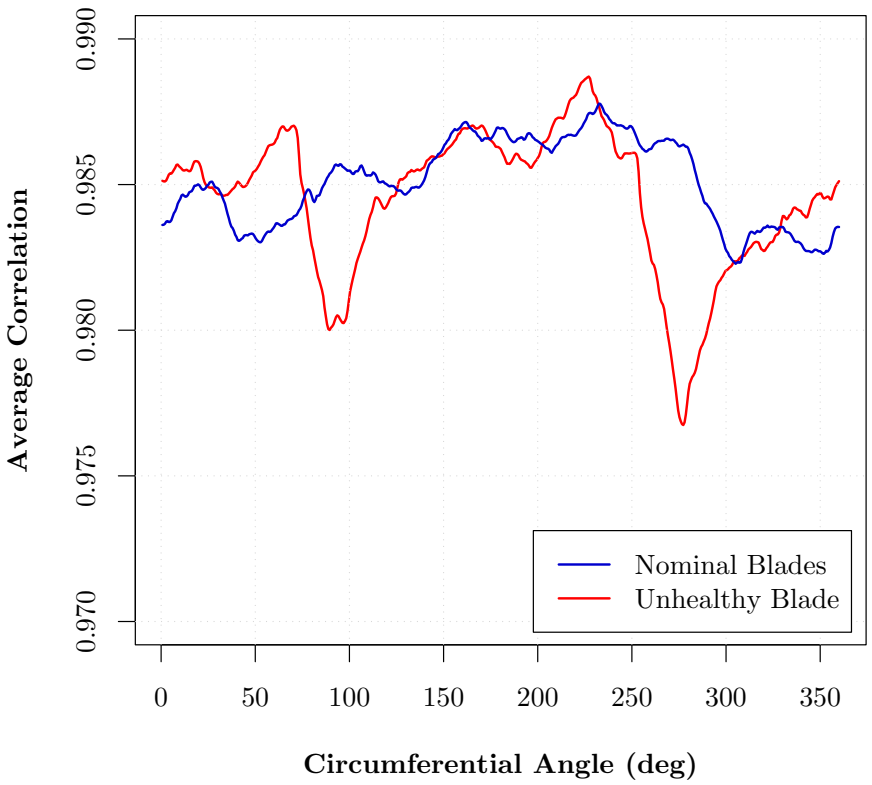

Figure 52: The use of ensemble averages for the detection of unhealthy blades.

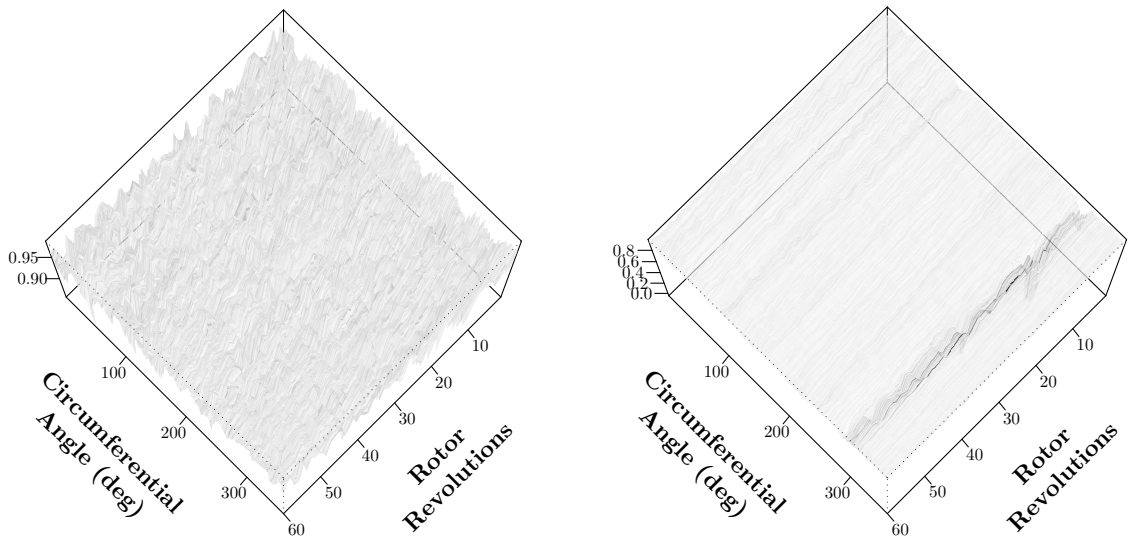

(a) Nominal Blades

(b) Unhealthy Blade Case: One "unhealthy" blade

Figure 53: Application of the correlation measure to blade aerodynamic health monitoring. These results have been obtained on the LSRC facility.

as "unhealthy" case are given in Figure 53. The dark band at roughly 280° circumferential angle, apparent in Figure 53(b), corresponds to the tampered blade.

Correlation measure can be used to identify blades with aerodynamic deficiencies. However, these deficiencies can only be identified if they degrade the dynamic nature of the flow, i.e., make it more chaotic. It follows that it would be possible to detect structural defects, provided they affect the regularity of flow over the associated blades.

5.3 Summary

The correlation measure technique has been derived to facilitate compressor stability limit detection. It captures flow phenomena local to a specific rotor, and even a particular blade. Its local nature can be exploited in applications other than stability limit detection. In particular, results illustrate its potential for problems pertaining to stage matching and health monitoring.

CHAPTER VI

CONCLUDING REMARKS

Over the last five decades, extensive research has been carried out in the area of compressor stability. The focus of these efforts has ranged from investigating the nature of aerodynamic instabilities to controlling them via feedback control methods. Specifically, the development of a control oriented analytical model spurred several studies in active stall control. However, recent experimental investigations on stall inception have found multiple routes to stall that are not predicted via any available model. The inability of analytical models to predict all types of stall inception mechanisms signifies the existence of unmodeled, yet non-negligible, flow phenomena. Consequently, model based stall control techniques are currently infeasible.

The research carried out as part of this dissertation has adopted a different philosophy. Specifically, compressor stability management is emphasized over active stabilization. Steady operation at the peak of the compressor characteristic is precluded, not only from stability concerns, but also from efficiency and performance considerations. In this light, the objective has been defined as the active management of available compressor stability margin. A limit detection and avoidance approach can be used to keep the compressor free from aerodynamic instabilities. This ability can benefit the engine design in two related ways. It can either improve the dynamic response of a gas turbine engine, or lower the stall margin requirements at the design point, while ensuring existing dynamic response. The appropriate choice would depend on the particular application.

6.1 Conclusions

As part of the investigations pertaining to compressor stability management, three experimental facilities associated with four compressors have been utilized. Some aspects of the problem have also been explored in a simulation framework. This simulation models a turbo-shaft gas turbine engine, a type typically used on helicopters. The results of these

studies can be summarized as:

- Active stability management can lead to improved transient engine performance. It is important to note that this improvement is not contingent upon new actuation mechanisms or improved actuators.

- Previous work has suggested that the stability of a compression system can be related to the trajectory followed by the tip-leakage vortex. Hence, the dynamic nature of flow over the rotor tip contains information relevant to the stability of the entire system. This information can be quantified by application of the correlation measure technique. Statistical analysis of the experimentally obtained correlation measure shows that sharp drops in its value, that can be observed from time to time, are more relevant to compressor stability detection than its average value.

- Sensor location has a significant impact on the behavior of correlation measure. In general, a sensor located at the axial projection of rotor mid-chord is suitable for correlation measure application. Specifically, correlation measure of the pressure signals obtained from this location decreases as the compressor is progressively loaded. It is reiterated that unusual compressor configurations may require a survey of sensor locations.

- The significance of the sharp drops in correlation measure can be captured by tracking threshold crossings. A stochastic model for the time between successive crossings has been developed. The exponential distribution of the stochastic model closely emulates the experimentally observed behavior. However, differences between the two exist, possibly due to the contributions of non-exponential and/or non-stochastic processes.

- The stochastic behavior of the threshold crossings has been incorporated into the engine simulation. A Monte-Carlo simulation carried out within this framework, highlights the importance of threshold selection to successful stability management.

- Correlation measure based active stability management is practically feasible. Closed loop control has been demonstrated on a laboratory compressor facility.

Although these aspects require further analysis, correlation measure can be used to address the compressor stage matching problem and blade aerodynamic health determination.

6.2 Contributions

A novel approach to compressor stability has been detailed in this work. The techniques necessary for its implementation have been developed. The approach has been successfully demonstrated in simulations, on compressor rigs, and in engine tests. The major contributions of this work can be summarized as:

- A different perspective to the problem of the compressor control has been introduced. In particular, the feedback control framework has been dropped in favor of the concept of stability management.

- A measure called the correlation measure has been developed. The threshold level crossings of this measure can be used for compressor stability limit detection. A successful application of correlation measure neither requires, nor utilizes any information about the compressor performance map.

- A model for the time between successive threshold crossing events has been derived. This model is an application of available formulae describing the properties of level-crossings by stochastic processes. This stochastic model can aid in simulation based evaluations of controller designs.

6.3 Recommendations

The successful demonstration of correlation measure based stability management has opened several avenues for future research efforts. Some of these include:

- The demonstration of correlation measure based compressor stability management has employed a simple architecture. A fixed, predetermined, control action is performed for each observed event. In particular, the events are binary and are not associated with any magnitude. Such a strategy could introduce "choppiness" in the system. The development of a smooth control law, one which may need to assign a magnitude

to the events, merits further consideration. It may also be necessary to incorporate the stochastic nature of the events into the control law. Further, an integrated control law should also take combustion instabilities into account and not excite any known undesirable frequencies of the system.

- The stochastic model of the time between successive events developed in this work could be refined, especially for smaller values of time between events. Moreover, this model may provide deeper insight into the flow phenomena quantified via the correlation measure. In turn, this could provide a better understanding of the end-wall flow, near the compressor casing.

- As the correlation measure quantifies the chaos in a pressure signal, it would be affected by measurement noise. It may be noted that all the experimental results obtained so far are already subject to measurement noise. This noise tends to lower the value of the correlation measure and may even generate spurious events at any given threshold setting. The sensitivity of the events to threshold setting in the presence of noise, with a special focus on the stochastic model, needs to be analyzed. It may be possible to use dual thresholds, one to generate an event and another, slightly higher value, to clear the event, and consequently reduce sensitivity to noise.

- In terms of deployment on production engines, it is necessary to realize that all aircraft control systems have to be certified as flightworthy. Due to the stochastic nature of the correlation measure based stability management, it cannot be characterized in terms of the classical control theory. New certification methods have to be developed that can characterize stochastic controllers and ensure continuing safety and reliability of aircraft systems.

- Although the correlation measure has been primarily developed as a stability limit detector, it may be employed in other applications. Two such applications have been evaluated. The results suggest that correlation measure can aid in balancing stage loads in a multi-stage compressor. Further, its localized characteristic can be exploited

to monitor aerodynamic health of the rotor blades. Future efforts should be concentrated on the applications of correlation measure beyond stability limit detection.

- Compressor stability management, within the broader framework of intelligent engines, requires sensors to be placed in high temperature environments. It is very important that the employed sensors should be reliable and possess a long operational life even under high temperatures. Optical sensors can fulfill these requirements and this subject needs to be explored.

- Another aspect of application on an engine is the problem of correlation measure fusion. Specifically, how should the different correlation measures, calculated using pressure signals from each stage on a multistage compressor, be combined? The solution could range from a simple "use the worst value", to moderately complex "weighted mean of the correlation measure", or even highly complex where each stage has an independent contribution to the overall fuel control law. The simple approach should be given preference. However, correlation measure should be calculated for all compressor stages in future tests and issues pertaining to information fusion studied.

APPENDIX A

GEORGIA TECH. AXIAL COMPRESSOR RIG

The axial compressor facility located in the School of Aerospace Engineering at Georgia Institute of Technology has been established to facilitate control-oriented studies in surge and rotating stall. This facility consists of an axial compressor rig, control hardware, as well as data acquisition hardware. The facility can be operated in dual modes: open loop data-acquisition mode and closed loop demonstration mode. The two modes have slightly different components, as shown in Figure 54. In the open loop mode (Figure 54(a)), human operator sets the throttle position. The throttle is essentially a butterfly valve and its position can be defined in terms of rotation angle. Any change in throttle setting is followed by a a short wait before data is acquired on a desktop computer based data acquisition system (DAQPC). The wait allows the system to settle into steady state operation prior to data acquisition. Each dataset contains eight different operating conditions, starting from fully open throttle position to one very close to stall. Typically, less than 1° rotation of the throttle from the last operating point pushes the entire system into surge. For each operating point, $20\,s$ of pressure signal from an over the rotor sensor as well as one located in the plenum (not shown in the schematic) are recorded at a sampling frequency of $100\,KHz$.

In the demonstration mode (Figure 54(b)), human operator sets the desired throttle position. This setting is modified by the limit avoidance controller based on the alarm signals received from the PXI-RT computer. In addition, there is a provision to turn off the stall/surge limit avoidance control. When the controller is off, the throttle command follows the operator dictated setting, thus emulating open-loop behavior. Although not detailed in the Figure 54, the pressure signals, correlation measure value, alarm signal, controller status and throttle command can all be recorded on the DAQPC system for later analysis.

The following sections provide details on the different parts of the facility.

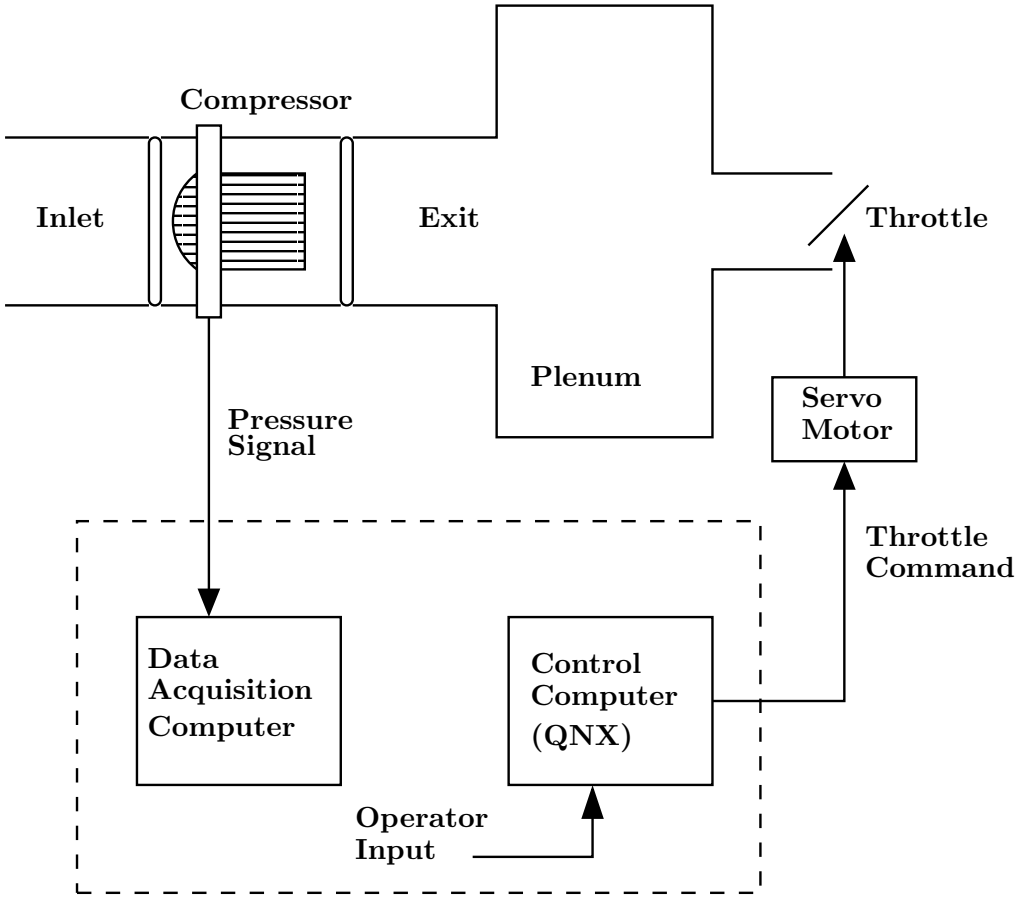

(a) Data Acquisition Mode

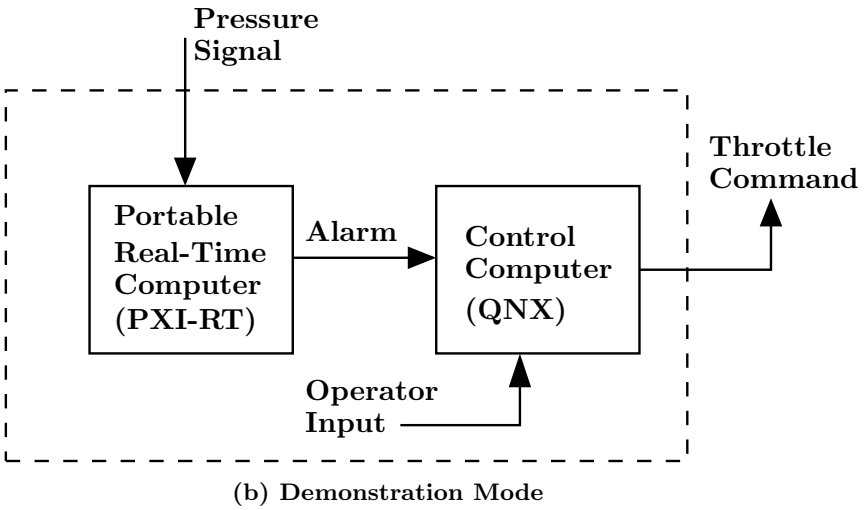

(b) Demonstration Mode

Figure 54: A functional schematic of GTAxial Rig, an axial compressor experimental facility. GTAxial Rig can be configured in either a data acquisition mode, or a demonstration mode.

A.1 Axial Compressor Rig

The axial compressor rig includes an inlet duct, a single-stage axial fan, a compressor discharge duct, a plenum, exhaust duct and a throttle. The room where the facility is housed, is equipped with inlet and exhaust vents. The room ducts prevent any local recirculation of flow, and thus maintain the compressor inlet conditions independent of its exit.

The low speed single-stage compressor, manufactured by Able Corporation, is an electrically driven unit. The 3-phase electric motor is contained within the compressor hub, and is connected to the rotor via a shaft assembly. The compressor delivers a pressure ratio of about 1.035 at sea level conditions. The rotor has fourteen low-aspect ratio blades. On the other hand, the stator has only eleven blades. The design speed is about 11800 RPM at which the tip Mach number is about 0.3. Consequently, the flow through the compressor is entirely subsonic.

The plenum is a large metal chamber with a volume of approximately $1m^3$. It is constructed of $3in$ $(7.62cm)$ aluminium plate and is capable of withstanding pressures up to 400psi. It incorporates a self-entraining burner and is thus capable of simulating a combustor. The burner is equipped with fuel pipes, an igniter, a flame detector and uses propane fuel. The flame detector is a UV-sensor that observes the flame. For ignition purposes the flame detector can be bypassed. In regular operation, the detector cuts off fuel flow if no flame is present. This ensures safe operation of the facility.

The flow exits the plenum through a duct connecting it to the laboratory exhaust. A butterfly valve in thus connecting duct can be used to throttle the mass flow and thus vary the compressor loading. The compressor is instrumented using six high bandwidth pressure sensors. These sensors, manufactured by Kulite Semiconductor Products, use a silicon on silicon Wheatstone bridge to measure pressure and possess natural frequencies of approximately $150\,KHz$. The six sensors are at the same axial location, corresponding to the rotor tip mid-chord, but are evenly distributed along the circumference. Moreover, all the sensors have been mounted such that they are flush to the inside of the compressor casing. The absence of any cavities combined with the high natural frequency of the sensor ensures that the sensing system has a large bandwidth. It may be noted that all the

measurements obtained as part of the present work are from a single sensor.

A.2 Data Acquisition Computer

The data acquisition computer (DAQPC) is a dual processor desktop computer equipped with a National Instruments data acquisition card, AT-MIO-16E-1. This card features a 12-bit analog to digital converter (ADC), with up to 16 single ended or eight differential analog inputs. The card is completely software configurable and does not require any manual setting of jumpers and switches. It has a throughput of 1.25 Mega samples per second. However, the experience to date with this card is that only a throughput of about 1 Mega samples per second can be sustained when acquiring multiple channels. As an example, it is possible to record 4 channels at $200\,KHz$ sampling rate but a combination of 5 channels at the same sampling rate cannot typically be sustained for more than a couple of seconds.

On the software side, the DAQPC uses Windows 2000® operating system. All the data acquisition and visualization functions have been programmed in the LabVIEW® programming environment. For compact data storage, acquired data is save in a binary format, where each sample occupies two-bytes.

A.3 Control Computer (QNXPC)

The control computer is a $200\,MHz$ Pentium™ based personal computer that runs a commercial real-time operating system called QNX. The version deployed is from a previous generation and is fairly primitive by current standards. On the positive side, it is stable, simple, and provides an extraordinary level of flexibility. The analog input and output functionality is available via two Analog Devices plug-in cards: RTI-800 and RTI-802.

The RTI-800 supports the measurement of 16 single-ended or 8 differential inputs. It has a 12-bit ADC with a conversion time of 25 μs, and provides a throughput of 31200 samples per second. The RTI-802 features eight independent channels for voltage output. Each output has a 12-bit digital to analog converter with a settling time of $20\mu s$, allowing for update rates of roughly $40\,KHz$. Both these cards are now obsolete but have been

retained due to their inherent simplicity. In particular, the cards can be directly accessed in a simple "C" program.

All the control software has been programmed in the "C" programming language. Although the hardware as well as the operating system are old, they have the benefit of being simple and easy to use. The simplicity of the system makes it less error prone and eliminates any driver overheads, thus increasing the rates at which control loops can be executed.

A.4 Portable Real-Time Computer

The portable real-time computer (PXI-RT) is an industrial computer manufactured by National Instruments. It consists of a chassis, NI-1042, with 8 slots. The first slot is occupied by a Pentium™ embedded controller and the rest are available for different plug-in cards. Of these, four slots are equipped with four simultaneous sampling multi-function data acquisition cards, PXI-6115. Each of these cards has four analog inputs providing a total of 16 input channels. The cards have a high sampling rate capability coupled with a large onboard memory. An interface to external data storage can be provided by a fifth expansion card. Consequently, this system can serve as a convenient and portable data acquisition system. Moreover, the PXI-6115 cards also feature two digital to analog converters for voltage output.

When used for data acquisition and storage, the embedded controller runs Windows XP® operating system. However, due to the availability of dedicated DAQPC, the data acquisition mode is not used in GTAxial experiments. In the real-time demonstration mode, the systems executes a proprietary operating system, LabVIEW-RT®. This real-time operating system (RTOS) can run standard LabVIEW programs with real-time constraints. In order to optimize execution times, custom compiled code created in the "C" programming language can also be embedded in LabVIEW programs. This technique has been extensively used on the GTAxial Rig. In fact, only the data input and output is performed using standard LabVIEW routines and all other aspects have been implemented via custom "C" routines.

REFERENCES

[1] Badmus, O. O., Chowdhury, S., Eveker, K. M., Nett, C. N., and Rivera, C. J., "Simplified approach for control of rotating stall Part 1: Theoretical development," *Journal of Propulsion and Power*, vol. 11, no. 6, pp. 1195–1209, 1995.

[2] Badmus, O. O., Chowdhury, S., Eveker, K. M., Nett, C. N., and Rivera, C. J., "Simplified approach for control of rotating stall Part 2: Experimental results," *Journal of Propulsion and Power*, vol. 11, no. 6, pp. 1210–1223, 1995.

[3] Ballin, M. G., "A high fidelity real-time simulation of a small turboshaft engine," NASA TM–100991, Ames Research Center, Moffett Field, california, July 1988.

[4] Bindon, J., "Measurement and formation of tip clearance loss," *Journal of Turbomachinery*, vol. 111, no. 3, pp. 257–263, 1989.

[5] Bright, M. M., Qammar, H. K., Weigl, H. J., and Paduano, J. D., "Stall precursor identification in high-speed compressor stages using chaotic time series analysis methods," *Journal of Turbomachinery*, vol. 119, pp. 491–499, July 1997.

[6] Camp, T. R. and Day, I. J., "A study of spike and modal stall phenomena in a low speed axial compressor," in *Proceedings of the 1997 International Gas Turbine and Aeroengine Congress and Exhibition*, June 1997. Paper No. 97-GT-526.

[7] Chen, G., Greitzer, E., Tan, C., and Marble, F., "Similarity analysis of compressor tip clearance flow structure," *Journal of Turbomachinery*, vol. 113, no. 2, pp. 260–269, 1991.

[8] Christensen, D., Cantin, P., Gutz, D., Szucs, P., Wadia, A., Armor, J., Dhingra, M., Neumeier, Y., and Prasad, J., "Development and demonstration of a stability management system for gas turbine engines," in *Proceedings of the ASME Turbo Expo 2006: Power for Land, Sea and Air*, (Barcelona, Spain), May8 – 11 2006. Paper No. GT-2006-90324, In review.

[9] Cramer and Leadbetter, *Stochastic Processes*. Longman Scientific & Technical, 1st ed., 1967.

[10] Cumpsty, N. A., *Compressor Aerodynamics*. Longman Scientific & Technical, 1st ed., 1989.

[11] D'Andrea, R., Behnken, R. L., and Murray, R. M., "Rotating stall control of an axial flow compressor using pulsed air injection," *Journal of Turbomachinery*, vol. 119, pp. 742–752, Oct. 1997.

[12] Day, I. J., "Stall inception in axial flow compressors," *Journal of Turbomachinery*, vol. 115, pp. 1–9, Jan. 1993.

[13] Day, I. J., Breuer, T., Escuret, J., Cherrett, M., and Wilson, A., "Stall inception and the prospects for active control in four high-speed compressors," *Journal of Turbomachinery, Transactions of the ASME*, vol. 121, no. 1, pp. 18–27, 1999.

[14] Day, I. J., Greitzer, E. M., and Cumpsty, N. A., "Prediction of compressor performance in rotating stall.," *Journal of Engineering for Power, Transactions of the ASME*, vol. 100, no. 1, pp. 1–14, 1978.

[15] Denton, J. D., *Loss mechanisms in turbomachines*. Lecture Series Monograph 1999-02, Rhode Saint Genese, Belgium: von Karman Insititute for Fluid Dynamics, Feb. 8–12.

[16] Dhingra, M., Armor, J., Neumeier, Y., and Prasad, J. V. R., "Compressor surge: A limit detection and avoidance problem," AIAA Paper 2005–6449, Aug. 15–18, 2005. Proceedings of the AIAA Guidance, Navigation, and Control Conference and Exhibit, San Francisco, California.

[17] Dhingra, M., Neumeier, Y., Prasad, J. V. R., and Shin, H., "Stall and surge precursors in axial compressors," AIAA Paper 2003–4425, July 20–23, 2003. Proceedings of the 39th AIAA/ASME/SAE/ASEE Joint Propulsion Conference and Exhibit, Huntsville, Alabama.

[18] Emmons, H. W., Pearson, C. E., and Grant, H. P., "Compressor surge and stall propagation," *Transactions of the ASME*, vol. 77, pp. 455–469, 1955.

[19] Epstein, A. H., Williams, J. E. F., and Greitzer, E. M., "Active suppression of aerodynamic instabilities in turbomachines," *Journal of Propulsion and Power*, vol. 5, pp. 204–211, Mar.–Apr. 1989.

[20] Escuret, J. F. and Garnier, V., "Stall inception measurements in a high-speed multistage compressor," *Journal of Turbomachinery*, vol. 118, pp. 690–696, Oct. 1996.

[21] Greitzer, E. M., "Surge and rotating stall in axial flow compressors: Part 2 - Experimental results and comparison with theory.," *Journal of Engineering for Power, Transactions ASME*, vol. 98 Ser A, pp. 199–217, Apr. 1976.

[22] Greitzer, E. M., "Surge and rotating stall in axial flow compressors: Part I - theoretical compression system model," *Journal of Engineering for Power, Transactions of the ASME*, vol. 98 Ser A, pp. 190–198, Apr. 1976.

[23] Gysling, D. L. and Greitzer, E. M., "Dynamic control of rotating stall in axial flow compressors using aeromechanical feedback," ASME Paper 94-GT-292, 1994.

[24] Hoss, B., Leinhos, D., and Fottner, L., "Stall inception in the compressor system of a turbofan engine," *Journal of Turbomachinery*, vol. 122, pp. 32–43, Jan. 2000.

[25] Hoying, D. A., Tan, C. S., Vo, H. D., and Greitzer, E. M., "Role of blade passage flow structures in axial compressor rotating stall inception," *Journal of Turbomachinery*, vol. 121, pp. 735–742, Oct. 1999.

[26] Inoue, M. and Kuroumaru, M., "Structure of tip clearance flow in an isolated axial compressor rotor," *Journal of Turbomachinery*, vol. 111, no. 3, pp. 250–256, 1989.

[27] Inoue, M., Kuroumaru, M., Iwamoto, T., and Ando, Y., "Detection of a rotating stall precursor in isolated axial flow compressor rotors," *Journal of Turbomachinery*, vol. 113, no. 2, pp. 281–289, 1991.

[28] Inoue, M., Kuroumaru, M., Tanino, T., and Furukawa, M., "Propagation of multiple short-length-scale stall cells in an axial compressor rotor," *Journal of Turbomachinery, Transactions of the ASME*, vol. 122, pp. 45–54, Jan. 2000.

[29] Kirtley, K. R., Graziosi, P., Wood, P., Beacher, B., and Shin, H.-W., "Design and test of an ultralow solidity flow-controlled compressor stator," *Journal of Turbomachinery*, vol. 127, no. 4, pp. 689 – 698, 2005.

[30] Liaw, D.-C. and Abed, E. H., "Stability analysis and control of rotating stall," *IFAC Symposia Series*, no. 7, pp. 295–300, 1993.

[31] Longley, J. P., Shin, H.-W., Plumley, R. E., Silkowski, P. D., Day, I. J., Greitzer, E. M., Tan, C. S., and Wisler, D. C., "Effects of rotating inlet distortion on multistage compressor stability," *American Society of Mechanical Engineers (Paper)*, pp. 1–12, 1994.

[32] Markopoulos, N., Neumeier, Y., Prasad, J. V. R., and Zinn, B. T., "Linear versus quadratic amplitude feedback in active control of compressor rotating stall," *Journal of Propulsion and Power*, vol. 16, no. 6, pp. 1164–1173, 2000.

[33] Marsaglia, G. and Tsang, W. W., "The ziggurat method for generating random variables," *Journal of Statistical Software*, vol. 5, Oct. 2000.

[34] Moore, F. K., "Theory of rotating stall of multistage axial compressors: Part I. Small disturbances; Part II. Finite disturbances; Part III. Limit cycles.," *Journal of Engineering for Gas Turbines and Power, Transactions of the ASME*, vol. 106, no. 2, pp. 313–336, 1984.

[35] Moore, F. K. and Greitzer, E. M., "Theory of post-stall transients in axial compression systems: Part I - Development of equations.," *Journal of Engineering for Gas Turbines and Power, Transactions of the ASME*, vol. 108, pp. 68–76, Jan. 1986.

[36] Moore, F. K. and Greitzer, E. M., "Theory of post-stall transients in axial compression systems: Part II - Application.," *Journal of Engineering for Gas Turbines and Power, Transactions of the ASME*, vol. 108, pp. 231–239, Apr. 1986.

[37] Prasad, J. V. R., Krichene, A., and Neumeier, Y., "Active control of compressor surge using a real time observer," in *Proceedings of the NATO Symposium on Active Control Technology*, May8 – 11 2000. Braunchschweig, Germany.

[38] Prasad, J. V. R., Neumeier, Y., Lal, M., Bae, S. H., and Meehan, A., "An experimental investigation of active and passive control of rotating stall in axial compressors," *IEEE Conference on Control Applications - Proceedings*, vol. 2, pp. 985–990, 1999.

[39] Stein, A., Niazi, S., and Sankar, L. N., "Computational analysis of centrifugal compressor surge control using air injection," *Journal of Aircraft*, vol. 38, pp. 513–520, May–June 2001.

[40] Stetson, H. D., "Designing for stability in advanced turbine engines," *Engine Handling*, p. 11, Oct. 1982. AGARD CP3424.

[41] Storace, A. F., Wisler, D. C., Shin, H.-W., Breacher, B. F., Ehrich, F. F., Spakovsky, Z. S., and Martinez-Sanchez, M., "Unsteady flow and whirl-inducing forces in axial-flow compressors. Part I - Experiment," in *Proceedinds of ASME TURBO EXPO 2000: International Gas Turbine & Aeroengine Congress & Exhibition*, May 2000. Paper No. 2000-GT-0564.

[42] Storer, J. and Cumpsty, N., "Tip leakage flow in axial compressors," *Journal of Turbomachinery*, vol. 113, no. 2, pp. 252–259, 1991.

[43] Strazisar, A. J., Bright, M. M., Thorp, S., Culley, D. E., and Suder, K. L., "Compressor stall control through endwall recirculation," *Proceedings of the ASME Turbo Expo 2004*, vol. 5 A, pp. 655–667, 2004.

[44] Tahara, N., Kurosaki, M., Ohta, Y., Outa, E., Nakakita, T., and Tsurumi, Y., "Early stall warning technique for axial flow compressors," in *Proceedings of the ASME Turbo Expo 2004: Power for Land, Sea and Air*, (Vienna, Austria), June14 – 17 2004. Paper No. GT-2008-53292.

[45] Tryfonidis, M., Etchvers, O., Paduano, J. D., Epstein, A. H., and Hendricks, G. J., "Prestall behaviour of several high-speed compressors," *Journal of Turbomachinery*, vol. 117, pp. 62–80, Jan. 1995.

[46] Wang, Y. and Murray, R. M., "Bifurcation control of rotating stall with actuator magnitude and rate limits: Part I - Model reduction and qualitative dynamics," *Automatica*, vol. 38, pp. 597 – 610, Apr. 2002.

[47] Wang, Y., Yeung, S., and Murray, R. M., "Bifurcation control of rotating stall with actuator magnitude and rate limits: Part II - Control synthesis and comparison with experiments," *Automatica*, vol. 38, no. 4, pp. 611 – 625, 2002.

[48] Weigl, H. J., Paduano, J. D., Frechette, L. G., Epstein, A. H., Greitzer, E. M., Bright, M. M., and Strazisar, A. J., "Active stabilization of rotating stall and surge in a transonic single-stage axial compressor," *Journal of Turbomachinery*, vol. 120, pp. 625–636, Oct. 1998.

[49] Wisler, D. C., Breacher, B. F., and Shin, H.-W., "Effects of loading and clearance variation on tip vortex and endwall blockage," in *Proceedings of The 9th International Symposium on Transport Phenomena and Dynamics of Rotating Machinery*, (Honolulu, Hawaii), Feb.10 – 14 2002.